İSTANBUL TECHNICAL UNIVERSITY ★ INSTITUTE OF SCIENCE AND TECHNOLOGY

ENCAPSULATION OF MAGNETITE NANOPARTICLES IN CROSSLINKED POLY(VINYL ALCOHOL) VIA INVERSE EMULSION PROCESS

M.Sc. Thesis by

Meral AKDÜZEN

Department : Chemistry

Programme: Polymer Science and Technology

JUNE 2006

İSTANBUL TECHNICAL UNIVERSITY ★ INSTITUTE OF SCIENCE AND TECHNOLOGY

ENCAPSULATION OF MAGNETITE NANOPARTICLES IN CROSSLINKED POLY(VINYL ALCOHOL) VIA INVERSE EMULSION PROCESS

M.Sc. Thesis by

Meral AKDÜZEN

(515031021)

Date of submission : 8 May 2006

Date of defence examination: 20 June 2006

Supervisor (Chairman): Prof. Dr. Niyazi BIÇAK

Members of the Examining Committee Prof.Dr. Tuncer ERCİYES (İTÜ.)

Prof.Dr. Gürkan HIZAL (İTÜ.)

JUNE 2006

İSTANBUL TEKNİK ÜNİVERSİTESİ ★ FEN BİLİMLERİ ENSTİTÜSÜ

ÇAPRAZ BAĞLI PVA İÇİNE TERS EMÜLSİYON YÖNTEMİ İLE MANYETİT NANOTANECİKLERİNİN HAPSEDİLMESİ

YÜKSEK LİSANS TEZİ
Meral AKDÜZEN
(515031021)

Tezin Enstitüye Verildiği Tarih : 8 Mayıs 2006
Tezin Savunulduğu Tarih : 20 Haziran 2006

Tez Danışmanı :	**Prof. Dr. Niyazi BIÇAK**
Diğer Jüri Üyeleri	**Prof.Dr. Tuncer ERCİYES (İ.T.Ü.)**
	Prof.Dr. Gürkan HIZAL (İ.T.Ü.)

HAZİRAN 2006

ACKNOWLEDGEMENT

This master study has been carried out at Istanbul Technical University, Chemistry Department of the Science & Letter Faculty.

First of all, I would like to express my gratitude to my supervisor Prof. Dr. Niyazi Bıçak who brought this subject to my attention and for his deep interest, help and constructive discussions throughout my research.

I am also acknowledged to Dr. Orhan Kamer and Prof. Dr. Yusuf Yağcı for sharing their deep knowledge and experience during my research.

I am also indepted to my laboratory colleagues Bünyamin Karagöz, Atilla Taşdelen, Özgür Akdemir and Muzaffer Erdoğan for their helpful attitude during my laboratory works.

I would like to thank to Prof. Dr. Süleyman Tanyolaç, Prof. Dr. Ayşe Yusufoğlu, and Assoc. Prof. Dr. Cemal Özeroğlu for their encouragement in making up my mind to study in the field of polymer science.

I would like to thank to Ergin Arıoğlu, Başar Arıoğlu, Ülkü Arıoğlu, Emre Aykar, Celal Akın, Güzide Ünlü, Yusuf Ünlü, Tülay Çiçekuzman, Edibe Benekçi, Neslihan Arapoğlu, and Serap Karagöz for their kind interest and support during my studies.

Finally, I would like to dedicate this thesis to my parents Faruk and Serap AKDÜZEN, grandmother Fatma Kevser MERAL. I owe much to my family for all their self-sacrifice, patience and support during all my education.

May 2006 Meral AKDÜZEN

TABLE OF CONTENTS

ABBREVIATIONS

SEM : Scanning Electron Microscopy
FT-IR : Fourier Transform-Infrared
H : Interparticle Distance
G : Gibbs Energy
CA : Cetyl Alcohol
SDS : Sodium Dodecylsulfate
PIT : Phase Inversion Temperature
CMC : Critical Micelle Concentration
HD : Hexadecane
PCS : Photon Correlation Spectroscopy
TEM : Transmission Electron Microscopy
DLS : Dynamic Light Scattering
PMMA : Poly(Methyl Methacrylate)
MAA : Methacrylic Acid
COOH : Carboxylic Acid
AIBN : Azo Bis (İsobutyro Nitrile)
TGA, TG : Thermogravimetric Analysis
HEMA : Hydroxyethyl Methacrylate
PANI : Polyaniline
NaDS : Dodecylbenzene Sulfonic Acid Sodium Salt
Ms : Saturation Magnetization
Hc : Coecervity Force
FTIR : Fourier Transform İnfrared
UV : Ultra-Visible Spectrum
XRD : X-Ray Diffraction
MRI : Magnetic Resonance İmaging
Sty-DVB : Styrene- Divinyl Benzene
CLPANI : Cross-Linked Polyaniline
PPy : Polypyrole
PAH : Poly(Allylamine Hydrochloride)
MAPPs : Magnetically Active Polymer Particles

LIST OF TABLES

LIST OF FIGURES

LIST OF SYMBOLS

$\mathbf{Bu_4N^+}$	: Tetrabutyl ammonium
Au	: Gold
Ni	: Nickel
Pt	: Platinum
Pd	: Palladium
Ti	: Titanium
Ru	: Rubidium
ψ_d	: Helmholtz potential
$\psi_{H/2}$	: Potential half way
$\Delta \mathbf{G_{el}}$	: Free energy of electrical double layer
a	: Particle radius
n_1	: The number of molecules
$\mathbf{C_c}$	: Coagulation concentration
Q	: Total particle charge
V_1	: Solvent molecular volume
V_2	: Polymer molecular volume
V_s	: Steric interaction
V_E	: Electrostatic interaction energy
AgI	: Silver iodide
β_{11}	: A constant referring to identical particles of material
A_{11}	: Hamaker constant
$\mathbf{SiO_2}$	: Silicium dioxide
ψ_d	: Surface potential
Γ_2	: Adsorbed amount of polymer (number of chains/area)
χ	: Flory polymer/solvent interaction parameter
$\mathbf{S_{mix}}$ **and** S_{el}	: Geometric functions
$\rho(z)$	: Segment concentration profile
ξ	: Zeta potential
ε	: Permittivity of the medium
$\mathbf{Fe_2O_3}$	: Iron (III) oxide
$\mathbf{FeCl_3}$	: Iron (III) chloride
$\mathbf{Fe_3O_4}$	: Magnetite
$\mathbf{FeCl_2}$	: Iron (II) chloride
$\mathbf{ZrO_2}$	: Zirconium oxide
$\mathbf{ZrOCl_2}$	: Zirconium oxychloride
$\mathbf{CaCO_3}$	: Calcium carbonate
γ	: Interfacial surface tension
$\varepsilon(t)$	: Net power density
t	: Time
$p_{\mathbf{Laplace}}$	: Laplace pressure

γ_{LL}	: Interface energy of oil droplet and water phase
R	: Droplet radius
π_{osm}	: Osmotic pressure
$[Fe(CN)_6]^{4-}$	: Ferrocyanide
$G^{(2)}(\tau)$	: Photocount correlation function
τ	: Correlation delay time
$G^{(1)}(\tau)$	: Normalised correlation function of the scattered electric field
γ	: A constant
Γ	: Decay rate or inverse coherence time
D	: Translational diffusion coefficient
K	: Scattering vector
θ	: Scattering angle
η_0	: Viscosity of the medium
NaOH	: Sodium hydroxide
v_2	: Volume ratio of dry polymer in swollen state
ρ	: Density of polymer in dry state
v_1	: Molar volume of solvent
$\bar{M}_c$	: Molecular weight of the polymer segments between two crosslinking points
v_2^0	: Molar ratio of the dry polymer at the beginning
f	: Degree of ionization

ENCAPSULATION OF MAGNETITE NANOPARTICLES IN CROSSLINKED POLY(VINYL ALCOHOL) VIA INVERSE EMULSION PROCESS

SUMMARY

A preparative method for magnetite nanoparticles stabilized with in situ crosslinked poly (vinyl alcohol) is presented. We have observed for the first time that, poly (vinyl alcohol), even in 2.2 % concentrations, undergoes rapid post-crosslinking by Fenton Reagent (Fe (II) + H_2O_2) in aqueous solutions. By proper adjusting of the feed composition (using 50 % excess of Fe (II) for the peroxide equivalent), the iron dots in which 2/1 ratios of Fe (III) / Fe (II) are tightly entrapped into cross linked poly (vinyl alcohol) gel matrix. This procedure gives finely disperse emulsions by inverse emulsion (water in xylene: 1 /5) without using additional emulsifier. Treatment with aqueous ammonia results in formation of magnetite nanoparticles coated with cross linked poly (vinyl alcohol). SEM (scanning electron microscopy) showed that the products are amorphous and size of the particles are in the range of 280-460 nm. By the method presented, nano particles with magnetite contents as high as 45 % can be prepared. The nanoparticles shows high saturation magnetization with nearly zero hysteresises in 2-51 Oe of magnetic fields.

ÇAPRAZ BAĞLI POLİ(VİNİL ALKOL) İÇİNE TERS EMÜLSİYON YÖNTEMİ İLE MANYETİT TANECİKLERİNİN HAPSEDİLMESİ

ÖZET

Bu çalişmada aninda çapraz kılınmış Poli (vinil alkol) içine hapsedilmiş manyetit nano taneciklerinin hazırlanması için bir yöntem geliştirilmiştir. Ilk defa tarafımızdan Poli(vinil alkol)'ün %2.2 konsantrasyonlarındaki Fenton Reaktifi tarafından çok hızlı bir şekilde çapraz bağlandığı gözlenmiştir. Buradan yola çıkarak başlangıç bileşiminde hidrojen peroksite göre % 50 fazla Fe(II) kullanmak suretiyle içinde 2/1 oranında Fe(III)/Fe(II) içeren demir sülfatlarını çapraz bağlı poli(vinil alkol) içinde hapsetmeyi başardık. Bu işlem 1/5 su-toluen emulsiyonunda gayet ince dağılmış tanecikler vermektedir. Bu bileşimin amonyakla muamele edilmesiyle çapraz bağlı poli(vinil alkol) içine hapsedilmiş manyetit tanecikleri içeren bir dispersiyon hazırlanmıştır. Ortaya konulan bu yöntemle manyetit içeriği % 45 lere varan manyetit nano tanecikleri hazırlanabilmektedir. Elde edilen bu ürünlerin SEM (Taramalı elektron mikroskobu) fotoğrafları tanecik boyutlarının ortalama 260-480 nm aralığında olduğunu göstermiştir. Manyetiklik ölçümlerinde doygunluk manyetikliklerinin bileşim oranlarına bağlı olarak 47 emu/g'a kadar çıkabildiğini ve nano taneciklerden beklendiği gibi çok küçük histeresis (2-51 Oe) gösterdikleri belirlenmiştir.

1. INTRODUCTION

Preparation of nanosized ferromagnetic particles has gained growing interest due to their potential applications in various areas such as magnetic data storage, medical diagnosis, magnetic separation of biochemicals, and cells, targeted drug delivery and laser printing.

Magnetite (Fe_3O_4) is naturally occurring material having strong magnetization properties. Since its laboratory synthesis by co precipitation from aqueous solution of Fe (II) and Fe (III) mixture, magnetite has found considerable attention. Apparent advantages of magnetite over γ-iron or its ferromagnetic alloys are their processibility and relative stability against air oxygen.

In recent years considerable attention has been focused on polymer assisted dispersions of magnetite nanoparticles. There appear two common approaches for preparing magnetite and metal oxide nanoparticles.

i) Formation of magnetite in presence of polymeric or low molecular-weight surfactants dispersed in water,

ii) Seeded polymerization of a suitable monomer such as acrylamide on magnetite particles.

Although the first approach has proven to be more successful in preparation of stable magnetite nanoparticles, it is not easy task owing to rapid coalescence of the particles by means of magnetic forces. Particle sizes have been greatly reduced by micro-emulsion method, providing kinetic control of particle growths.

Prerequisite of nanoparticle stabilization is of course adsorption of the dispersing surfactant or polymer on the particle surface. However, this stability is greatly affected by external factors such as ionic strength and temperature. Any disturbing effect may cause destabilization of the particles, by removing adsorbed polymer on the surface. In order to attain more stable magnetite nanoparticles, irreversible

attachment of stabilizer molecules onto the particle surface seems to be essential. However covalent linking of surfactant molecules to the oxide surfaces is almost impossible in practice.

Alternatively, coating of the particles with a cross linked polymer can be considered for long lasting stabilities. Bio-compatibility of the polymer is sought for medical applications of those materials.

For biological applications, polyvinyl alcohol has been considered as suitable host matrix. Acid catalyzed crosslinking of polyvinyl alcohol with glutar dialdehyde has been demonstrated to be useful method for entrapment of nano size magnetite particles. Although simplicity of the post-crosslinking in this procedure is attractive, the aldehyde component used is not biologically safe.

Herein we report a novel and simple strategy for preparing submicron magnetite particles coated with crosslinked PVA without using additional crosslinking agent. In this strategy Fenton Reagent was used for crosslinking of PVA and generating the Fe (III) component of the magnetite which will be formed in the next step.

Fenton Reagent is well-known radical source in which hydrogen peroxide is decomposed by Fe (II) to give hydroxyl radical and Fe (III). This reagent has been widely used as redox initiator for polymerization of water miscible vinyl monomers, in the past.

It was demonstrated for the first time that, Fenton Reagent causes to instantaneous crosslinking of PVA in aqueous solution. In the present study this chemistry was employed to deposit Fe (II) and Fe (III) salts within the crosslinked PVA matrix. In the study stoichiometry of the reagents and process conditions of the magnetite formation in nanosizes were investigated. Magnetic measurements, FT-IR and Scanning Electron Microscopy (SEM) techniques were used for characterization of the products.

A preparative method for magnetite nanoparticles stabilized with in situ crosslinked poly (vinyl alcohol) is presented. For the first time, we have observed that, poly

(vinyl alcohol) even in 2.2 % concentrations undergoes rapid post-crosslinking by Fenton Reagent (Fe (II) + H_2O_2) in aqueous solutions.

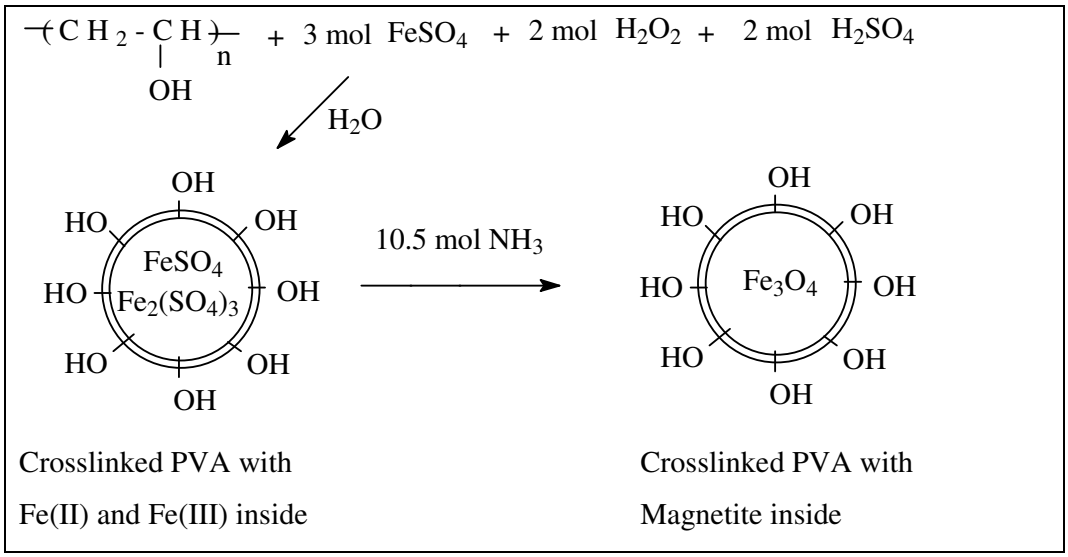

Figure 1.1: Formation and entrapment of submicron size magnetite particles in crosslinked PVA.

By proper adjusting of the feed composition (using 50 % excess of Fe (II) for the peroxide equivalent), the iron dots in which 2/1 ratios of Fe (III) / Fe (II) are tightly entrapped into cross linked poly (vinyl alcohol) gel matrix. This procedure gives finely disperse emulsions by inverse emulsion (water in toluene: 1 /5) without using additional emulsifier. Treatment with aqueous ammonia results in formation of magnetite nanoparticles (260-480 nm in diameters) coated with cross linked poly (vinyl alcohol). By the method presented, nano particles with magnetite contents as high as 45 % can be prepared.

It was observed that those dispersions are stable over tree weeks upon standing at room temperature.

Magnetic measurements showed that resulting products have high saturation magnetizations (up to 47 emu g^{-1}) with nearly zero hysteresises in 2-51 Oe.

2. THEORITICAL PART

2.1. Nanoparticles and Colloids

The word “colloid” was introduced for the first time by Graham in 1861 to describe the very slow sedimentation and noncrystalline state, two characteristic appearances of aqueous solution made of compounds well-known to be insoluble in water such as silver or gold chloride. In its starting definition, this term implied the suspension of a phase (solid or liquid) into a second phase, and was used for suspensions, which neither settled nor deposited spontaneously. These properties have led Graham to postulate that these colloidal particles should be large enough (above 1 nm) and of relatively weak size in order not to settle out (below 1 μm).

There are, in this way, very different types of colloids according to the physical phase of dispersed compounds and the environment of dispersion. The term “colloid” brings together a great diversity of compounds such as polymer suspensions in solution, emulsions constituted by amphiphilic molecules in aqueous or organic mixture, and finally dispersions of inorganic particles. For long time, the properties of inorganic colloids and more precisely metal nanoparticles have interested scientists. This interest is mainly due to their aesthetic properties as pigments in ceramics or their technological properties as catalysis. During the 20th Century, substantial progress has been obtained in the synthesis of metal colloids. Ostwald and Turkevitch [1] works have thus allowed understanding better the nucleation processes, growing and agglomeration linked up to the preparation of metal nanoparticles.

Recently, several criteria have been summarized to distinguish modern nanoclusters from traditional colloids such as the control over the composition, size, surface-ligating anions and other ligands, and finally the control over the desired properties: solubility in an appropriate solvent, isolability, and redissolvability. Additional kinetic and mechanistic studies in modern transition metal nanoclusters formation have also been performed, and, finally, a novel mechanism consisting of slow

continuous nucleation followed by fast autocatalytic surface growth leading to near-monodispersed nanocluster has been proposed [2].

2.2. Metal Nanoparticles

Now, essential challenges must be taken up: (i) finding new and reproducible methods of synthesis allowing stable and monodispersed suspensions of metal colloids which have a size between 1 and 10 nm, (ii) using new methods of characterization to elucidate the microstructures of these nanoparticles, and (iii) developing new applications.

Today, catalysis is the essential application of metal nanoparticles, but they find also application in such diverse fields as photochemistry, nanoelectronics, or optics. As catalysts, these systems show a great potential because of the large surface area of the particles. Many chemists suggest that metal colloids are very efficient catalysts because of a great ratio of atoms remaining at the surface, and so available to chemical transformation of substrates. In fact, these catalysts are microheterogeneous systems bearing metal nanoparticles. Undoubtedly, many catalytic transformations have been carried out with microheterogeneous metal catalysts while chemists believed that they were performed by homogeneous catalysts [3]. Since that time, modern methods to distinguish homogeneous from heterogeneous catalysts were described [4].

The original catalytic approach is to use colloidal metallic particles finely dispersed in organic or aqueous solution or a solvent mixture. Generally, these suspensions must be stabilized by protective agents to prevent aggregation and/or to facilitate recycling. One disadvantage of soluble colloidal metals is the recovery of the catalyst from the reaction products. This can be overcomed by using aqueous/organic biphasic conditions or other immobilization systems such as, for instance, fluorinated solvents or thin films of liquids on porous supports.

2.2.1. Synthesis of Metal Nanoparticles

Dispersions of metallic nanoparticles can be obtained by two main methods (Figure 2.1): (i) mechanic subdivision of metallic aggregates (physical method) or (ii) nucleation and growth of metallic atoms (chemical method).

The physical methods yield dispersions where the particle size distribution is very broad. Traditional colloids are typically larger (>10 nm) and not reproducibly prepared giving irreproducible catalytic activity. Chemical methods such as the reduction of transition metal salts are the most convenient ways to control the size of the particles. Today, the key goal in the transition metal colloid area is the development of reproducible nanoparticles (or modern nanoclusters) syntheses in opposition to traditional colloids. Nanoclusters should be or have at least (i) specific size (1-10 nm), (ii) welldefined surface composition, (iii) reproducible synthesis and properties, and (iv) isolable and redissolvable ("Bottleable").

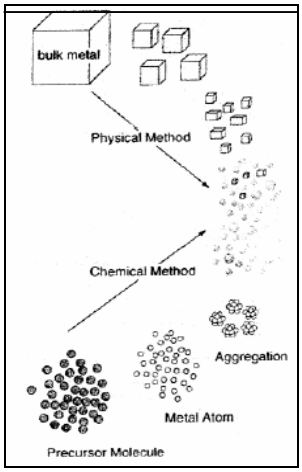

Figure 2.1: Schematic illustration of preparative methods of metal nanoparticles.

Chemical methods

Colloidal suspensions can be obtained by various methods leading to various particles size distributions. Nevertheless, whatever the method used a stabilizing agent is always necessary to prevent the aggregation of the colloids formed into larger particles. Five general synthetic methods are mainly used in the literature to synthesize transition metal colloids:

1. Chemical reduction of transition metal salts,
2. Thermal, photochemical, or sonochemical decomposition,
3. Ligand reduction and displacement from organometallics,
4. Metal vapor synthesis, and
5. Electrochemical reduction.

2.3. Stabilization of Colloids

One of the main characteritics of colloidal particles is their small size. Unfortunately, these metallic nanoparticles are unstable with respect to agglomeration to the bulk. In most cases, this aggregation leads to the loss of the properties associated with the colloidal state of these metallic particles. For example, during catalysis the coagulation of colloidal particles used as catalyst leads to a significant loss of activity. The stabilization of metallic colloids and thus the means to preserve their finely dispersed state is a crucial aspect to consider during their synthesis. Several general discussions on the stability of colloids and nanoclusters have been already reported [5].

At short interparticle distances, the Van der Waals forces will attract two metallic particles to each other. These forces vary inversely as the sixth power of the distance between their surfaces. In the absence of repulsive forces opposed to the Van der Waals forces, the colloidal metal particles will aggregate. Consequently, the use of a stabilizing agent able to induce a repulsive force opposed to the van der Waals forces is necessary to provide stable nanoparticles in solution.

The general stabilization mechanisms of colloidal materials have been described in Derjaguin-Landau-Verwey-Overbeek (DLVO) theory [6]. Nanocluster stabilization is usually discussed in terms of two general categories: (i) charge stabilization and (ii) steric stabilization.

For example, nanoparticle dispersions may be stabilized against flocculation by electrostatic repulsion, due to ions adsorbed at the particle surface, by steric effects arising from solvated polymer attached to the particle or by combinations of the two effects. In the preparation of dispersions there is often considerable uncertainty concerning the exact nature of the stabilization because of the possibility of adventitious contributions from components that are present for other reasons, for example persulphate initiators in emulsion polymerization, which result in sulphate end groups in the interface and may play a dominant role in stabilization. The particle size of a dispersion, its shear stability, viscosity and its stability to added salts or polymers are all properties that may be affected by the nature of the stabilizing mechanism. In setting out to make a dispersion, it is therefore essential to consider the mode of stabilization in relation to the end use and whether the presence

of more than one stabilizing mechanism in the same dispersion will complicate interpretation of subsequent measurements.

Based on the stabilizing agents used, it was suggested to distinguish four kinds of stabilization procedures:

1. The electrostatic stabilization by the surface adsorbed anions,
2. The steric stabilization by the presence of bulky groups,
3. The combination of these two kinds of stabilization with the electrosteric stabilization such as surfactants,
4. The stabilization with a ligand or solvent.

2.3.3. Electrostatic (Double-Layer) Stabilization

Particles may be stabilized by the electrostatic forces that arise as a result of each particle being surrounded by a layer of ionized surface groups and the associated diffuse atmosphere of counter ions. The ionized double layer may be provided by (i) chemically bound ionized groups or (ii) physically adsorbed ionized groups. Chemically bound groups are frequently encountered in emulsion polymers, either through the use of ion-containing initiators, to which reference has already been made, or by incorporation of functional monomers (e.g. acrylic acid, maleic acid or sulpho-ethyl methacrylate). In inorganic colloids, ions may be present in the surface of the particle as part of the crystal structure.

Adsorbed groups are usually present in the form of conventional surfactants and emulsifiers (e.g. sodium lauryl sulphate, sodium dioctyl sulphosuccinate). Adsorbtion is normally dependent on rejection of the hyrocarbon moiety from water on the particle surface, although chemical affinity between the rejected group and the surface may be important (e.g. dispersion of fluoropolymers). The effectiveness of a given surfactant will depend on other inter-related factors, such as the critical micelle concentration under the dispersion conditions, temperature and on the balance of polar/nonpolar constituents in the surfactant. Charge-stabilized dispersions are flocculated by multivalent ions or by 1:1 electrolytes at high ionic strengths. They may also coagulate under shear, depending on the particle size and ionic strength. At high disperse-phase concentrations or low ionic strength, electroviscous effects may

cause a steep rise in viscosity. In preparing charge-stabilized dispersions due attention must therefore be paid to these factors.

Figure 2.2(a) illustrates schematically the potential energy versus distance of separation for charge-stabilized particles in aqueous media. It can be seen that the potential-energy barrier opposing close approach of the particles diminishes rapidly with increasing electrolyte concentration.

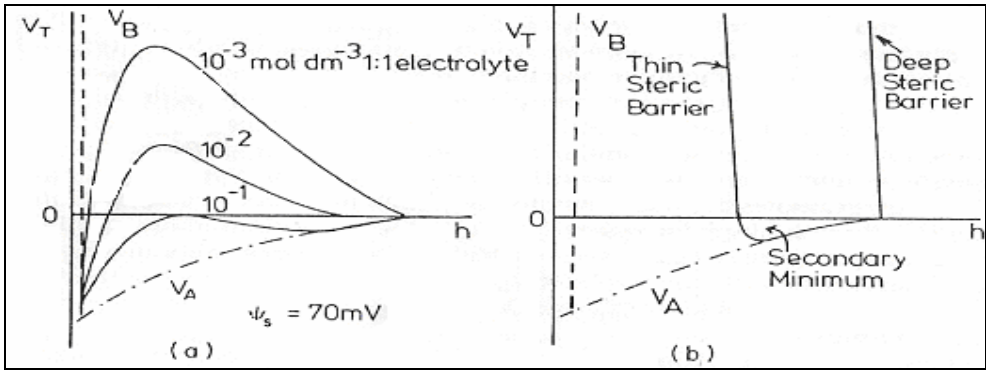

Figure 2.2: Schematic representations of potential energy versus distance of separation of (a) charge-stabilized particles in aqueous media (Buscall, 1985) and (b) sterically stabilized particles in nonaqueous media.

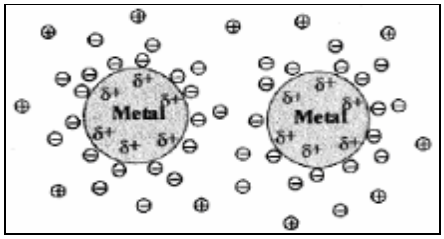

Figure 2.3: Schematic representation of electrostatic stabilization of metal colloid particles.

2.3.2. Steric Stabilization

Colloidal dispersions may be stabilized in either aqueous or nonaqueous media by solvated polymeric or oligomeric moieties adsorbed on the particle surface. In the simplest terms the adsorbed layer can be regarded as providing a barrier around each particle, preventing their close approach to one another to within a distance at which Van der Waal's attractions would cause flocculation. The adsorbtion of these molecules at the surfaces of the particles will provide a protective layer. The way in which these large adsorbed molecules prevent aggregation can be explained in a

simplified manner by visualizing the approach of 2 metallic colloids. In the interparticle space, adsorbed molecules will be restricted in motion, which causes a decrease in entropy and thus an increase in free energy (Figure 2.4). A number of conditions must be met if stable dispersions are to be prepared:

(i) The medium must be a good solvent (better than a theta solvent) for adsorbed polymer;
(ii) The surface coverage must be complete and the adsorbed stabilizer must be firmly attached to resist displacement under shear induced collisions;
(iii) The depth of the steric barrier must be sufficient to prevent flocculation.

In practice, molecular weights above 1000 are to be preferred, but useful stabilization can be achieved at much shorter chain lengths given full surface coverage.

Figure 2.2(b) is a schematic potential-energy versus distance diagram for a sterically stabilized dispersion**.** Unlike electrostatic stabilization, that is no long-range repulsion, and the particles are subject only to attractive forces until the outer fringes of the adsorbed molecules are in physical contact. The existence of a secondary minimum, i.e. a small net attraction, is therefore quite probable for strongly attracting particles or for shallow steric barriers.

Steric stabilizers take many forms. Naturally occurring polymers such as gelatin, casein, gum arabic, egg-white and vegetable oils have long been used in paints and inks as pigment dispersants. In modern solvent-borne coatings, alkyd and acrylic polymers are used. In the preparation of polymer latices, effective steric stabilizers are often generated by grafting reactions that result in the formation of amphipathic polymers, for example grafting of water soluble cellulose derivatives in emulsion polymerization. Fortunately there are many examples of well-characterized block and graft copolymers that have been synthesized for industrial use or for scientific studies, chiefly in nonaqueous media. In aqueous media block or graft copolymers are less easy to use except in their low-molecular-weight form as non-ionic surfactants, The *insitu* formation of stabilizer either in solution or at the particle surface is often simpler.

Sterically stabilized dispersions are very shear-stable over a wide range of particle sizes and can be made at high solids without difficulty. They may be flocculated by

changing the solvency of the medium or by desorbing the stabilizer, but otherwise remain stable indefinitely.

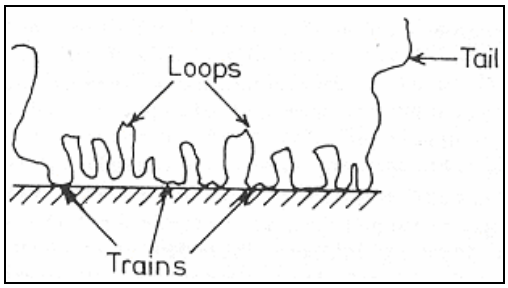

Figure 2.4: Schematic represantation of adsorbtion of nonionic polymer on a solid surface.

2.3.3. Combined Electrostatic And Steric Stabilization

Many of the dispersions are stabilized by a combination of charge and steric stabilization. The term electrosteric stabilization has been proposed for such systems. Many industrial and naturally occurring dispersions fall into this category. The contribution to stability of the two mechanisms in aqueus media may be varied independently to some extent. This possibility can be exploited in the study of one or other effect [8].

The electrostatic and steric stabilization can be combined to maintain metallic nanoparticles stable in solution [9]. This kind of stabilization is generally provided by means of ionic surfactants. These compounds bear a polar headgroup able to generate an electric double layer and a lypophilic side chain able to provide steric repulsion. The electrosteric stabilization can be also obtained from polyoxoanions such as the couple ammonium (Bu_4N^+)/polyoxoanion ($P_2W15Nb_3O_{62}^{9-}$). The significant steric repulsion of the associated bulky Bu_4N^+ countercations associated with the highly charged polyoxoanion (Coulombic repulsion) provide an efficient electrosterical stability toward agglomeration in solution of the resultant nanoclusters [9]. The variation of potential energy versus interparticle distance is shown in Figure 2.5.

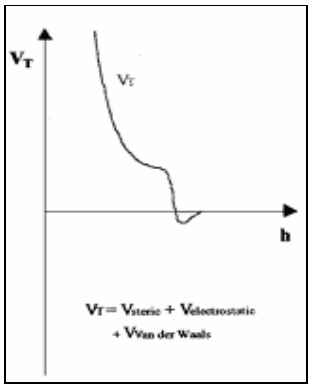

Figure 2.5: Plot of energy (V_T) vs interparticular distance (h) for electrosteric stabilization.

2.3.4. Stabilization by a Ligand or Solvent

The term *ligand stabilization* has been chosen to describe the use of traditional ligands to stabilize transition metal colloids. This stabilization occurs by the coordination of metallic nanoparticles with ligands such as phosphines, [10] thiols, [11] amines, [12] or carbon monoxide [13]. For example, Au, Pt, Pd, and Ni colloids were synthesized stabilized by phosphines. The phenanthroline and its derivatives and octanthiol have also been used to prepare Pt and Pd colloids.

It has recently been reported that nanoparticles can be stabilized only by solvent molecules. Thus, Ti [14] and Ru [7] nanoparticles were synthesized in tetrahydrofuran or thioethers without adding steric or electrostatic stabilizers. However, in both cases, it has not been established that there is no coordination of the heteroatoms of the solvents with the metallic surface. Moreover, proof of the absence of stabilizing agents such as anions or cations is lacking. Sometimes, elemental analysis shows that potentially coordinating bromide or chloride anions still remain.

2.4. Mechanisms Of Charge Stabilization And Steric Stabilization

Colloidal particles dispersed in a continuous medium are in constant Brownian movement. During these perpetual wanderings they experience interactions of various kinds, the magnitudes of which strongly depend on the particles' transient mutual distances. The combination of interaction energies determines whether the particles remain separate, so that the dispersion is stable in the colloidal sense, or stick together, in which case destabilization (coagulation or flocculation) occurs. Four types of

interaction can be distinguished:

1. Electrical double-layer repulsion or attraction;
2. Van der Waals attraction or repulsion;
3. Steric effects, mainly due to (adsorbed) polymers;
4. Short-range structural forces.

2.4.1. Electrical Double Layer Repulsion or Attraction

The effect of structural layers on stability has not yet fully been assessed, although recently a suggestion for its incorporation in the DLVO-theory has been made [15].

Another limitation will be that we restrict our considerations to two-particle interactions.

When charged colloidal particles in a dispersion approach each other, a situation gradually arises in which the individual double layers can no longer develop unrestrictedly, since the limited space does not allow complete potential decay. Restricting our considerations to two particles that are identical in all respects, and also assuming the surfaces to be flat, the potential distribution at an interparticle distance *H* is schematically depicted by the full line in Figure 2.6.

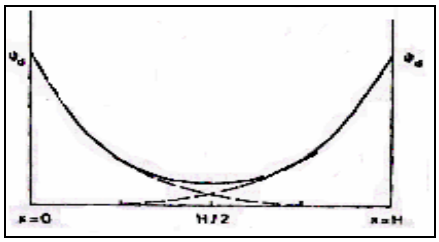

Figure 2.6: Potential distrubition between two flat plates of identical o.H.p. potential ψ_d (full line). The dashed lines give the potential decay of th individual particles had they been fully independent.

Note that ψ_d is considered to be independent of the particle distance. The dashed curves show the potential as a function of the distance x to the outer Helmholtz plane, had the particles been at infinite distance. The potential $\psi_{H/2}$ halfway between the two plates is no longer zero, implying that the first integration of the Poisson-Boltzmann equation has to be performed with the boundary conditions $\psi = \psi_{H/2}$ and $d\psi/dx=0$ at $x=H/2$, rather than with $\psi=0$ and $d\psi/dx=0$ at $x \rightarrow \infty$ as for isolated particles. The

second integration has to be performed with the boundary conditions $\psi = \psi_d$ (i.e. the o.H.p. potential) at x=0, $\psi = \psi_{H/2}$ at x=*H*/2, and leads to an elliptic integral of the first kind. The resulting combinations of $\kappa H/2$, ψ_d and $\psi_{H/2}$ have been tabulated [16]; κ is the reciprocal Debye-Hülckel length. Since tables are not easily read, for better understanding it is useful to note that for the interaction only the tails of the potential distribution are relevant. As a first approach, $\psi_{H/2}$ can be approximated by the sum of the ψ(x=H/2) values that the two particles would have if they did not sense each other's neighbourhood. For the low potential values under consideration, this amounts to [16]

$$\gamma = \left(\tanh \frac{1}{4} \gamma_d \right) \tag{2.1}$$

Combining (2.1) with the equation

$$\sigma_0 = -\varepsilon\varepsilon_0 \left(\frac{d\psi}{dx} \right)_{x=0} \tag{2.2}$$

$$\sigma_d = -\varepsilon\varepsilon_0 (d\psi / dx)_{x=0} \tag{2.3}$$

leads to

$$\sigma_d = (2n\varepsilon\varepsilon_0 kT)^{1/2} (2\cosh y_d - 2\cosh y_{H/2})^{1/2} \tag{2.4}$$

From (2.3) it can easily be inferred that decreasing the interparticle distance (and hence increasing $y_{H/2}$ at constant y_d) implies a decrease in the diffuse-charge density σ_d. Since decreasing σ_d requires energy, a situation with double-layer overlap goes along with an increase in the Gibbs energy *G* of the system. Thus the conclusion must be that two identical double layers repel each other. The quantitative elaboration of the free energy of the electrical double layer, G_{el}, and its variation due to double-layer overlap, ΔG_{el}, is rather involved, and it was referred the reader to the original literature [16]. Figure 2.7 illustrates the dependence of ΔG_{el}, on *H/2* for three different values of κ. Although the details show a number of intricacies, the general picture is that increasing the concentration of indifferent electrolyte causes the electrostatic repulsion to decrease. If the concentration of potential-determining ions

is increased, the concomitant increase in ψ_d causes, to increase, as demonstrated in Figure 2.8 Another important parameter is the valence z of the counterions. Its effect is shown in Figure 2.9, where the dashed line referring to $z = 3$ is almost everywhere below that for $z = 1$, despite the fact that the o.H.p. potential is chosen three times as large. Obviously, increasing the valence of the counterion dramatically reduces the repulsion.

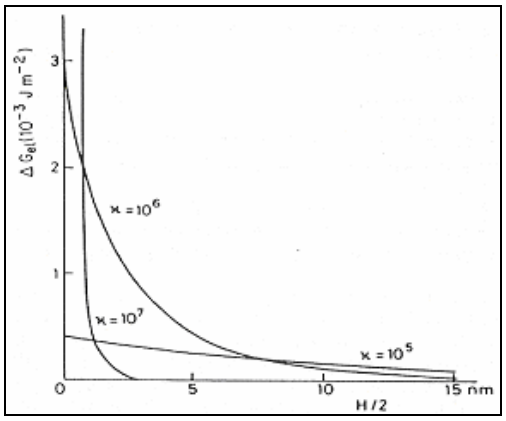

Figure 2.7: Increase in the electrical free energy of two flat plates as a function of decreasing mutual distance for three values of the reciprocal Debye-Hückel length. ψ_d = 154 mV; 1-1 electrolyte in aqueous solution.

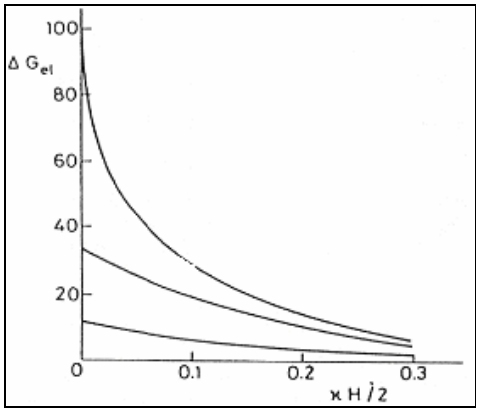

Figure 2.8: Increase in electrical free energy of two flat plates as a function of κ *H/2.* From top to bottom the three lines correspond to dimensionless potentials y_d of 8,6 and 4 respectively. The units on the vertical axis are only relative.

The cohesion of the numerical results has been condensed in a number of approximate analytical expressions. An important representative is the equation

$$\Delta G_{el} = \frac{64nkT}{\kappa}\gamma^2 \exp(-\kappa H) \tag{2.4}$$

Since in the derivation of (2.4) [16] the approximate formula (2.1) has been used, the results are only applicable at low potentials ($y_d \sim 1$), but for $kH/2$ exceeding 1 it is then virtually correct. Note that , ΔG_{el} is expressed in J m^{-2}.

Although colloidal particles may vary largely in size and shape, considering them to be spherical can be at least as appropriate as treating them as flat plates. For spherical geometry, the following two following cases considered:

(i) large particles with thin double layers, so that $\kappa a >> 1$;

(ii) conditions of small κa.

In dealing with case (i) they used an approach, and which has also proved useful when interaction energies are of a nature other than electrical. In this approximation the two spheres are considered as being divided into infinitesimal parallel rings, which then represent an infinite number of pairwise flat-plate interactions. The calculations are again rather involved, so that in using the complete Poisson-Boltzmann equation, ultimately a graphical or numerical method has to be employed. For low potentials, the approximate equation (2.4) may be used as the starting point, resulting in

$$\Delta G_{el} = \frac{64\pi nkTa}{\kappa^2}\gamma^2 \exp(-\kappa H_0) \tag{2.5}$$

An interesting aspect of (2.5) (in which H_o is the shortest distance between the surfaces of the spheres) is that it shows ΔG_{el} to be linearly dependent on the particle radius a.

For a small κa, case (ii) had to introduce the linear approximation of the Poisson-Boltzmann equation, so that these results only apply to low potentials. Also, under these conditions the repulsion free energy is proportional to the particle radius.

An important aspect of the Verwey-Overbeek [16] treatment concerns the assumption that at any stage of the particles' approach the electrical double layers adjust to the new conditions, so that equilibrium is always maintained. This is equivalent to stating that interaction takes place at constant potential. If, on the other hand, the relaxation time of the surface charge is appreciably longer than the time the particles are in each other's interaction sphere as a result of the Brownian motion, the charge rather than

the potential will be the constant parameter. Verwey and Overbeek themselves have already shown that constant charge leads to larger repulsion than constant potential. Whether one or the other condition prevails, will be different from system to system. Lykiema and Van Leeuwen (1982) [17] have analysed this topic for the much-studied AgI/eleclrolyte-solution interface. Based on a number of exchange reactions taking place at the interface and taking into account that the charge density has to relax only over the small areas directly involved in the contact of the particles, they arrive at the conclusion that for this system the potential can be considered to be the constant parameter. An even more recent analysis of Polder (1984) [18] has confirmed this assertion.

As is well known, in a one-component system individual atoms or molecules always attract each other at short distances, owing to van der Waals forces. These attractive forces can be of three different kinds: dipolo-dipole interaction (Keesom), dipole-induced dipole interaction (Debye) and interactions based on fluctuations in the electron-density distribution (London). Whatever the specific nature of the interaction, for not too large distances of separation the dependence of the corresponding free energy G_a on the particle distance r in vacuum is always of the form

$$G_a = -\beta_{11} r^{-6} \tag{2.6}$$

β_{11} is a constant referring to identical particles of material. The minus sign in Equation (2.6) expresses that attraction always goes along with lowering of the free energy.

Since colloidal particles are essentially assemblies of molecules, the individual contributions have to be compounded. In this process, only the London interactions have to be considered, since large assemblies have neither a net dipole moment nor a net polarization. The result relies on the assumption that the interaction energies between all molecules in one particle with all those in the other are simply additive. The interaction between two identical half-infinite parallel plates at distance H in vacuum is then represented by

$$G_a = -\frac{A_{11}}{12\pi H^2} \tag{2.7}$$

whereas for two identical spheres in vacuum the result is

$$G_a = -\frac{A_{11}}{6}\left(\frac{2}{s^2-4}+\frac{2}{s^2}+\ln\frac{s^2-4}{s^2}\right) \qquad (2.8)$$

A_{11} is known as the Hamaker constant and is defined by

$$A_{11} = \pi^2 \beta_{11} n_1^2 \qquad (2.9)$$

Where n_1 is the number of molecules of type 1 per unit volume, and $s = (2a + H_0)/a$. Equation (2.8) shows that A_{11} has the dimensions of energy.

For very short distances ($H_0 << a$, and *only* then), (2.8) may be approximated by

$$G_a = -\frac{aA_{11}}{12H_0} \qquad (2.10)$$

From (2.7) and (2.10), in comparison with (2.6), it becomes apparent that the range of attractive forces between macroscopic particles is orders of magnitude larger than for individual molecules. A striking aspect of (2.10) is that it shows G_a to be proportional to a, just like ΔG_{el}.

We have to realize, however, that the preceding treatment refers to particles in vacuum, and that the dispersion medium has not yet been accounted for . When doing so, the important conclusion emerges that (2.7) and (2.8) can be retained if *only* A_{11} is replaced by $A_{11(2)}$, the Hamaker constant of particles of material 1 dispersed in medium 2. $A_{11(2)}$ is defined by

$$A_{11(2)} = A_{11} - 2A_{12} + A_{22} = (A_{11}^{1/2} - A_{22}^{1/2})^2 \qquad (2.11)$$

$A_{11(2)}$ is a positive quantity, so that in a dispersion medium also two particles of the same material always attract each other. Anticipating the next section, it is important to note that in this treatment $A_{11(2)}$ is not only independent of the distance, but also of the electrolyte concentration in the solution. In Table 2.1 some data on the Hamaker constant in aqueous dispersions have been collected.

This classical approach is a "microscopic" theory, in that it is based on interactions between pairs of atoms. In contrast is the more modern Lifshits theory, in which

colloidal systems are considered from a macroscopic point of view. The principle of this macroscopic approach is that the spontaneous electromagnetic fluctuations in two particles become correlated when the latter approach each other, causing a decrease in the free energy of the system. The elaboration of this theory is rather complex and in its application requires extensive data on the electromagnetic interaction energies. Nevertheless, it allows the important conclusion to be drawn that most qualitative aspects displayed by (2.7)-(2.10) are fully confirmed [19]. An interesting exception concerns the rate of decay of G_a at large separations. Owing to the time required for electromagnetic waves to cover the distance between two particles, the H^{-2} dependence in (2.7) gradually changes into a H^{-3} dependence at large separations, a phenomenon known as retardation.

Table 2.1: Hamaker constants A_{nm} for some aqueous dispersions.

Colloid	$10^{20}A_{11(2)}$ (J)
Metals	10-20
SiO_2	0.3-0.9
Low-molecular-weight organic compounds	0.08-1.8
Polymers	0.2-2.5
AgI	2-4

Having established the distance dependence of ΔG_{el} as well as that of G_a, the two relations can be combined to provide the distance dependence of the total free energy of interaction G_T. A schematic example for two flat plates is presented in Figure 2.9, where curve A represents Ga Line B refers to ΔGel for relatively high ψ d. From the combination of A and B, line D, it is apparent that upon approach of the two particles, GT = Ga + ΔGel gradually increases. Only when the thermal energy of the particles is large enough to surmount the maximum in D can they approach to closer distances than that corresponding to this maximum. If this is the case then ultimately the particles come into contact with each other (H=0), which is equivalent to coagulation. The next step may then be that they fully merge, leading to a new entity. Such a process is known as coalescence, a phenomenon regularly occurring in emulsions, for example if the maximum in D is sufficiently greater than the energy of the Brownian motion then the particles have to remain at distances beyond this maximum, and the dispersion is stable. Obviously, instability can be promoted by

lowering the activation energy. This can be accomplished, for example, by decreasing Ψ_d to an extent corresponding with line C, which results in line E for GT. Not only can lowering the o.H.p. potential induce coagulation, increasing the ionic strength can also give the same effect. It is clear that increasing the valence of the counterion also greatly enhances destabilization. At this stage it is worth emphasizing that the interaction curves clearly show electrostatically stabilized (electrostatic) sols always to be unstable in the thermodynamic sense. Only because the activation energies can be (made) so high as to make the coagulation process unnoticeably slow can colloid stability be kinetically realized.

For spherical particles (or indeed for particles of other geometries) the situation is similar to that depicted in Figure 2.9. It may be remarked that for large radii (as for flat plates) G_T shows a shallow minimum. This so-called secondary minimum (the primary minimum is to the left of the energy maximum) gives rise to weak and reversible coagulation, a phenomenon that has been treated [20].

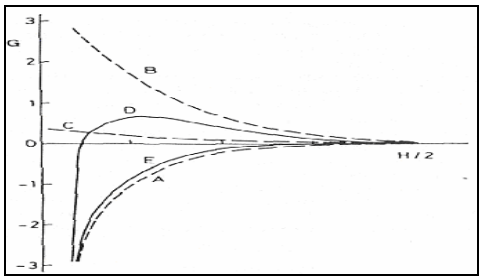

Figure 2.9: G_a, ΔG_{el} and $G_T=G_a+\Delta G_{el}$ as functions of half the distance between two flat plates. The units on the axis are only relative.

Since approximate formulae for ΔG_{el} and G_a are available, quantitative expressions for $G_T(d)$ can also be formulated. These can be used to derive expressions for the coagulation concentration, which is that concentration that causes every encounter between two colloidal particles to lead to destabilization. The following criteria has been introduced [16] for the transition between stability and instability:

$$G_T(=\Delta G_{el} + G_a) = 0, \qquad (2.12a)$$

$$dG_T/dd = 0, \qquad (2.12b)$$

so that

$$d\Delta G_{el}/dd = -dG_a/dd \qquad (2.13)$$

Inserting (2.5) and (2.7) into (2.12) and (2.13) shows the maximum in G_T to be always situated at $kH/2 = 1$. For the corresponding coagulation concentration c_c, when applied to aqueous solutions at 298 K, one obtains

$$C_{cx} = 8.0x10^{-36} \frac{\lambda}{A^2 z^6} \text{ mol m}^{-3} \qquad (2.14)$$

As expected, (2.14) illustrates that c_c increases with ψ_d, and decreases upon increasing the van der Waals attraction and the valency of the coagulating counterions. For very high values of ψ_d, γ approaches unity, in which case the coagulation concentrations would be proportional to the inverse sixth power of the valence. In practice, however, the condition $\gamma = 1$ is hardly ever met, so that the extremum ψ_d so low that $\gamma \approx \frac{1}{4} y_d$ is at least as interesting. In that case, c_c would be proportional to z^{-2} which still illustrates the large valence sensitivity. Qualitatively, the nonlinear dependence of c_c on z, was formulated about a century ago as the rule of Schulze and Hardy.

Using the same line of reasoning as for flat plates, for spherical particles also an approximate formula can be obtained. It appears to be identical with (2.14), except for the proportionality constant, which is now $3.6x10^{-36}$.

It should be reminded that (2.14) holds for conditions of constant potential, and that for conditions of constant charge c_c would be higher.

Adding organic solutes affects colloid stability in various ways. Not only does one have to cope with possibly incomplete electrolyte dissociation, but in addition the organic compounds usually get adsorbed at the interface. The latter effect induces changes in the structure of the inner part of the double layer, and may alter the amount of specifically adsorbed ions. This has yet to be combined with the variation in the dielectric constant of the solution and in the Hamaker constant.

In fully apolar nonaqueous solvents the amount of electrolyte that can be dissolved is very low. Consequently, electrical double layers in such systems are very thick, despite the fact that the low dielectric constant exerts the opposite effect. Also, the mechanisms by which the surface acquires its charge are rather different from those in water. Usually the values of the surface-charge density are low. For the prevailing

low potentials and low values of ka, it shown that [16] for two identical spheres the following approximate equation for ΔGel holds:

$$\Delta G_{el} = \frac{4\pi\varepsilon\varepsilon_0 a^2\psi_0^2}{R}\exp(-\kappa H) \approx \frac{4\pi\varepsilon\varepsilon_0 a^2\psi_0^2}{R} \tag{2.15}$$

ψ_0 is the surface potential, which in these systems is virtually identical with ψ_d, and $R=2a + H_0$.

Equation (2.15) can be combined with the equation correlating the total particle charge Q with ψ_0,

$$Q=4\pi\varepsilon\varepsilon_0 a\psi_0, \tag{2.16}$$

To give

$$\Delta G_{el} = \frac{Q^2}{4\pi\varepsilon\varepsilon_0 R} \tag{2.17}$$

Which is actually Coulomb's law. This result thus expresses the fact that the screening effect of the ions in the double layer, so important a phenomenon in aqueous systems, is virtually absent in nonaqueous ones.

2.4.2. Mechanism of Steric Stabilization

All of the states of aggregation referred to may be achieved by the judicious use of polymers. The polymer molecules may be chemically bonded (grafted) to the particle surface, physisorbed from solution, or simply present in solution. This topic is the subject of a recent book [21]. A detailed review has also been compiled [22].

The presence of adsorbed (or grafted) polymer molecules around the particles also leads to a "structured" layer, usually of much greater thickness (e.g. δ may be up to ~100 run with very high-molecular-weight polymers). The nature of V_s is now even more complex, since, for $h < 2\delta$, perturbation of the conformations of the adsorbed chains, as well as displacement of solvent from the interfacia! region into bulk, must occur. These two contributions to V_s, are known classically as the elastic (or volume restriction) and the mixing *(or osmotic)* contributions to what is generally referred to overall as the "steric interaction" [22]. More recent

theories of the steric interaction have avoided this artificial split (see below). However, it is useful to retain this division in order to understand the principal factors involved. For example, it has been given that the following approximate expression for the steric interaction V_s between two spheres with an adsorbed polymer layer [21]:

$$V_s = \overbrace{\frac{2\pi akTV_2^2\Gamma_2^2}{V_1}\left(\frac{1}{2}-\chi\right)S_{mix}}^{\text{mixing term: } V_{s,mix}} + \overbrace{2\pi akT\,\Gamma_2 S_{el}}^{\text{elastic term: } V_{s,el}} \qquad (2.18)$$

Where $a(>>\delta)$ is the particle radius, V_1 is the solvent molecular volume, V_2 the polymer molecular volume, Γ_2 the adsorbed amount of polymer (number of chains/area), χ the Flory polymer/solvent interaction parameter, and S_{mix} and S_{el} are geometric functions that depend on the form of the segment concentration profile, $\rho(z)$ in the adsorbed layer normal to the interface. Analytical expressions for S_{mix} and S_{el} have been derived by Napper {1977, 1983) for various assumed forms for $\rho(z)$. Although $\rho(z)$ has now been determined experimentally using small-angle neutron scaltering for individual particles, one really needs to establish how $\rho(z)$ varies with their separation in order to calculate V_s accurately. Alternatively one may determine V_s directly using force-balance methods [22].

A theory has been developed for V_s [23], based on their earlier lattice model of polymers at the solid/solution interface. In their approach it is assumed that adsorption equilibrium is maintained as a function of particle separation *h.* Hence $\rho(z, h)$ is calculated for flat places. The theory may be extended to spheres using the Derjaguin approximation.

The presence of adsorbed polymer on the particles may modify the Van der Waals forces, and also the electrostatic forces in the case of charged particles. Both these effects are difficult to model exactly. With regard to the Van der Waals forces, it has been considered that the effect of adsorbed polymer layers [24], extending Void's treatment for composite particles. Provided that the mean segment volume

fraction in the adsorbed layer is not too high, and the Hamaker constant of the polymer not too different from that of the solvent, the modification to the van der Waals forces is small.

The effect of the adsorbed polymer on the electrical double layer around a charged particle, and hence on the electrostatic interaction, is complex: both the surface-charge density and the distribution of counterions between the Stern layer and the diffuse layer may well be changed. The simplest approach [25] is to simply calculate the electrostatic interaction energy V_E prior to overlap of the adsorbed layers, i.e. at $h > 2\delta$. One may then, to a first approximation, use the appropriate equation for $V_E(h)$, with the zeta potential ξ replacing the surface or Stern potential, and $h - 2\delta$ replacing h. For example, for $\kappa a > 1$, where κ^{-1} is the Debye thickness of the electrical double layer,

$$V_E = 2\pi\varepsilon a\xi^2 \ln\{1 + \exp[-\kappa(h - 2\delta)]\ \} \tag{2.19}$$

where ε is the permittivity of the medium.

In practice, homopolymers are not the most efficient type of polymer molecule to provide effective steric stabilization. The necessary requirements are as follows:

*(a)*high coverage: Γ needs to be of order of $\Gamma_{plateau}$;

*(b)*efficient anchoring: χ_s for the adsorbed segments (in trains) needs to be $>> \chi_{s,c}$, the critical value of χ_s, for adsorption;

*(c)*extended tails (and loops, if present): δ needs to be sufficiently large, such that at $h = 2\delta$ the van der Waals energy is $< kT$ *or* so;

(d)''good'' solvent environment for the segments in tails (loops): $\chi < 0.5$.

Clearly, conditions (b) and (d), for example, can not be fulfilled simultaneously by a homopolymer. Hence various types of copolymers have been devised to overcome this difficulty. In particular, block or graft copolymers have been used (see Figure 2.12). In order to increase the χ_s value for the A ''backbone'', polymer interactions stronger than dispersion forces may be introduced (e.g. dipole-dipole, anion-cation, or even chemical bonds). A useful review of stabilizer design and chemistry is given [26].

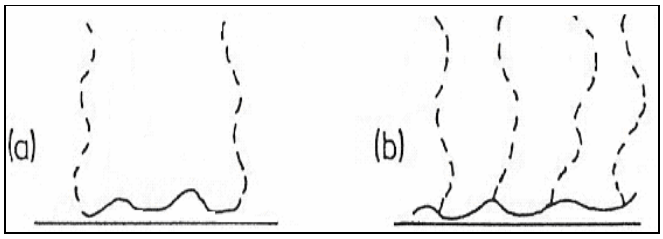

Figure 2.10: (a) ABA block copolymer; (b) AB graft copolymer.

2.5. Preparation of Stable Polymer Dispersions

The processes employed in the preparation of polymer dispersions fall into three broad categories: emulsion polymerization, dispersion polymerization and suspension polymerization.

In emulsion polymerization, monomer is emulsified in a nonsolvent, commonly water, usually in the presence of a surfactant. A water-soluble initiator is added, and particles of polymer form and grow in the aqueous medium as the reservoir of monomer in the emulsified droplets is gradually used up.

In dispersion polymerization, which has been exploited chiefly in non-aqueous media, monomer, initiator, stabilizer, and solvent initially form a homogeneous solution. Polymer precipitates when the solubility limit is exceeded, and again particles continue to grow until the monomer is consumed.

In suspension polymerization monomer is emulsified in the continuous phase using a surfactant or polymeric suspending agent. The initiator is often dissolved within the monomer droplet rather than in the continuous phase. The droplets are gradually converted into insoluble particles, but no new particles are formed.

Emulsion and dispersion polymerization both pass through nucleation and growth stages. In both types of process, the most commonly observed form of nucleation is the precipitation of primary particles comprising oligomeric free radicals, which originate from solution polymerization of dissolved monomer. These primary particles may be the result of homogeneous self-nucleation of single oligomers by collapse onto themselves or by aggregation of several oligomeric free radicals.

Solution polymerization continues even after the main locus of polymerization has moved into the monomer-swollen particles. It is therefore prefarable to conduct the second stage of the polymerization with only the minimum quantity of stabilizer

necessary to maintain stability. Addition of further stabilizer or surfactant can nucleate a second crop of particles to give a bimodal size distribution.

In dispersion polymerization, renucleation can also be caused by a fall in monomer concentration, causing a reduction in solvency and a fresh precipitation of particles. Control of the reaction conditions can be used to produce either monodisperse bimodal or polymodal dispersions.

In order to control the particle size more precisely, the technique of seeded polymerization is often employed. A small fraction of the total monomer is included in the initial reaction mixture, polymerization is initiated to form a seed, then the remaining monomer and extra surfactant if required is fed at a controlled rate commensurate with the rate of polymerization and surface growth. In this way renucleation can be minimized, so the technique is of special value in the preparation of large particles of the order of several micrometres in diameter.

Emulsion polymerization in the presence of ionic surfactants in general gives very fine particle dispersions *(ca.* 0.2 μm diameter or less). Larger particle sizes can be made by control of surfactant concentration, but in the manufacture of concentrated polymer latices for the coatings and adhesive industries, this approach frequently results in instability under shear and unwanted build up in the reactor. Fortunately, the incorporation of small amounts of high-molecular-weight soluble polymer (e.g. hydroxyethyl-cellulose) in the aqueous phase produces a much coarser seed slage. It is then relatively easy to prepare latices with particle sizes in the 0.2-1.5 μm range.

2.5.1. Miniemulsion Technique

A system where small droplets with high stability in a continuous phase are created by using high shear is classically called a "miniemulsion". One of the tricks to obtaining stability of the droplets is the addition of an agent that dissolves in the dispersed phase, but is insoluble in the continuous phase. The small droplets can be hardened either by subsequent polymerization or by decreasing the temperature (if the dispersed phase is a low-temperature melting material). For a typical oil-in-water miniemulsion, an oil, a hydrophobic agent (or several), an emulsifier, and water are homogenized by high shear to obtain homogeneous and monodisperse droplets in the size range of 30 to 500 nm.

To create a stable emulsion of very small droplets, which -for historical reasons- is called a miniemulsion, the droplets must be stabilized against Ostwald ripening by diffusion processes (τ_1 mechanism) and against coalescence by collisions (τ_2 mechanism). Stabilization against coalescence is effected by adding an appropriate surfactant. If the small droplets are not stabilized against Ostwald ripening they will disappear. In creating a miniemulsion, diffusional stabilization is achieved by adding a small quantity of a highly monomer-soluble and water insoluble agent. The idea of miniemulsion polymerization is to initiate the polymerization in each of the small stabilized droplets meaning that polymerization takes place in small nanodroplets. First published results where droplets with sizes of less than 0.7 μm were nucleated leading to polystyrene polymer particles. Homogenization was obtained by stirring; sodium dodecylsulfate (SDS) was used as a surfactant and cetyl alcohol (CA) was used as a hydrophobe resulting in a broad distribution of particles. A continuation of this early work was published one year later. It was shown that the addition of cetyl alcohol increases the stability of the droplets [27]. It was stated that miniemulsion polymerization leads to a broad size distribution, which, however, from a current point of view is due to the imperfection of homogenization at that time. The preparation of still broadly distributed droplets using hexadecyltrimethylammonium bromide/cetyl alcohol mixtures was published. In 1979, the use of sonication for the homogenization process in miniemulsions was described [28]. The term miniemulsion itself was created later. Key factors of miniemulsion formulation are the type of homogenization and the addition of the hydrophobe.

The process of miniemulsification allows the generation of small, homogeneous, and stable droplets of monomer or polymer precursors, which are then transformed by (as many as possible) polymer reactions to the final polymer latexes, keeping their particular identity without serious exchange kinetics being involved. It will be shown that the strength of miniemulsions is the formation of polymeric nanoparticles consisting of polymers or polymer structures, which are not accessible by other types of heterophase polymerization. Non-radical polymerizations and the formation of hybrid materials by the encapsulation of resins, inorganic materials, or liquids are some examples showing the wide applicability of miniemulsions also for technologically relevant questions. With the miniemulsification of molten inorganic

materials followed by a reaction, miniemulsions cross the border of polymers and open new possibilities in the fabrication of solid particles for material science.

The formulation and application of polymeric nanoparticles dispersed in a non-solvent, so-called polymer latexes, enjoy great popularity in academia and industry. Usually, (macro) emulsion or microemulsion polymerization is used to prepare these latexes. But even though this type of heterophase polymerization is widely applied, on has to be aware that an inconceivable restricted set of polymer reactions can be performed in this way. Strictly spoken, emulsion polymerization is good for the radical homopolymerization of a set of barely water-soluble monomers, but already heavily restricted in radical copolymerization. The reason for this is the polymerization mechanism where the polymer particles are the product of a kinetically controlled growth and are built from the center to the surface, where all the monomer has to be transported through the water phase by diffusion. Because of the dictate of kinetics even for radical copolymerization, serious disadvantages, such as the lack of homogeneity and restrictions in the accessible composition range, have to be accepted. In order to overcome these disadvantages, one has to perform a heterophase polymerization where small, homogeneous, and stable droplets of monomer or polymer precursors are generated, which are then transformed by (as many as possible) polymer reactions to the final polymer latexes, keeping their particular identity without serious exchange kinetics being involved. This means that the droplets have to become the primary locus of the initiation of the polymer reaction. With the concept of nanoreactors where the essential ingredients for the formation of the nanoparticles are present in the droplets, one can take advantage of a potential thermodynamic control for the design of nanoparticles. Polymerization in such nanoreactors should take place in a highly parallel fashion, i.e., the synthesis is performed in 1018±1020 nano-compartments per liter, which are separated from each other by a continuous phase. In miniemulsion polymerization, the principle of such small nanoreactors is realized as demonstrated in Figure 2.13 [29]. In the first step of the miniemulsion process, small stable droplets of 30±500 nm are formed by shearing a system containing the dispersed phase, the continuous phase, a surfactant and an osmotic pressure agent. In a second step, these droplets are polymerized without changing their identity. The droplets are small enough that the system benefits from all the advantages of conventional systems during polymerization, e.g.,

high rates of polymerization and high molecular weights of the resulting polymers. A main interest is laid on the stability principle of miniemulsions, the kinetics during the polymerization process, and the formation of polymer particles. The lack of monomer transport through the water phase easily allows the incorporation of severely hydrophobic components as well as solids. It will be shown that the concept developed is not restricted to a single procedure, such as radical polymerization in water, but opens the way to new polymers via a liquid/liquid technology both in a direct (aqueous solvent) and inverse (organic or hydrocarbon solvent) fashion. The principle is also highly favorable for the generation of nano-particulate metals and ceramics.

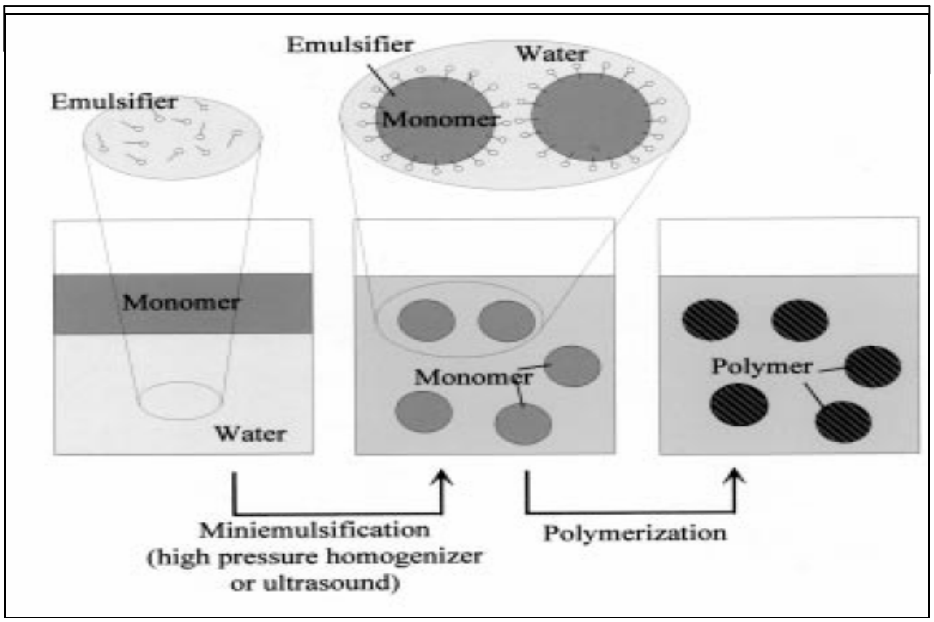

Figure 2.11: The principle of miniemulsion polymerization [29].

The characteristics of miniemulsions can be summarized as follows:

(1) Steady state-dispersed miniemulsions are osmotically stable, but critically stabilized with respect to colloidal stability.

(2) The interface energy between oil and water phase in a miniemulsion is larger than zero. The surface coverage of the miniemulsion droplets by surfactant molecules is not complete.

(3) The formation of a miniemulsion requires high mechanical agitation to reach a steady state given by a rate equilibrium of droplet fission and fusion.

(4) The osmotic stability of miniemulsion droplets results from an osmotic pressure in the droplets, which controls solvent or monomer evaporation. The osmotic pressure results from the addition of a hydrophobe, which has an extremely low water solubility. This crucial prerequisite is usually not present in thermodynamically stable microemulsions, but can be added to increase the stability. It is also expected that such miniemulsions undergo structural changes to establish a situation of zero effective pressure instead of zero Laplace pressure.

(5) During polymerization, the growth of droplets in miniemulsions can be suppressed. Monomer diffusion is balanced by a high osmotic background of the hydrophobe, which makes the influence of the polymer less seriously.

(6) The amount of surfactant required to form a polymerizable miniemulsion with SDS is small, usually between 0.5 and 25% with respect to the monomer phase, which is well below the surfactant amounts required for microemulsions. For high values, some overlap might occur. Also in these regions, miniemulsions represent the state with higher dispersity, as indicated by their surface tensions or characteristic sizes.

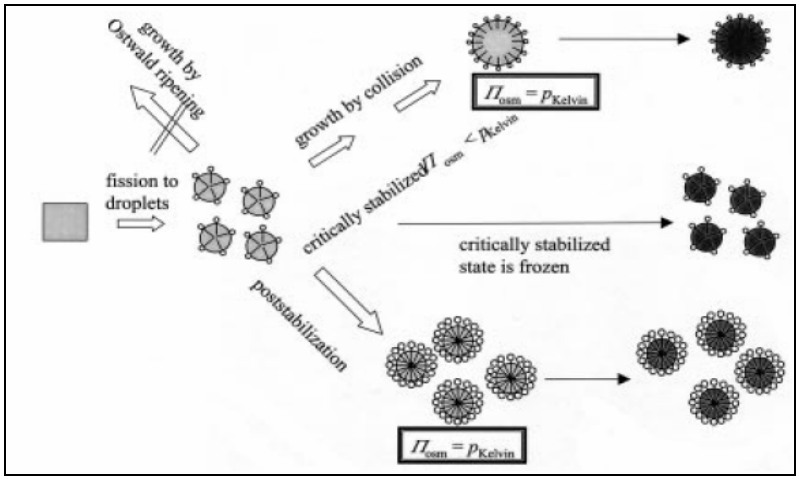

Figure 2.12: Schematic summary of the process of miniemulsion polymerization.

It was shown that miniemulsification can also be applied to low melting salts and metals to obtain colloids of high homogeneity with diameters between 150 nm and 400 nm. There are many salts or metals with low melting points. These systems can be heated above their melting points and can be miniemulsified in organic solvents. Subsequent cooling below the melting temperature results in a recrystallization of the

particles. The formation of high-melting materials can be achieved by a further reaction in which the low-melting material is used as a precursor.

In the dispersed state, heterophase reactions such as precipitations, oxidations, or carbonizations can be performed, which essentially occur under preservation of the colloidal entities as single nanoreactors. Miniemulsification and further reaction to iron oxide, magnetite, zirconia, and calcium carbonate was shown. The miniemulsification process is also suited to prepare metallic nanoparticles by using gallium or alloys with a low melting point (see same examples in Figure 2.13) [29]. The application of sterically appropriate stabilizers makes those dispersions colloidally stable in non-polar organic solvents. Due to the simplicity of liquid/liquid reactions, the quality of the particle size distributions and the smoothness of the particle surfaces, the technique is a considerable alternative to other techniques of colloid generation, such as milling or controlled precipitation reactions.

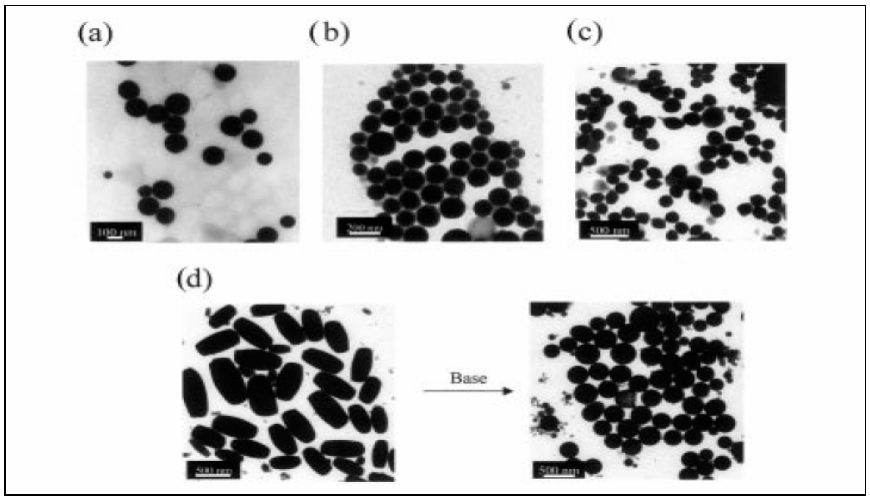

Figure 2.13: Miniemulsification of molten salts and metals: (a) Wood's metal particles, (b) Fe_2O_3 particles obtained from $FeCl_3$ droplets, (c) Fe_3O_4 particles obtained from $FeCl_2/FeCl_3$ droplets, and (d) ZrO_2 obtained from $ZrOCl_2$ [29].

The same procedure of miniemulsification can be performed to obtain polymer particles. Hydrophilic monomers are miniemulsified in an organic phase and hydrophobic monomers in water. Hardening of the droplets can then be achieved by subsequent polymerization in each droplet. The type of polymerization is not just limited to radical reactions: polyaddition or polycondensation reactions can also be carried out in such miniemulsion droplets. As one example, polymeric particles

formed via polyaddition of a diepoxide and a diamine are shown in Figure 2.14 [30] Particles such as these may be well suited to dentures.

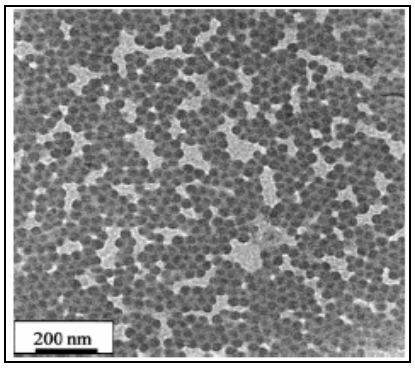

Figure 2.14: Particles obtained by polyaddition in miniemulsion [30].

The first two examples showed the fabrication of either pure inorganic or pure polymeric particles. It is of course of high interest to combine the inorganic and the polymeric part in order to obtain hybrid particles. If the inorganic particles shown in the first example are dispersed in a monomer and if this dispersion is subjected to miniemulsification, polymeric particles that fully encapsulate inorganic material are obtained. The polymeric shell effectively protects the inorganic particle. It is possible to incorporate just one (large) inorganic particle per polymer particle as was shown in the case $CaCO_3$, one can also cover a larger carbon black aggregate by a thin polymeric layer (see Figure 2.15a), [31] or one can incorporate many small particles, e.g., magnetite particles, in each polymer particle (see Figure 2.15b) [30]. Successful incorporation has been proven by many techniques. The dispersion with encapsulated carbon black may, for example, be used for ink jet printing, and the magnetic particles may be used for medical applications, e.g., for the destruction of cells via magnetic fields.

It has been shown that the encapsulation process is not limited to solid materials, but also liquids that are insoluble in the polymeric shell material can be encapsulated in order to obtain nanocapsules. For the synthesis, a monomer and oil are chosen in such a way that the two components are miscible in the monomeric state. But as soon as polymerization takes place, phase separation occurs. The differences in the hydrophilicities of the oil/polymer and polymer/water interfaces have to be designed so that the formation of nanocapsules is favored (Figure 2.15c) [30]. The wall can either be formed so that no leakage occurs, or it can be formed as a permeable shell that allows controlled release, e.g., of a perfume or a medicine.

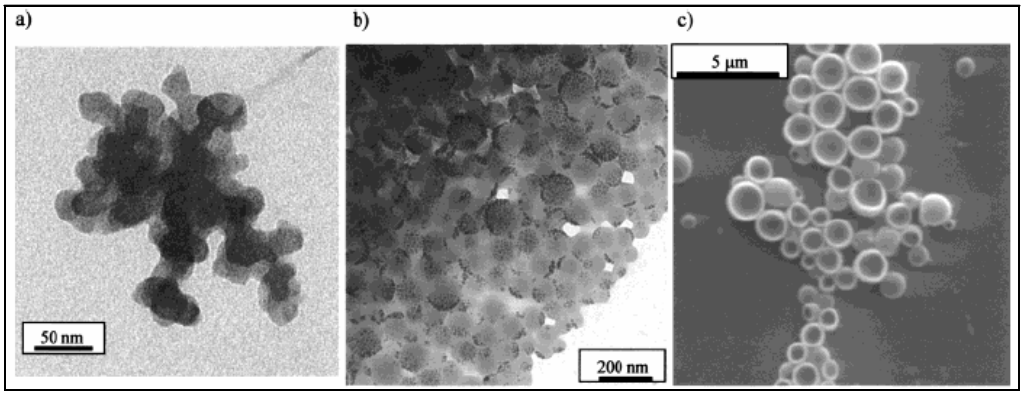

Figure 2.15: Encapsulation of materials by the miniemulsion process: a) carbon black aggregates, b) magnetite, c) a liquid to form nanocapsules [30].

Consequently, dispersion of liquid matter in stable nanodroplets into a miniemulsion opens new vistas for the synthesis of homogeneous inorganic particles using fluid precursor systems. Not only inorganic particles but also liquids can be encapsulated in a subsequent second miniemulsion step in a polymer shell in order to avoid leakage. This protects the interior against external influences, but may also protect the environment, e.g., the human body, against toxic materials. A permeable shell allows the controlled slow release of substances into the environment. The miniemulsion principle can also be exploited to obtain polymer particles. The strength of miniemulsions is that polymeric nanoparticles consisting of polymers or polymer structures that are not accessible using other types of heterophase polymerization can be produced.

2.5.2 Preparation of Nano-Emulsions

Three methods may be applied for the preparation of nano-emulsions (covering the droplet radius size range 50–200 nm). The use of high pressure homogenisers (aided by appropriate choice of surfactants and cosurfactants), the use of low energy emulsification method at constant temperature or application of the phase inversion temperature (PIT) concept.

The production of small droplets (submicron) requires application of high energy. The process of emulsification is generally inefficient.

Simple calculations show that the mechanical energy required for emulsification exceeds the interfacial energy by several orders of magnitude. For example, to produce an emulsion at $\varphi = 0.1$ with a $d_{32} = 0.6\ \mu$m, using a surfactant that gives an

interfacial tension $\gamma = 10$ m·Nm^{-1} , the net increase in surface free energy is $A\gamma = 6\gamma / d_{32} = 10^4 Jm^{-3}$. The mechanical energy required in a homogenizer is 10^7 Jm^{-3} , i.e. an efficiency of 0.1%. The rest of the energy (99.9%) is dissipated as heat.

The intensity of the process or the effectiveness in making small droplets is often governed by the net power density ($\varepsilon(t)$).

$$p = \varepsilon(t)\ \mathrm{d}t \tag{2.20}$$

Where t is the time during which emulsification occurs. Break up of droplets will only occur at high ε values, which means that the energy dissipated at low ε levels is wasted. Batch processes are generally less efficient than continuous processes. This shows why with a stirrer in a large vessel, most of the energy applies at low intensity is dissipated as heat. In a homogenizer, p is simply equal to the homogenizer pressure.

Several procedures may be applied to enhance the efficiency of emulsification when producing nano-emulsions: One should optimise the efficiency of agitation by increasing ε and decreasing dissipation time. The emulsion is preferably prepared at high volume fraction of the disperse phase and diluted afterwards. However, very high φ values may result in coalescence during emulsification. Add more surfactant, whereby creating a smaller γ_{eff} and possibly diminishing recoalescence. Use surfactant mixture that shows more reduction in γ the individual components. If possible dissolve the surfactant in the disperse phase rather than the continuous phase; this often leads to smaller droplets.

It may be useful to emulsify in steps of increasing intensity, particularly with emulsions having highly viscous disperse phase.

A study of the phase behaviour of water/oil/surfactant systems demonstrated that emulsification can be achieved by three different low energy emulsification methods, as schematically shown in Figure 2.16(a) [32] stepwise addition of oil to a water surfactant mixture; (b) stepwise addition of water to a solution of the surfactant in oil; and (c) mixing all the components in the final composition, pre-equilibrating the samples prior to emulsification. In these studies, the system water/Brij 30

(polyoxyethlene lauryl ether with an average of 4 mol of ethylene oxide/decane was chosen as a model to obtain O/W emulsions.

The results showed that nano-emulsions with droplet sizes of the order of 50 nm were formed only when water was added to mixtures of surfactant and oil (method b) [32].

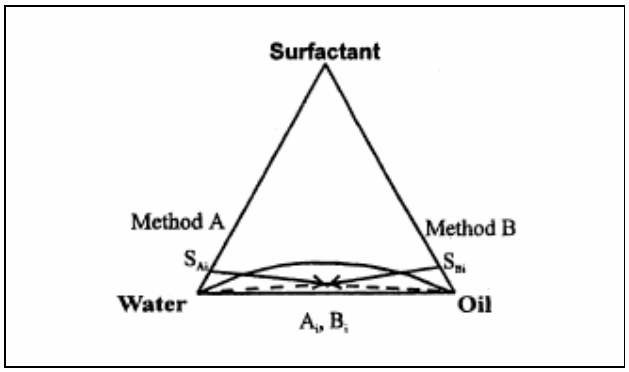

Figure 2.16: Schematic representation of the experimental path in two emulsification methods: Method A, addition of decane to water/surfactant mixture; method B, addition of water to decaneyBrij 30 solutions.

Phase inversion in emulsions can be one of two types: Transitional inversion induced by changing factors which affect the HLB of the system, e.g. temperature and/or electrolyte concentration; catastrophic inversion, which is induced by increasing the volume fraction of the disperse phase.

Transitional Inversion can also be induced by changing the HLB number of the surfactant at constant temperature using surfactant mixtures. This is illustrated in Figure 2.17 [32], which shows the average droplet diameter and rate constant for attaining constant droplet size as a function of the HLB number.

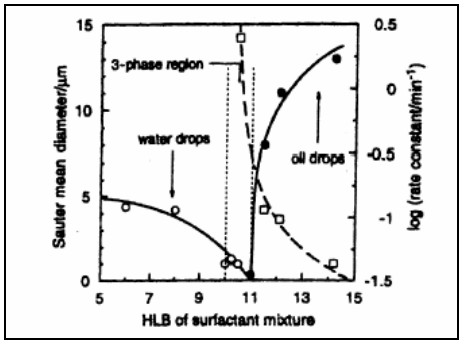

Figure 2.17: Emulsion droplet diameters (circles) and rate constant for attaining steady size (squares) as function of HLB CyclohexaneyNonylphenol Ethoxylate.

It can be seen that the diameter decreases and the rate constant increases as inversion is approached. For application of the phase inversion principle one uses the transitional inversion method which has been demonstrated by Shinoda and coworkers [33] when using non-ionic surfactants of the ethoxylate type. These surfactants are highly dependent on temperature, becoming lipophilic with increasing temperature due to the dehydration of the polyethyleneoxide chain. When an O/W emulsion is prepared using a non-ionic surfactant of the ethoxylate type is heated, then at a critical temperature (the PIT), the emulsion inverts to a W/O emulsion. At the PIT the droplet size reaches a minimum and the interfacial tension also reaches a minimum. However, the small droplets are unstable and they coalesce very rapidly. By rapid cooling of the emulsion that is prepared at a temperature near the PIT, very stable and small emulsion droplets could be produced.

A clear demonstration of the phase inversion that occurs on heating an emulsion is illustrated from a study of the phase behaviour of emulsions as a function of temperature. This is illustrated in Figure 2.18 [32], which shows schematically what happens when the temperature is increased [33].

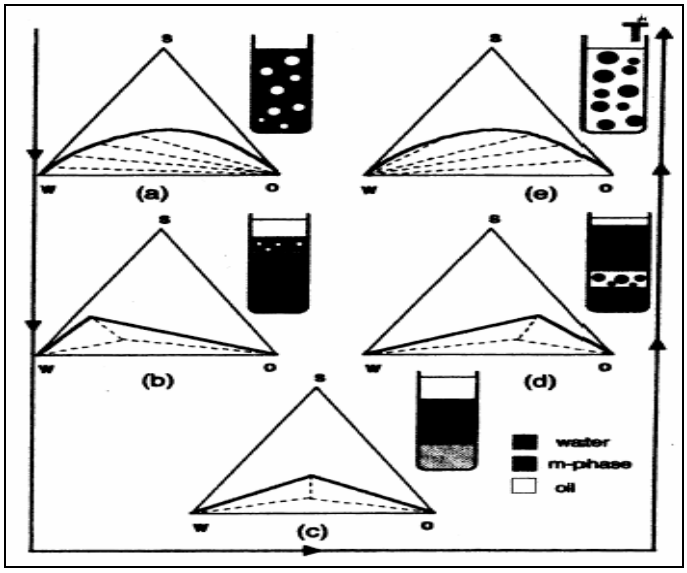

Figure 2.18: The PIT concept [32].

At low temperature, over the Winsor I region, O/W macroemulsions can be formed and are quite stable. On increasing the temperature, the O/W emulsion stability decreases and the macroemulsion finally resolves when the system reaches the

Winsor III phase region (both O/W and W/O emulsions are unstable). At higher temperature, over the Winsor II region, W/O emulsions become stable.

Figure 2.19 [33] shows the most clear-cut image of the macroemulsion inversion as a function of temperature. Equal volumes of oil and water are emulsified at various temperatures. Five hours after preparation, macroemulsions turned out to completely sediment. Below the balanced temperature (HLB temperature), a stable O/W macroemulsion is formed, whereas above the balanced temperature a stable W/O emulsion is formed.

Close to the balanced point (60–68 ^{0}C), a three phase equilibrium is observed and neither O/W or W/O emulsions are stable.

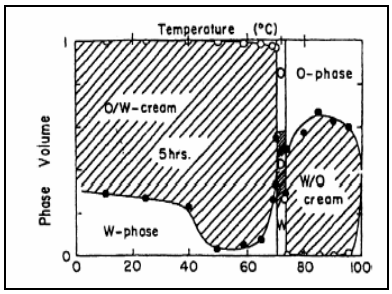

Figure 2.19: Macroemulsion stability diagram of cyclohexane-waterpolyoxyethylene (9.7) nonyl phenol ether system [33].

Near the HLB temperature, the interfacial tension reaches a minimum. This is illustrated in Figure 2.20 [32]. Thus by preparing the emulsion at a temperature 2–4 ^{0}C below the PIT (near the minimum in γ) followed by rapid cooling of the system, nano-emulsions may be produced.

The minimum in γ can be explained in terms of the change in curvature H of the interfacial region, as the system changes from O/W to W/O.

For O/W system and normal micelles, the monolayer curves towards the oil and H is given a positive value.

For a W/O emulsions and inverse micelles, the monolayer curves towards the water and H is assigned a negative value. At the inversion point (HLB temperature) H becomes zero and γ reaches a minimum.

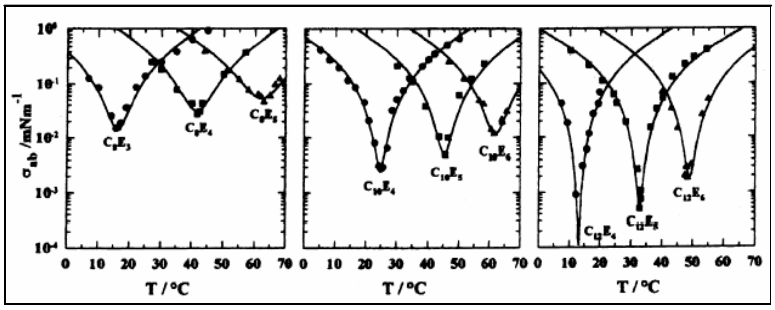

Figure 2.20: Interfacial tensions of n-octane against water in the presence of various *C E* surfactants above the cmc as a function of temperature [32].

Emulsions are understood as dispersed systems with liquid droplets (dispersed phase) in a liquid (continuous phase). Stabilization can be obtained electrostatically or sterically. Either molecular diffusion degradation (Ostwald ripening) or coalescence may lead to the destabilization and breaking of emulsions.

When an oil-in-water emulsion is created by the application of shear force to a heterogeneous fluid containing surfactants, a distribution of droplet sizes results. Interdroplet mass transfer (Ostwald ripening) determines the fate of this distribution because of their higher Laplace pressure. If the small droplets are not stabilized against diffusional degradation, they will disappear, increasing the average droplet size. It was shown that this disappearance can be very fast for small droplets [35].

It was shown that emulsion stability is proportional to particle volume. It has been demonstrated that [36] by statistically analyzing experimental data that the changes of the particle size distribution function is in accordance with the predictions of the Lifshitz-Slyozov theory. An extension with respect to fluorocarbon emulsions was achieved later [37]. Due to the low solubility in water, fluorocarbon emulsions exhibit a higher stability and can, therefore, also be used for medical applications, e.g., artificial blood.

It was proposed in 1962 that unstable emulsions may be stabilized with respect to the Ostwald ripening process by the addition of small amounts of a third component, which must distribute preferentially in the dispersed phase [29].

The evolution of the emulsion is driven by the competition between the osmotic pressure of the trapped species and the Laplace pressure of the droplets. This is of high importance for the production of stable emulsions. Increased stability is desired

for anesthetic/analgesic emulsions, the stability of which is provided by white mineral or other ripening inhibitors [38].

The rate of Ostwald ripening depends on the size, polydispersity and solubility of the dispersed phase in the continuous phase. This means an already ultra-hydrophobic oil dispersed in small droplets of low polydispersity shows low diffusion. But by adding a hydrophobe, the stability can even be increased by additionally building up an osmotic pressure. This was shown for fluorocarbon emulsions based on perfluorodecaline droplets and stabilized with lecithin. By adding a hydrophobic component, e.g. perfluorodimorphinopropane, the droplets' stability was increased and could be introduced as stable blood substitutes [29].

Davis et al. [39] described that the added material reduces the total vapor pressure as defined by Raoult's law. Hexane and hexadecane (HD) demonstrate a slight negative deviation from ideality, and HD/fluorochemicals a slight positive deviation from ideality. As in the case of the pure oil system, smaller droplets will have a slightly higher vapor pressure (or solubility) than larger ones. To reach the equilibrium state, hexane will leave the small droplets and pass to larger ones. This loss of hexane will cause an increase in the mole fraction of the third component in the small droplets and a decrease in the large droplets. Thus, the small droplets will have a more reduced vapor pressure as compared to the larger ones than originally was the case.

Besides the molecular diffusion of the dispersed phase, a destabilization of an emulsion can also occur by collision and coalescence processes. It was found that, in the case of rapid Brownian coagulation in dilute oil-in-water emulsions, the deformation influence on droplet interaction and drainage is negligible [29]. Observing the weak influence of droplet deformation on rapid coagulation and taking into account the Borwankar-Ivanov theory [40] that the transition to charged droplets and lower electrolyte concentrations decreases droplet deformation, it was concluded that both slow and reversible coagulation cannot be influenced by droplet deformation in miniemulsions. A droplet surface is homogeneous in contrast to solid particle surfaces.

A usual surfactant is anionic SDS, which is used for many model systems. In 1976, the possibility of using cationic surfactants, such as octadecylpyridinium bromide, was shown for the preparation of miniemulsions. However by stirring the emulsion,

droplets were obtained resulting in broadly distributed droplet sizes [41]. It has also been reported that the use of cationic surfactants to create miniemulsions [42]. It has been shown that cationic and non-ionic surfactants can be used to create well defined miniemulsions for further miniemulsion polymerization processes, resulting in a narrow size distribution of stable cationic and non-ionic latex particles [43]. Similar molecular amounts of simple cationic surfactant CTMABr and anionic SDS result in similar particle sizes showing that the particle size is essentially controlled by a limit of the surfactant coverage of the latex particles. From surface tension measurement results, this surface coverage was determined to be of the order of 30%, which proves the very efficient use of surfactants in the miniemulsification process. Two cationic counterion-coupled gemini surfactants, so-called cocogems, which were shown to be extremely efficient in the formation of microemulsions [44] resulted in only a moderate activity in miniemulsification. Rather large latex particles with a close-to-complete surfactant layer were obtained. This shows that the underlying energetic rules of micro- and miniemulsions are different and that efficiency relies on different surfactant properties. It is speculated that, for miniemulsions, the ability of surface spreading is advantageous, whereas low absolute interface energies and a high area requirement per surfactant is favorable for microemulsions.

A new class of cationic surfactants with sulfonium headgroups can also be employed effectively for the synthesis of miniemulsion polymers. The use of common and easily accessible reactants allows a broad variation of the molecular surfactant structures, i.e. the synthesis of linear homologues, but also of bola- or star-shaped surfactants [45]. The complexation of miniemulsions stabilized with sulfonium surfactants with delaminated clay sheets is a convenient way to generate armored latexes and crystalline nanocapsules with a wall thickness of 1.5 nm. The stability of the shells can be increased by a condensation reaction with silicic acid, which reacts with itself, but also with residual surface OH-groups of the clay [46].

Non-ionic miniemulsions can be made by using 3-5% of a poly (ethylene oxide) derivative as the surfactant, resulting in larger, but also very well-defined latexes [43].

Chern and Liou used the non-ionic surfactant nonylphenol polyethoxylate with an average of 40 ethylene oxide units per molecule [47]. Particle sizes between 135 and 280 nm were realized. The particle size mainly depends on the type and amount of

the hydrophobe and, therefore, on the degree of the suppression of Ostwald ripening [47].

Poly-(methyl methacrylate)-block-poly[(N,N-diethylamino-)ethyl methacrylate)] diblock copolymer as the surfactant and HD as the hydrophobe for the stabilization of miniemulsions was used [48]. Particles with sizes between about 150 and 400 were produced. Increasing the surfactant level in the miniemulsion could increase the polymerization rate. It is also possible to create stable vinyl acetate miniemulsions employing non-ionic poly(vinyl alcohol) (PVA) as the surfactant and HD as the hydrophobe [49].

It is also possible to use comb-like polymers with molecular weights of about 46104, for the formation of polystyrene miniemulsion latexes. In this case, the polymer acts as surfactant and hydrophobe at the same time, which is of high industrial significance. The polymers are comprised of octadecyl acrylate and acrylic or methacrylic acid groups. A typical organization of the comb-like polymer is anticipated at the oil-water interface, in view of the different polarities of the comonomer components [50]. Compared to cetyl alcohol, the water solubility is shown to be very low, which ensures the stability of the miniemulsion droplets.

Homogenization of the emulsions to miniemulsions can be obtained by means of different methods. In the first articles published, stirring was used. The use of an omnimixer and ultra-turrax was also described in early articles. However, the shear obtained by these techniques is not sufficient in order to obtain small and homogeneously distributed droplets [51]. A much higher energy, with respect of the thermodynamic part ($\Delta G = \gamma \Delta A$ with ΔG-free Gibbs energy difference, γ – surface/interfacial tension and ΔA - the newly formed interface) is required, since the comminution of large droplets into smaller ones involves additional forces, so that the viscous resistance during agitation absorbs most of the energy [52]. The excess energy is dissipated as heat. As high shear devices, today ultrasonication is used, especially for the homogenization of small quantities, whereas the microfluidizer or high pressure homogenizers are necessary for the emulsification of bigger quantities.

Mechanical emulsification starts with a premix of the fluid phases containing surface-active agents and further additives. Emulsification includes two steps. First,

the deformation and disruption of droplets, which increase the specific surface area of the emulsion, and secondly, the stabilization of this newly formed interfaces by surfactants.

Homogenization can be efficiently obtained by means of ultrasonication or high pressure homogenizers. For the miniemulsification of small quantities in a batch process, the ultrasonifier is an appropriate tool, but can also be used as continuous apparatus. For larger quantities, the use of a high pressure homogenizer is advised in order to achieve high homogeneity of the sample. However, the process of homogenization by ultrasound should be started with stirring the sample in order to already reach droplet sizes about ten times as large as the final droplet size after ultrasonication. During ultrasonication, the droplet size decreases constantly until reaching an equilibrium size. In the beginning of homogenization, the polydispersity of the droplets is still quite high, but by constant fusion and fission processes, polydispersity decreases. The miniemulsion then reaches a steadystate (see Figure 2.21)[53]. The process of homogenization can be followed by different methods, e.g., turbidity and surface tension measurements. With increasing time of ultrasonication droplet size decreases and, therefore, the entire interface oil/water increases as well. The constant amount of surfactant now has to be distributed at a larger interface. Since there always is an equilibrium between the surfactant at the interfaces water/oil and water/air, surface tension increases if the droplets are not fully covered by surfactant molecules.. The smaller the droplets are the higher the coverage is in order to obtain stable droplets, but in any case, full coverage is usually not obtained. The surface tension measurement is sensitive to the total interface oil/water, but can hardly allow to distinguish between polydisperse and monodisperse systems as long as the interfacial area is constant. Therefore, a constant value is reached after 500 s, but from turbidity measurements, the steady state is not yet reached at that point. This is due to the fact that turbidity measurements are also sensitive to the size distribution of the droplets. The homogenization of the droplet size distribution is reached after about 1000 s.

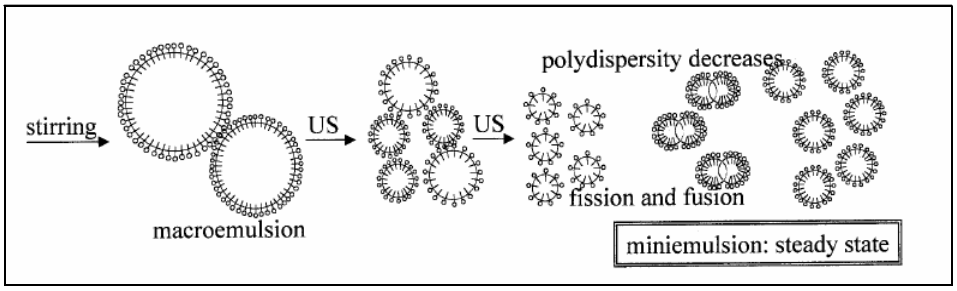

Figure 2.21: Scheme for the formation of a mini emulsion by ultrasound [53].

Minidroplets after the homogenization process are rather unstable dispersions and can undergo growing by Ostwald ripening (mechanism τ_1) or by collisions (coalescence, mechanism τ_2). The suppression of both processes is requested for the formulation of a stable miniemulsion. Coalescence can be controlled by the effective use of a surfactant. Ostwald ripening can efficiently be suppressed by the addition of a hydrophobic agent to the dispersed phase, which now counteracts the Laplace pressure of the droplet. This agent cannot diffuse from one droplet to the other and is trapped in each droplet, thus providing an osmotic pressure inside the droplets, which counteracts the Laplace pressure. The effectiveness of the hydrophobe increases with decreasing water solubility in the continuous phase. There is a minimum content of HD in order to efficiently suppress Ostwald ripening. For the hydrophobic agent, the term costabilizer might also be used. The term cosurfactant, which is also used in the literature, is rather misleading because, in most cases, the agent is not a cosurfactant in the traditional sense. A cosurfactant by definition [54] is a surface-active agent, which acts in addition to the surfactant by further lowering the interfacial energy, but can not form micellar aggregates itself.

Using an adequate amount of hydrophobe and undergoing an efficient homogenization process, the question is whether the pressure equilibrium between Laplace pressure and osmotic pressure is already given. It was found that steady-state miniemulsification results in a system of critical stability, i.e. the droplet size is the product of a rate equation of fission by ultrasound and fusion by collisions, and the minidroplets are as small as possible for the time scales involved. The pressure equilibrium right after the homogenization step is not fulfilled. It turned out that the droplet growth by monomer exchange (or mechanism τ_1) is effectively suppressed by the addition of a very hydrophobic material, whereas slow droplet growth by collisions (or mechanism τ_2) is subject to the critical conditions. The droplets grow

until the pressures are equilibrated (see Figure 2.21). It is, however, possible to obtain a long-term colloidal stability of miniemulsions by the addition of an appropriate second dose of surfactant after the dispersion step (see Figure 21).

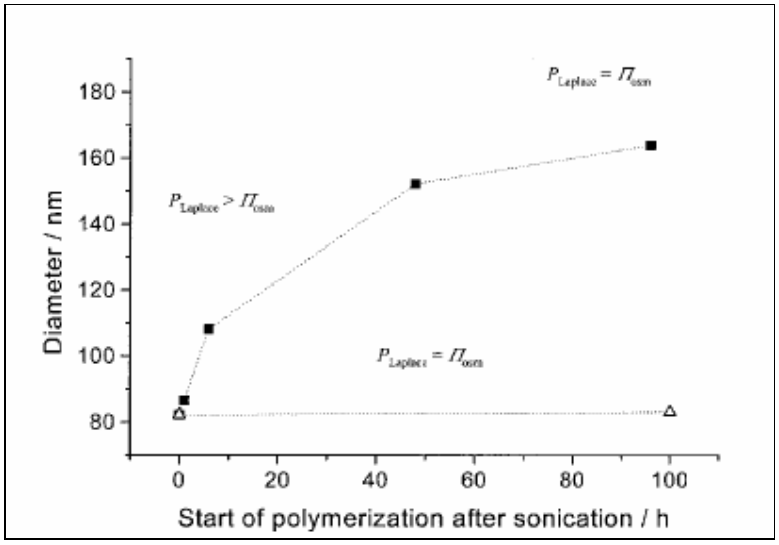

Figure 2.22: Growth of the droplets after ultrasonication until the pressures are equilibrated. Post-stabilizing allows to keep the droplet size constant.

The recalculation of latex interface energies allows one to calculate an accurate Laplace pressure p_{Laplace} inside the original miniemulsion droplet according to

$$\frac{2\gamma_{LL}}{R} = p_{\text{Laplace}} \tag{2.21a}$$

with

$$\gamma_{LL} = \frac{A_{\text{dense}}}{A_{\text{surf}}}\gamma_{LL,\text{dense}} + \left(1 - \frac{A_{\text{dense}}}{A_{\text{surf}}}\right)\gamma_{LL,\text{naked}} \tag{2.21b}$$

with droplet radius R and γ_{LL} being the interface energy of oil droplet and water phase. γ_{LL}, naked and γ_{LL}, dense are the interfacial tensions at the water/styrene interface without and with SDS coverage and are determined to be 35 mN N m^{-1} and 2 mN N m^{-1} , respectively. For a typical recipe, e.g., S = 0.012 (R = 50 nm and, therefore, γ_{LL} = 30 mN N m^{-1}), this results in a Laplace pressure of 12 bar as a maximum driving force for Ostwald ripening.

This Laplace pressure is counterbalanced by an osmotic pressure which is given by:

$$\Pi_{osm} = \frac{RTc}{M} \tag{2.22}$$

In order to check the influence of the effect of osmotic pressure, two miniemulsions with a different amount of hydrophobe, but otherwise similar to each other are mixed together. In this case, the droplets with lower hydrophobe content shrink, whereas the droplets with higher hydrophobe content increase in size until the osmotic pressure in all droplets is equilibrated. In an ideal case, a bimodal dispersion can be created.

Once the droplets are in the equilibrium state, the question remains whether or not there are exchange processes between the droplets. If the dispersed phase shows solubility in the continuous phase, some molecules can diffuse through the continuous phase, but all together, the sizes of the droplets do not change.

Analogous to direct miniemulsions, the osmotic pressure in inverse miniemulsions can be suppressed by an agent insoluble in the continuous phase, a so-called lipophobe. Most salts show a low solubility in organic solvents and can be used as lipophobes in water-in-oil miniemulsions [55]. The extraordinary high droplet stability after sonication against exchange can now be demonstrated in a very illustrative way. A miniemulsion with droplets containing a $FeCl_3$ solution, and one containing a $[Fe(CN)_6]^{4-}$ solution are mixed and, as can be seen from Figure 2.23a, the miniemulsion mixture stays colorless. This indicates that droplets with $FeCl_3$ and droplets with $[Fe(CN)_6]^{4-}$ coexist and no fusion/fission process takes place. If one performs the same experiment with two microemulsions, an immediate reaction takes place because the low interfacial tension close to zero leads to high dynamic processes in the system. The microemulsion droplets do not hold their identity.

In miniemulsions, higher energy is required to perform this dynamic exchange process. This can be obtained by ultrasonication. In this case, fusion and fission processes are induced and it can be seen that, with increasing ultrasonication time, the miniemulsion indeed turns blue (see Figure 2.23b)**.** The overall droplet size does not change.

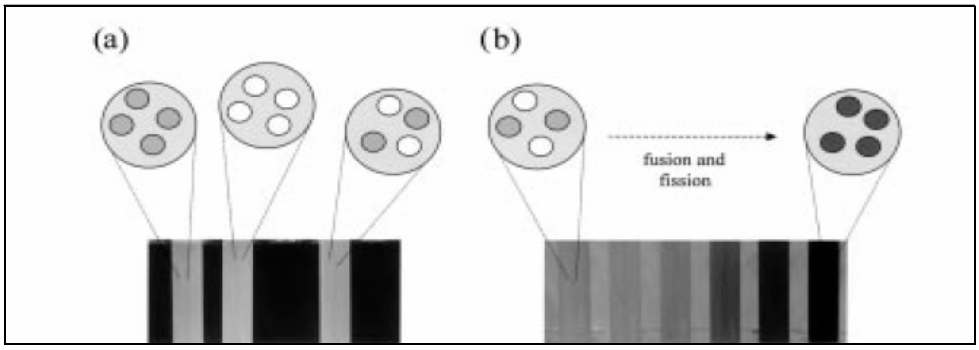

Figure 2.23: (a) Mixing of 2 inverse miniemulsions, the one containing a $FeCl_3$ solution, the other one $[Fe(CN)_6]^{4-}$; (b) ultrasonication is applied.

As hydrophobes many different molecules can be used. As a standard molecule, HD is used. But it is also possible to use molecules, which act as a dye, comonomer, or other additives. Silanes, siloxanes, isocyanates, polyester, fluorinated alkanes and many others turned out to be very efficient in suppressing Ostwald ripening. It is evident that the less water-soluble the hydrophobe is, the more effective it is as an osmotic pressure agent.

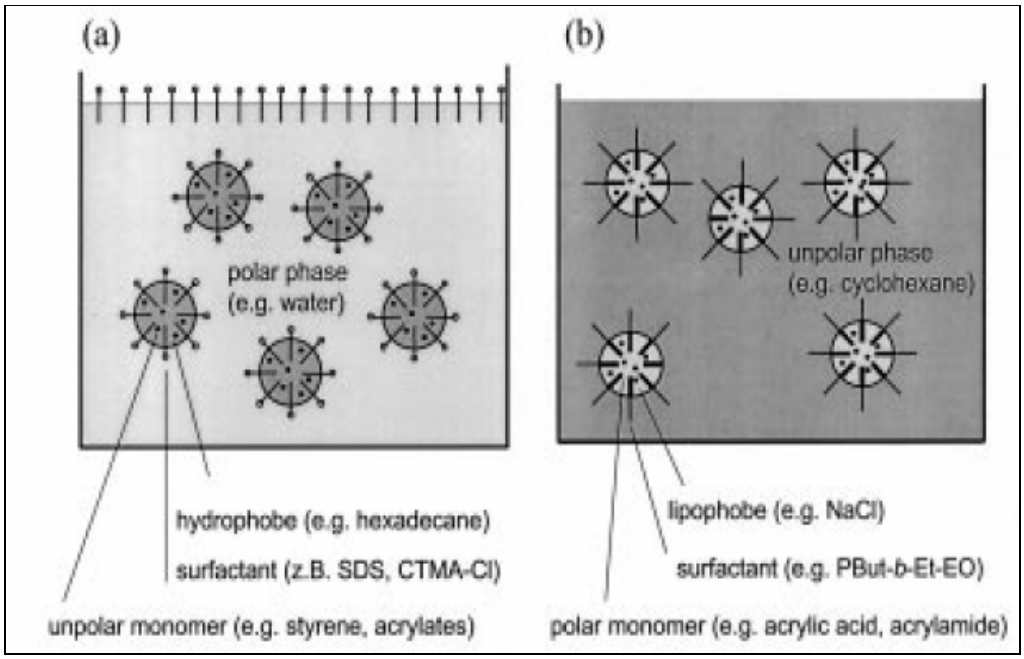

Figure 2.24: Comparison between direct miniemulsion and inverse miniemulsion.

The requirement that the costabilizer or hydrophobe must be of low molecular weight is based on swelling experiments reported and theoretical swelling experiments. Data reported herein demonstrate that it is possible to create miniemulsion latexes with a polymer as a poor hydrophobe [56]. Polymer makes an

ideal hydrophobe for numerous reasons. Primarily, it is able to fulfill the major requirements of any hydrophobe: water insolubility and monomer compatibility. It was shown that the use of polymer (without cetyl alcohol (CA)) as a hydrophobe allows to sufficiently stabilize the droplets during the course of polymerization [57]. Therefore, it was concluded that the addition of a small amount of polymer stabilizes the droplets kinetically, but not thermodynamically since the molecular weight is high and the number of chains does not reach a high number in order to provide an osmotic pressure in the droplets, which is high enough to fully counteract the Laplace pressure. The amount of both surfactant and polymer concentration allows one to control the droplet and micellar nucleation. A low surfactant level increases stability by decreasing the solubility of the monomer and hydrophobe in the aqueous phase. High hydrophobe levels, in contrast, impart diffusional stability.

2.5.3. Microemulsion Polymerization

The criterion for microemulsion polymerization is that a threshold emulsifier concentration exists above which a thermodynamically stable microemulsion is formed spontaneously for a given organic and aqueous phase. Contrary to that, miniemulsions are critically stabilized and require high shear to reach a steady state. Microemulsions are thermodynamically stable with an interfacial tension at the oil/water interface close to zero, whereas in miniemulsions, the interfacial tension is much larger than zero. The high amount of surfactant, which is required for microemulsion preparation leads to a complete coverage of the particles, and, therefore, the surface tension of the microemulsion reaches a minimum value. Additionally, a cosurfactant is often used to further minimize interfacial tension. During microemulsion polymerization, the polymerization starts from this thermodynamically stable state. Since initiation can not be achieved in all microdroplets simultaneously, polymer chains are formed only in some droplets. This thermodynamic non-equilibrium state usually leads to an increase in particle size (5 to 50 nm in latexes, in coexistence with empty micelles) [58].

2.5.4. Macroemulsion Polymerization

Below a threshold of surfactant amount, which also depends on temperature, monomer concentration and the chemistry of the emulsifier, no microemulsion, but kinetically stabilized macroemulsions are formed. Therefore, large monomer droplets

(1±10 μm in diameter), which are stabilized by surfactant, and empty or monomer-swollen surfactant micelles coexist in the initial state. For polymerization, one starts from large monomer droplets and surfactant micelles in the water phase. The watersoluble initiator forms oligoradicals from slightly watersoluble monomer units. These oligoradicals then enter the micelles and start to form particles. During polymerization, monomer diffuses through the water phase to the micelles in order to sustain polymer particle growth. Particles with a diameter of usually more than 100 nm are formed. Due to the increase of the interfacial area, the surface tension of a latex increases with polymerization. In the literature, the term emulsion polymerization is used for this process [59]. For clarity, we defined it as a macroemulsion polymerization as compared to micro- and miniemulsion polymerization.

The differences between macroemulsion polymerization and miniemulsion polymerizations are obvious. In macroemulsion polymerization, the latex particle does not correspond to the primary emulsion droplet, and the size is established by kinetic processes where kinetic parameters, such as temperature or the amount of initiator, play a predominant role. These factors remain unseen in miniemulsion polymerization where the latexes are essentially a polymerized copy of the original droplets, the size of which is essentially given by dispersion process and droplet stability, but not by polymerization parameters. In terms of the stability of the emulsion and in terms of the size of the resulting particles, miniemulsions are in between macroemulsions and microemulsions.

2.5.5. Suspension Polymerization

In the case of large monomer droplets in the continuous phase, nucleation predominantly occurs in the droplets, and each polymerizing droplet behaves as an isolated batch polymerization reactor. This principle of nanoreactors is very similar to the idea of miniemulsion. Indeed, the main difference is the size and stability. The notation suspension polymerization is reserved for systems where nucleation occurs in the monomer droplets and the average number of radicals per particle $\bar{n}$ is very high (102 to 106). This is usually obtained if the droplets are larger than 1 μm.

2.5.6. Difference between Micro-, Macro- And Suspension Polymerization

Miniemulsions are not defined by size range, but by a mode of operation. Differences to other heterophase polymerization types, namely microemulsion, (macro)emulsion, miniemulsion, and suspension polymerization, are delineated below. The different processes are shown in Figure 25 [29].

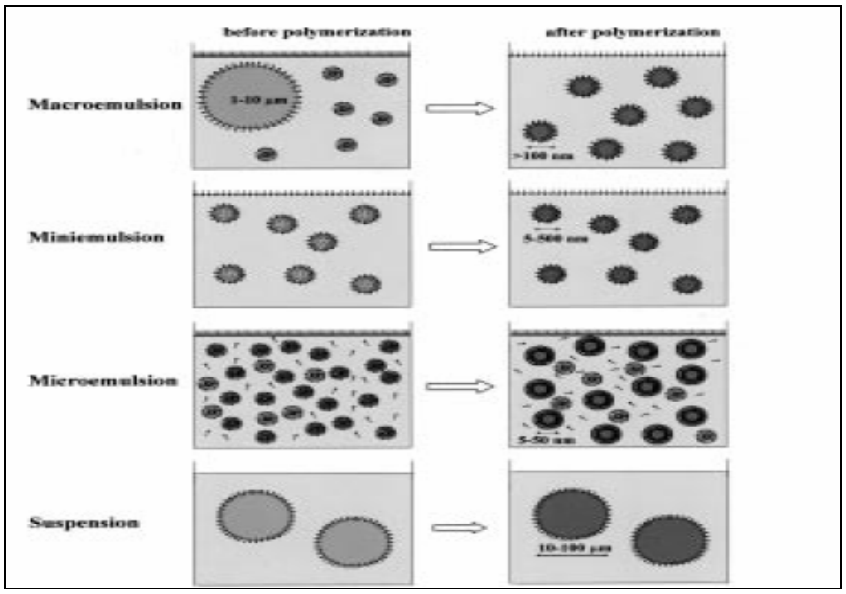

Figure 2.25: Comparison of heterophase polymerization processes.

2.6. Mechanism of Emulsification

To prepare an emulsions oil, water, surfactant and energy are needed. This can be considered from a consideration of the energy required to expand the interface, $\Delta A\,\gamma$ (where ΔA is the increase in interfacial area when the bulk oil with area A_1 produces a large number of droplets with area A_2 ; $A_2 << A_1$, γ is the interfacial tension). Since γ is positive, the energy to expand the interface is large and positive. This energy term cannot be compensated by the small entropy of dispersion $T\Delta S$ (which is also positive) and the total free energy of formation of an emulsion, ΔG is positive,

$$\Delta G = \Delta A\gamma - T\Delta S \tag{2.23}$$

Thus, emulsion formation is non-spontaneous and energy is required to produce the droplets. The formation of large droplets (few micrometers) as is the case for macroemulsions is fairly easy and hence high speed stirrers such as the Ultraturrax or Silverson Mixer is sufficient to produce the emulsion. In contrast the formation of small drops (submicron as is the case with nano-emulsions) is difficult and this requires a large amount of surfactant and/ or energy.

The high energy required for formation of nanoemulsions can be understood from a consideration of the Laplace pressure p (the difference in pressure between inside and outside the droplet,

$$p = \gamma \left(\frac{1}{R_1} + \frac{1}{R_2} \right) \tag{2.24}$$

where R_1 and R_2 are the principal radii of curvature of the drop.
For a spherical drop, $R_1 = R_2 = R_3$ and,

$$p = \frac{2\gamma}{R} \tag{2.25}$$

To break up a drop into smaller ones, it must be strongly deformed and this deformation increases p. This can be shown when a spherical drop deforms into a prolate ellipsoid. For a spherical drop, there is only one radius of curvature R_a, whereas for a prolate ellipsoid there are two radii of curvature $R_{b,1}$ and $R_{b,2}$. Consequently, the stress needed to deform the drop is higher for a smaller drop. Since the stress is generally transmitted by the surrounding liquid via agitation, higher stresses need more vigorous agitation, hence more energy is needed to produce smaller drops [60].

Surfactants play major roles in the formation of nanoemulsions: By lowering the interfacial tension, p is reduced and hence the stress needed to break up a drop is reduced. Surfactants prevent coalescence of newly formed drops.

Various processes occurring during emulsification, namely break up of droplets, adsorption of surfactants and droplet collision (which may or may not lead to coalescence occur [60]. Each of these processes occurs numerous times during emulsification and the time scale of each process is very short, typically a

microsecond. This shows that the emulsification process is a dynamic process and events that occur in a microsecond range could be very important. To describe emulsion formation one has to consider two main factors: Hydrodynamics and interfacial science.

To assess nano-emulsion formation, one usually measures the droplet size distribution using dynamic light scattering techniques (photon correlation spectroscopy, PCS). In this technique, one measures the intensity fluctuation of scattered light by the droplets as they undergo Brownian motion [61]. When a light beam passes through a nano-emulsion, an oscillating dipole moment is induced in the droplets, thereby reradiating the light. Due to the random position of the droplets, the intensity of scattered light will, at any instant appears as a random diffraction or 'speckle' pattern. As the droplets undergo Brownian motion, the random configuration of the pattern will, therefore, fluctuate such that the time taken for an intensity maximum to become a minimum, i.e. the coherence time corresponds exactly to the time required for the droplet to move one wavelength. Using a photomultiplier of active area about the diffraction maximum, i.e. one coherence area, this intensity fluctuation can be measured. The analogue output is digitised using a digital correlator that measures the photocount (or intensity) correlation function of the scattered light. The photocount correlation function $G^{(2)}(\tau)$ is given by the equation,

$$G^{(2)}(\tau) = B\left(1 + \gamma^2 \left[g^{(1)}(\tau)\right]^2\right) \tag{2.26}$$

where τ is the correlation delay time. The correlator compares $G^{(2)}(\tau)$ for many values of τ. B is the background value to which $G(\tau)$ decays at long delay times. $G^{(1)}(\tau)$ is the normalised correlation function of the scattered electric field and γ is a constant (approx.1). For monodisperse non-interacting droplets,

$$g^{(1)} = \exp(-\Gamma\tau) \tag{2.27}$$

where Γ is the decay rate or inverse coherence time, that is related to the translational diffusion coefficient D by the equation,

$$\Gamma = DK^2 \tag{2.28}$$

where K is the scattering vector,

$$K = \frac{4\pi n}{\lambda_o} \sin\left(\frac{\theta}{2}\right) \tag{2.29}$$

λ is the wavelength of light in vacuo, n is the refractive index of the solution and θ is the scattering angle.

The droplet radius R can be calculated from D using the Stokes–Einstein equation,

$$D = \frac{kT}{6\pi \eta_o R} \tag{2.30}$$

η_0 is the viscosity of the medium.

The above analysis is valid for dilute monodisperse droplets. With many nano emulsions, the droplets are not perfectly mono-disperse (usually with a narrow size distribution) and the light scattering results are analysed for polydispersity (the data are expressed as an average size and a polydispersity index that gives information on the deviation from the average size).

2.7. The Mineral Magnetite

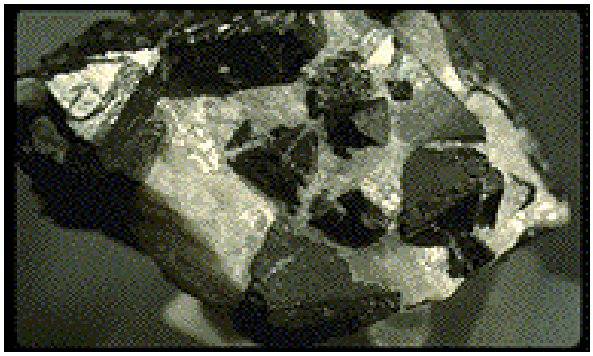

Figure 2.26: The mineral magnetite.

- Chemical Formula: Fe_3O_4, Iron Oxide
- Class: Oxides and Hydroxides
- Group: Spinel
- Uses: Major ore of iron and as mineral specimens

Magnetite is a natural magnet, hence the name, giving it a very nice distinguishing characteristic. Explaining the magnetism is not easy but here is a go at it. Remember, electricity produces magnetic fields just as magnetism produces electic fields. Magnetite is a member of the spinel group which has the standard formula $A(B)_2O_4$. The A and B represent usually different metal ions that occupy specific sites in the crystal structure. In the case of magnetite, Fe_3O_4, the A metal is Fe^{+2} and the B metal is Fe^{+3}; two different metal ions in two specific sites. This arrangement causes a transfer of electrons between the different irons in a structured path or vector. This electric vector generates the magnetic field.

2.7.1. Physıcal Characteristics

- Color is black.
- Luster is metallic to dull.
- Transparency: Crystals are opaque.
- Crystal system is isometric; 4/m bar 3 2/m
- Crystal habits are typically octahedrons, but rarely rhombododecahedron and other isometric forms, most commonly found massive or granular. Twinning of octahedrons into spinel law twins is seen occassionally.

- Cleavage is absent although octahedral parting can be seen on some specimens.
- Fracture is conchoidal.
- Hardness is 5.5 - 6.5
- Specific Gravity is 5.1+ (average for metallic minerals)
- Streak is black.
- Associated minerals are talc and chlorite (schists), pyrite and hematite.
- Other Characteristics: Magnetism stronger in massive examples than in crystals, striations on crystal faces (not always seen).
- Notable occurrences include South Africa, Germany, Russia and many locallities in the USA.
- Best field indicators are magnetism, crystal habit and streak.

2.7.2. Synthesis of Magnetic Polymer Nanoparticles

Recently, nanosized magnetic materials have gained increasing interest because of the development of nanotechnology [62]. Among these nanotechnology studies, polymer-blended magnetic materials are now extensively studied because of their high process ability, versatility, and lower cost. [63] However, there is indeed a major difficulty in obtaining well-characterized materials because of the assembly of the particles.

Ferrofluids or magnetic fluids are stable dispersions of ultrafine magnetic particles or encapsulated magnetic particles in an organic or aqueous carrier medium. The stabilization of these particles is achieved through a surfactant which hinders the particles from flocculation or sedimentation. Ideally, these particles remain uniformly dispersed in the carrier medium although they are or have been exposed to magnetic fields.

It is well known that magnetite crystals have an inverse spinel structure. It is also well known that magnetite is formed by Fe^{2+} and Fe^{3+} ions with a molar ratio of 1:2.

Since new synthetic approaches of nanoscaled magnetic particles are based on size distribution control and improved magnetic properties, functionalized polymers have been increasingly recommended as dispersing agents for

aggregates [64]. Coating and encapsulation of magnetic particles with natural polymers such as proteins and polyglucosides [65], synthetic ones such as polyelectrolytes [66] and non-ionic polymers bearing lateral functionality (PVA) [67] have been used in order to obtain colloidal suspensions. Polymers randomly adsorb on surface involve affinities to the surface. Homo- and co-polymers produce adsorbed layers which consist of segments laying flat on the surface, and non-adsorbed loops and tails which ensure electrosteric stabilization of the particles. However colloidal stabilization depends on polymer layer thickness and it is known that particle destabilisation may occur by the lack of layer thickness or by polymer bridging mechanism. Because of this limitation, the molecular weight has to remain moderate while a brush monolayer adsorbtion mode will better satisfy steric stabilization of dispersed particles.

The desire for robust encapsulation, control over the loading of magnetic nanoparticles within the polymer particles, and control over the size of the resulting magnetic polymer particles drives interest in precipitation, suspension, and emulsion polymerization methods. Recipes for the creation of monodisperse polymer latex and microspheres exist; heterocoagulation of nanoparticles [68] or the direct precipitation of magnetic materials [69] onto the surfaces of monosized latex results in magnetic latex, monodisperse in size. Further polymerization of a polymer layer to cap the latex surface creates hydrophobic [70] or hydrophilic [71] magnetic latex. Most often, such latex contains only small loadings of magnetic material; however, up to 24 wt% (6 vol%) magnetite has been demonstrated [71]. A commercially successful variation on this concept creates highly porous yet monosized latex, precipitates magnetic nanoparticles within the pores, and caps the pores with a polymer layer to seal in the magnetic particles [72]. Loadings of up to 30 wt% magnetic iron oxide result. The success of such methods is tempered by the complicated multistep processes required.

Rather than depositing magnetic particles on the surface of latex particles, uniformly dispersing the magnetic nanoparticles throughout the entire ensemble of latex particles should theoretically allow higher concentrations of nanoparticles per latex particle. A nonmagnetic and hydrophilic particle, silica, treated with coupling agent and dispersed in an ethanolic medium containing dissolved styrene monomers, becomes coated with hydrophobic polystyrene upon

polymerization. As clearly shown in these well characterized “dispersion polymerization” experiments, complete encapsulation of silica into latex, results under certain controlled conditions. Similarly, magnetic nanoparticles, treated with organic base, become coated with hydrophilic monomers in a “seed precipitation polymerization” [73]. However, polydisperse latex results and an incomplete characterization of the coated particles leaves questions open regarding the degree of encapsulation [73].

Magnetic polymer nanoparticles, which are usually dispersed in a carrier liquid, can be tailor-made depending on the final application. Several kinds of magnetic polymer nanoparticles have been produced from both natural and synthetic polymers with the intention to incorporate groups on the surface or to treat their surface to perform, for instance, selective separations.

Magnetic nanoparticles with polymer encapsulation can be produced by several methods:

Method 1

In early publications, magnetic fluids were produced by grinding magnetite with heptane or long chain hydrocarbon and a grinding agent, e.g., oleic acid. The most common method for the synthesis of magnetite particles is by coprecipitation from a solution of Fe(II) and Fe(III) salts using alkali metal hydroxide [74], Smaller and more uniform particles can be synthesized by using the microemulsion approach [75]. Magnetic fluids were produced by precipitation of an aqueous Fe^{3+}/Fe^{2+} solution with a base, coating these particles with an adsorbed layer of oleic acid and then dispersing them in a non-aqueous fluid. Both processes result in tiny magnetite particles, a surfactant coating these magnetite particles and a non-aqueous liquid carrier in which the hydrophobic magnetite particles will be dispersed. Obviously, the latter process is more feasible to apply in the production of more homogeneous magnetite particles.

Method 2

Other applications of ferrofluids rely on water as the continuous phase. An aqueous magnetic material suspension by the conversion of iron compounds to magnetic iron oxide in the aqueous medium under controlled pH conditions in presence of a petroleum sulfonate dispersant was produced [76]. Shimoiizaka *et.*

al. [76] developed a water-based ferrofluid from the oleic acid coated magnetite particles dispersed by an anionic or nonionic surfactant solution which is suitable to form a second surfactant layer.

Method 3

Polymer covered magnetic particles can also be produced by precipitation in situ of magnetic materials in the presence of polymer which acts as a stabilizer. In this way, magnetic polymer nanoparticles are produced in presence of the water-soluble dextran, polyethyleneimine, poly-(vinyl alcohol), poly(ethylene glycol), sodium poly-(oxyalkylene diphosphonates), and amylose starch. In all cases, the magnetic particles are surrounded by a hydrophilic polymer shell. In situ synthesis has the potential to control the mean particle size and size dispersion of the nanoparticle population. A further possibility might be to modify magnetic films and fibers by filling polymers that have high forming abilities with magnetite nanoparticles. Success in nanometric size control and homogeneous dispersion of particles easily leads to an easy preparation of magnetic materials with fine characteristics [76].

The hydrophilic magnetic latexes have been first reported by Kawaguchi et al. [78] by using acrylamide as the main monomer. The second type of hydrophilic magnetic particles has been reported by Sauzedde et al. using the Furazawa's methodology [78]. The hydrophilic thermally sensitive latexes have been obtained by encapsulating adsorbed iron oxide nanoparticles onto oppositely charged polystyrene-core/poly (N-isopropylacrylamide)-shell. The encapsulation has been performed using water-soluble monomers only (N-isopropylacrylamide, N, N'methylene bisacrylamide and itaconic acid). The final particles exhibit thermal-sensitive property. In addition, various original methods (via non-conventional polymerization) have been investigated using natural polymers or proteins. In this domain, various interesting papers have been reported such as cross-linked albumin magnetic microspheres and their uses in the separation of red blood cell from whole blood. It is worth noting that all reported methods in the elaboration of magnetic polymeric latexes lead to submicron particles size (generally above 500 nm) with appreciable iron oxide content. However, few works have been dedicated to the preparation of small hydrophilic magnetic polymeric latexes mainly appreciable in drug delivery domains [78].

An easy method for manufacturing homogeneous inorganic– organic materials, especially composite fibers, was obtained by the in situ synthesis of inorganic particles within polymer matrices have also been reported by Hai Lin and his coworkers. Nanosized magnetite particles were synthesized in situ within poly(vinylalcohol) (PVA) solutions by precipitating Fe^{2+} ions or a mixture of Fe^{2+} and Fe^{3+} ions with NaOH solution. As a result, magnetite particles with an average diameter of 20 nm were obtained homogeneously within the solutions because of the tridimensional structure and chelating capacities of PVA. In this study, the synthesis was conducted at 60°C in view of the solubility of PVA. Transparent films were obtained by a casting method, and six kinds of magnetic PVA fibers were also prepared by a wet-spinning method from the solutions containing magnetite nanoparticles. The mechanical properties and the saturation magnetization of the fibers were measured. These fibers, which contain iron ions with a maximum content of 17.63 wt %, can be successfully fabricated by the in situ synthesis and they exhibit excellent magnetization properties (i.e., the largest saturation magnetization is 13.38 emu/g) [79].

Ugelstad and coworkers were the pioneers to obtain monodisperse magnetic polymer microparticles by precipitation in situ of magnetic oxides inside preformed porous mono-sized polymer particles, taking account the microparticles used as seed (0.5–1 mm) contain metal-binding groups [79]. Magnetic polymer microparticles (0.5–100 mm) with high degree of monodispersity and up to 35% of iron as magnetic oxides were obtained. It is important to stress that although Ugelstad's work it is to be consider a great contribution in the magnetic carrier technology nevertheless our focus is addressed to the production of nano-sized magnetic polymer particles (50–500 nm) meanwhile his work was emphasized to produce microparticles. The methodology used by Ugelstad et al. is basically based on direct precipitation of iron salt inside in the pores of the porous polystyrene seed for the preparation of hydrophobic monosized polystyerene magnetic particles. The particles obtained exhibit large particles size (i.e. 2.8 and 4.5 mm) with a good magnetic separation [79].

Colloidal dispersion of magnetite nanoparticles via in situ preparation with sodium polyoxyalkylene di-phosphonates have also been reported by Pierre le

Perchec. In this study, hydrosoluble polymers attached to inorganic surfaces allow production of dispersed state particles. Functionalized end-chain polymers were used to prepare stable aqueous magnetite colloidal dispersions. The magnetite nanoparticles were synthesized from coprecipitation of aqueous Fe^{3+} and Fe^{2+} ions in the presence of sodium polyoxyalkylene di-phosphonates. Transmission electron microscopy (TEM), dynamic light scattering (DLS), pyroanalysis techniques and isotherm determinations are reported to characterize the nanosized particles. Because of the structure of the interface with the polymer tightly anchored to the surface and the biocompatibility of the polyoxyalkylene chain, new developments might be found in the forthcoming time. Recent work has shown that strongly adsorbed monolayer on particles can be obtained from end-chain functionalized nonionic polymer. This block co-polymer is segmented into one strongly adsorbed group and a hydrosoluble nonadsorbed chain. We report on the use of such synthetic hydrosoluble polymer end-chain groups as a dispersing agent for magnetite particles. Polyoxyalkylene di-phosphonates used in this paper have been prepared starting either from primary aminopolyoxyalkylene issued by anionic polymerization of ethylene oxide initiated by potassium aminoalkylalcoholate or from commercially available monofunctionalized Jeffamine®. The di-phosphonate derivatives were prepared by means of the Mannich–Modritzer reaction. The following nonionic water soluble polymers containing di-phosphonate sodium groups at chain-end have been used for the production of magnetite nanoparticle dispersion:

$R_2\text{-}(O\text{-}CH_2\text{-}CH(R_1))_n\text{-}N\text{-}(CH_2PO_3H_2)_2$	n =	20	50	70
	R_1	H; CH_3	H	H; CH_3
	R_2	CH_3	H	CH_3

Figure 2.27: Represantation of nonionic water soluble polymers containing di-phosphonate sodium groups at chain-end.

TEM analyses allowed us to follow the efficiency of the polymer contribution on the dispersion state of the magnetite particles in water. The more the polymer concentration in water solution increases the more the aggregate size decreases allowing the production of stable dispersed magnetite particle suspensions. The analysis was completed from high resolution TEM microscopy pattern which led to precise and accurate determination of the morphological parameter of the

particles. At the magnification G=200000, it is shown that particles have narrow size distribution between 5–10 nm. The assembly looks like chaplet wires of light density material; although single particles appear well defined in size. DLS analyses have confirmed the production of self-assembly dispersed particles since the apparent particle size lay down from 22 to 40 nm. At low polymer concentrations C_i<3 mmol l^{-1}, two domains of size particles were found while at upper polymer concentrations Ci>8 mmol l^{-1}, a simple distribution was observed. In case of C_i=10 mmol l^{-1}, a narrow single distribution was observed with an average particle size of 30 nm [80].

Polymers with a tridimensional structure, especially chelating resins, such as derivatives of polystyrene, poly(vinyl pyridine), polyimine, and poly(vinyl acetate), have rigid pores that set upper limited inside growth space to the particles. One convincing reason for the formation of the tridimensional structure is the crosslinking reactions formed by coordinate bonds between the polymers and metal ions contained in particles. By this in situ synthesis of inorganic particles within polymer matrices, homogeneous inorganic– organic materials can be obtained easily. Among chelating resins, poly(vinyl alcohol) (PVA) has lately drawn considerable attention because of its capabilities of chelating hydroxyl groups to retain metal ions and hydrogen bonds leading to a tridimensional structure [79].

Method 4

Another method to produce magnetic polymer particles consists of the synthesis of magnetic particles and polymer particles separately and then mixing them together to enable either physical or chemical adsorption of the polymer onto the material magnetic. The polymer material can be produced by different ways, for instance by emulsion or precipitation polymerization. [79]

Method 5

Polymerization in direct miniemulsion can be used for the efficient encapsulation of water-insoluble materials in hydrophobic polymers to obtain hybrid particles which are homogenous in their size.

Direct miniemulsions are understood as stable aqueous dispersions of oil droplets having a size between 50–500 nm prepared by shearing a system containing oil,

water, a surfactant, and a highly water insoluble compound, the so-called hydrophobe which suppresses Ostwald ripening of the droplets. For the encapsulation process, the encapsulating material is dispersed in the monomer phase prior to miniemulsification. This strategy was also already used for the encapsulation of hydrophilic magnetite into polystyrene. To obtain a successful encapsulation, the magnetite aggregates have to be hydrophobized in order to make them dispersable in hydrophobic monomers such as styrene. A mixture of magnetite particles in styrene was miniemulsified in water and after polymerization, polymer encapsulated magnetite particles were obtained. However, the distribution of the magnetite in the polystyrene nanoparticles was still inhomogeneous, and the magnetite content in the polystyrene matrix was limited to 15 wt % [76].

Katharina Landfester has also developed a new 3 step route for the production of polymeric magnetic nanoparticles. The work has been based on miniemulsion processes for the production of aqueous ferrofluids consisting of uniform and stable magnetic polystyrene nanoparticles, which are highly homogeneous and possess high magnetite contents up to 40 wt.-%. The encapsulation of high amounts of magnetite into polystyrene particles can efficiently be achieved by a new three-step preparation route including two miniemulsion processes. In the first step, a dispersion of oleic acid coated magnetite particles in octane is obtained. In the second step, magnetite aggregates in water are produced in a miniemulsion process by using sodium dodecyl sulfate (SDS) as surfactant. In the third step, the dispersion with the magnetite aggregates which are covered by an oleic acid/SDS bilayer were mixed with a monomer miniemulsion and a second miniemulsion process, an ad-miniemulsification process, is used to obtain full encapsulation. After polymerization, polymer encapsulated magnetite aggregates having a particle size of about 60 nm were obtained. The weight-average molecular weight of the polymer formed in the particles was determined to be about 210.000 $g \cdot mol^{-1}$ which indicates that the presence of magnetite in the polystyrene does not have any effect on the final weight-average molecular weight of the polymer. Characterization by thermogravimetry, preparative ultracentrifugation, and transmission electron microscopy showed that up to 40% magnetite could be encapsulated resulting in particles with a high homogeneity of

the magnetite content. Magnetometry measurements reveal that the included iron oxide aggregates still consist of separated superparamagnetic magnetite particles [76].

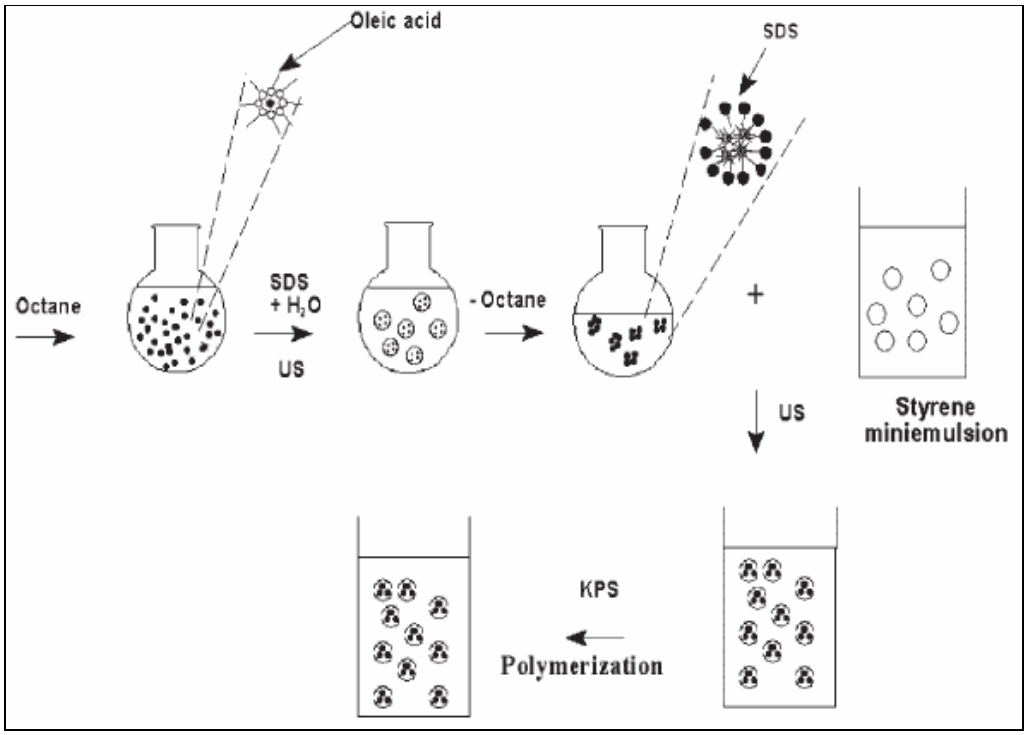

Figure 2.28: Formulation of polymer coated magnetite particles with high magnetite ratio.

In the first step, hydrophobized magnetite particles are produced and in a second step transferred to magnetite aggregates in water by using the miniemulsion process. In a third step, the principle of co-miniemulsion is used. The controlled fission/fusion process in the miniemulsification realized by high energy ultrasound or high pressure homogenization destroys all aggregates and liquid droplets, and only hybrid particles being composed of magnetite and monomer remain due to their higher stability [76].

It has also been reported by Wang and Chiu that magnetic poly(methyl methacrylate) (PMMA)/poly(methyl methacrylate/co-methacrylic acid) [P(MMA–MAA)] composite polymer latices were synthesized by two-stage soapless emulsion polymerization in the presence of magnetite (Fe_3O_4) ferrofluids. Different types and concentrations of fatty acids were reacted with the Fe_3O_4 particles, which were prepared by the coprecipitation of Fe(II) and Fe(III) salts to obtain stable Fe_3O_4 ferrofluids. The Fe_3O_4/polymer particles were monodisperse, and the composite

polymer particle size was approximately 100 nm. The morphology of the magnetic composite polymer latex particles was a core–shell structure. The core was PMMA encapsulating Fe_3O_4 particles, and the shell was the P(MMA–MAA) copolymer. The carboxylic acid functional groups (COOH) of methacrylic acid (MAA) were mostly distributed on the surface of the composite polymer latex particles. Antibodies (antihuman immunoglobulin G) were then chemically bound with COOH groups onto the surface of the magnetic core–shell composite latices through the medium of carbodiimide to form the antibody-coated magnetic latices (magnetic immunolatices). The MAA shell composition of the composite latex could be adjusted to control the number of COOH groups and thus the number of antibody molecules on the magnetic composite latex particles. With a magnetic sorting device, the magnetic immunolatices derived from the magnetic PMMA/P(MMA–MAA) core–shell composite polymer latex performed well in cell-separation experiments based on the antigen–antibody reaction.

Daniel and coworkers [76] obtained magnetic polymer particles by dispersing a magnetic material in an organic phase which consists of an organo-soluble initiator, vinyl aromatic monomers and/or a water insoluble compound. The mixture was emulsified in water by using an emulsifier and then polymerization took place in order to obtain polymer particles with a magnetite content between 0.5 and 35 wt.-% with respect to the polymer.However the resulting particle size distribution was rather broad (between 30–5 000 nm). Charmot and Vidil [76] used a similar method to produce magnetizable composite microspheres of a hydrophobic crosslinked vinylaromatic polymer, but they obtained a mixture of magnetizable particles and nonmagnetizable blank microspheres.

Method 5

It is also possible to use a strategy comprising the polymerization in heterophase in the presence of magnetic particles (preparation by inverse microemulsion or inverse miniemulsion process). The magnetic material preferably having a surfactant coated is embedded into a polymer using processes such as the suspension, the emulsion, or the precipitation polymerization. Magnetic particles were encapsulated in hydrophilic polyglutaraldehyde by suspension polymerization resulting in particles with an average diameter of 100 nm [76]. Magnetite containing nanoparticles of 150 to 200 nm were also synthesized by seed precipitation polymerization of methacrylic acid

and hydroxyethyl methacrylate in presence of magnetite particles containing tris(hydroxymethyl)aminomethane hydroxide in ethyl acetate medium [81]. Polymethacrylate/poly (hydroxymethacrylate) coated magnetite particles could be also prepared by a single inverse microemulsion process, leading to particles with a narrow size distribution, but only with a magnetite content of 3.3 wt.-% [82].

Another work has been reported by Fu et al. [78]. Hydrophilic submicron magnetic polymeric particles were prepared using inverse microemulsion polymerization process. Firstly, the magnetic properties of iron oxide nanoparticles elaborated were examined using X-ray diffraction and magnetization analysis of the chemical structure and the magnetic properties, respectively. The results obtained using stoichiometric precipitation of $FeCl_2$ and $FeCl_3$ revealed the magnetite iron oxide properties. Secondly, various magnetic polymeric latexes such as polyacrylamide latex were prepared by investigating the effect of surfactant (AOT) concentration, the amount of cross-linker (MBA), the initiator nature and the microemulsion elaboration methodology. The colloidal characterization of the final magnetic polymeric latexes revealed to be submicronic in size, spherical in morphology, containing 5–23wt% iron oxide and superparamagnetic in character. In this study firstly, Am and MBA were added to the iron oxide suspension previously synthesized (6%wt) in a desired proportion to form a stable colloidal dispersion, then added to an AOT-toluene solution to form a W/O microemulsion in ultrasonic bath. The microemulsion was then purged with nitrogen for 30 min. The polymerization of monomers (Am and MBA) was carried out with AIBN or V50 at 601C. The microemulsion is stable and has a black–red transparent color. A slight change in the color aspect of the microemulsion is observed a few minutes after the initiation of the polymerization. The final magnetic polyacrylamide latex with black–red color remained stable for several months without visible sedimentation. The influence of the AOT/H_2O ratio and the type of initiators applied on the final magnetic polymeric latex particle morphology, size and size distribution have been investigated [78].

Due to the different nature of AIBN and V50, two different polymerization mechanisms are possible during the polymerization. When AIBN is used, the polymerization was initiated principally from the organic phase. The formed radicals induce radical polymerization via the entry mechanism process. The Am monomer, which slightly dissolved in toluene, continuously deposited onto the latexes particles

during polymerization process. However, in the case of water-soluble initiator (V50), the polymerization starts in aqueus phase via classical emulsion polymerization process. In this study, two methods (i.e. phase inversion method and precipitation–redispersion process) are applied to disperse polyacrylamide magnetic particles in aqueous solution from W/O latexes. It is found that the particle size and size distribution of the magnetic polymeric particles prepared by two methods are different. When the phase reversion method was applied, the magnetic particles have DH values ranging from 80 to 180 nm (when AIBN was used), depending on the AOT/H_2O ratio and MBA amount. In fact, the average particle size (DH) decreases when the AOT/H_2O ratio or MBA concentration increase). The behavior observed is mainly attributed to the reduction of particle size with increasing AOT/H_2O by affecting the microemulsion surface tension as is well known in such polymerization process. When the concentration of MBA increases, the cross-linking density of the polymer particles also increases and consequently, the particles are more difficult to be swollen by water [78].

However, when the precipitation–redispersion method is applied, the particle size of the magnetic polymeric range from 140 to 300 nm, which is much larger than those prepared via phase inversion process, and found to be unrelated to AOT/H_2O ratio and the concentration of MBA . The observed behavior may be attributed to the influence of precipitation–redispesion and dryness on irreversible aggregated particles formation which induces uncertain particle size measurement. In fact, the large clusters formed during the process are difficult to be redispersed [78].

In addition to hydrophobic initiator AIBN, a water-soluble initiator 2,20 azobis-amidinoptopane di-hydrochlorides (V50) was also used in such W/O microemulsion polymerization. DLS analysis showed that the hydrodynamic diameter (DH) value of the latex (sample 1128A) obtained is about 76nm (Fig. 6A), which is of the same range as that of sample 1201A. The method of phase inversion was also performed on sample 1128A, and it is found that the DH value of the swelled particles is about 260nm (Fig. 6B), which is much larger than the size of the swelled sample 1201A with AIBN as initiator. Such a size difference between the two swelled magnetic polymeric particles is due to the fact that V50 is a charged initiator. The distrubution of the positive charges in the polyacrylamide matrix may enhance the swelling ability of the magnetic particles via intraelectrostatic repulsion and hydration

process, and consequently large hydrodynamic size was obtained after phase inversion [78].

A related method polymerizes emulsion droplets of styrene in the presence of an aqueous dispersion of surfactant-coated magnetic nanoparticles to yield magnetic latex [83]. To facilitate transfer of the inherently hydrophilic magnetic particles into the styrene and allow encapsulation, a double layer of surfactant (sodium oleate combined with sodium dodecyl benzene sulfonate) coats the magnetic nanoparticles. The method yields up to 20 wt% magnetite encapsulated into polystrene latex; however, polydisperse latex forms in the presence of sometimes large amounts of coagulant [83].

The dispersion polymerization or emulsion polymerization in the presence of surfactant-coated particles carries the risk of incomplete and nonuniform encapsulation. Reaction conditions must drive all the magnetic particles to transfer uniformly into the resulting polymer particle [83], or the magnetic particles must provide the only site for precipitation of polymer [81].

Oneway to potentially guarantee the uniform loading of magnetic particles into latex would be to directly disperse the magnetic particles into the monomer of interest, emulsify, and then polymerize. Surprisingly, a comprehensive search of the literature yielded a few patents and a mild scientific interest in nonmagnetic pigments [84] though no papers that carefully examine this potentially elegant and direct approach. Certainly in an aqueous medium, such an approach requires dispersion of high concentrations of hydrophilic magnetic particles into droplets of hydrophobic monomers—a difficult challenge. However, dispersion of significant amounts of magnetic iron oxide into hydrophilic monomers, “inverse” emulsification of this sol into oil, and subsequent polymerization would likely be easier. In addition, the method might lead to biocompatible magnetic latex in one step. In this paper, we describe how magnetic latex results from this inverse emulsion polymerization approach.

A related approach exploits the cross-linking of polymers, rather than the polymerization of monomers, to create biocompatible magnetic particles. First, the application of mechanical energy creates a dispersion of magnetite in the presence of aqueous albumin [85], chitosan [86], or polyvinylalcohol [87] polymers. The

addition of further energy creates an emulsion of the magnetic particle sol in cottonseed [85], mineral [86], or vegetable oil [87]. Depending upon composition and reaction conditions, addition of cross-linker and heat results in magnetic latex, 0.3 to 30 microns in average diameter, polydisperse in size, with up to 24 wt % magnetite [85]. Theoretically, the insolubility of the polymer and magnetic particles in the oil continuum should guarantee uniform loading of magnetite per latex; however, no proof is provided. Since significant amounts of water reside in the droplets during cross-linking, and nothing chemically binds the magnetic particles to the polymer matrix, questions arise as to the permeability of the resulting latex and the potential for leaching magnetite out of the latex.

Denser coatings around the magnetic particles may result from "inverse" emulsion polymerization of hydrophilic monomers around magnetic particles. Recent work exploits the properties of inverse microemulsions, thermodynamically stable mixtures of water in inverse micelles, to create magnetic latex. Upon polymerizing acrylamide monomers microemulsified in oil, 40-nm-diameter polyacrylamide latex results [88]. Upon microemulsifying and precipitating iron salts within the water droplets in microemulsions, magnetic nanoparticles result [89]. A combination of the two approaches results in magnetic nanoparticles encapsulated in hydrophilic polymers, with average diameters ranging from 80 to 320 nm [86]. However, the relatively polydisperse latex contains only contain 3.3 wt% (0.6 vol %) magnetic particles.

Greater concentrations of magnetic particles might arise using the larger droplets in inverse emulsions, created by using relatively low amounts of surfactant, as opposed to the nanodroplets in inverse microemulsions, created with significantly larger amounts of surfactant. First proposed by Vanderhoff et al. [86], polymerization of inverse emulsions yields latex from monomers such as acrylamide [90] and if tuned properly results in 100 nm diameter and narrowly distributed polyacrylamide latex [91] or similarly sized polyacrylic acid latex [92]. In recent work, polymerization of inverse "miniemulsions" of acrylamide, neutralized polyacrylic acid, or hydroxyethylmethacrylate also yields latex in the 80- to 160-nm size range [93]. Application of these "inverse" emulsion polymerization methods as a method to encapsulate magnetic particles remains unexplored.

Wormuth [86] used the inverse miniemulsion process [81] to encapsulate magnetic particles by a hydrophilic polymer. It has been reported that, The structure-directing nature of block copolymers, combined with the "miniemulsion" polymerization process, facilitate synthesis of superparamagnetic latex loaded with nanometric magnetic iron oxide. A "double-hydrophilic" diblock copolymer (polyethylene oxide block-co-polymethacrylic acid), present during the precipitation of magnetic iron oxide, directs nucleation, controls growth, and sterically stabilizes the resulting 5 nm superparamagnetic iron oxide. After drying, the coated particles spontaneously repeptize into a mixture of hydroxyethylmethacrylate and methacrylic acid monomers, creating a ferrofluid-like dispersion. Inverse emulsification of the ferrofluid (magnetic particles plus monomer) into decane, aided by small amounts of diblock copolymer emulsifier along with ultrasonication, creates minidroplets (180 nm) filled with magnetic particles and monomer. Subsequent polymerization generates magnetic latex. Extensive characterization by scanning electron microscopy, transmission electron microscopy, dynamic light scattering, thermogravimetric analysis, magnetic measurements, and x-ray diffraction shows complete and uniform encapsulation of 5 nm magnetic iron oxide into latex of average diameter between 140 and 220 nm depending upon emulsifier (poly(ethylene-co-butylene)-b-poly(ethylene oxide) concentration. The magnetically active latex contains 18 wt% magnetic iron oxide coated with hydrophilic polymers. In a minimum number of steps, the direct dispersion of magnetic particles in monomer and inverse miniemulsification process generates hydrophilic magnetic latex. The stability of the inverse emulsions examined here, sterically stabilized by the PBE block of the PBE-PEO emulsifier, depends upon the strength of the steric repulsive force, which in turn depends upon the molecular weight of the PBE block, the concentration at the interface, and the solubility of the PBE block in decane at the temperature of interest. Given the significant concentration of droplets in the emulsion (10 vol%), collisions likely occur during polymerization. The saturation magnetism found for the latex is 10 emu/g of total latex solids, which, when converted using the TGA-determined value of the iron oxide content (18 wt%), yields a value of 55 emu/g for the inorganic solids within the latex. The value is8%lower than that found prior to polymerization (60 emu/g); however, given the errors in determination of the magnetic properties (5%) combined with the error in

determining the iron oxide content via TGA (3%), the apparent decrease in saturation magnetism may not be significant.

A novel approach to prepare magnetic polymeric nanoparticles by synthesis of the magnetite core and polymeric shell in a single inverse microemulsion is reported by Zaitsev and his coworkers [82]. Stable magnetic nanoparticles colloid dispersion with narrow size distribution can thus be produced. The microemulsion seed copolymerization of methacrylic acid, hydroxyethyl methacrylate, and cross-linker results in a stable hydrophilic polymeric shell of the nanoparticles are available. The preparation of the nanoparticles was carried out also by the two-stage microemulsion process and the seed precipitation polymerization. The particle size was varied in the range 80-320 nm by changing of the monomer concentration and water/surfactant ratio. The magnetic properties and the size distribution of the nanoparticles synthesized by these three methods were compared. The polymeric nanoparticles synthesized in single microemulsion have superparamagnetic properties and the narrowest size distribution.

2.7.3. Synthesis of Polymeric Magnetic Particles by Seed Precipitation Polymerization

The magnetite particles (1 wt %) were dispersed in ethyl acetate. The polymerization of monomers was carried out with AIBN [82].

2.7.4. Synthesis of Polymeric Shells with Previously Synthesized Magnetite Particles in Microemulsion

The microemulsion was prepared by adding an aqueous suspension of previously synthesized magnetite particles (0.45 wt %), in some cases with a hydrophilic initiator,to a solution of methacrylic acid, hydroxyethyl methacrylate(MAA/HEMA)9:1 molar ratio), cross-linker,and AOT in toluene in the chosen proportions. Water/AOT/toluene ratio was 2:5:25 by weight. The monomer concentration was about 2.3 wt % with a cross-linker/monomer molar ratio of 1:200. The microemulsion was then purged with nitrogen for 45 min, and a hydrophobic initiator (0.2 wt %) was added to the solution in toluene. The polymerization of monomers was carried out with either AIBN or potassium persulfate at 55 °C [82].

2.7.5. Synthesis of Magnetite and Polymeric Magnetic Particles in the Same Microemulsion

First, the magnetite particles were synthesized by microemulsion method. Then, water, monomers (MAA/HEMA) 9:1 molar ratio), cross-linker, and an initiator were added to the reaction mixture in the desirable proportion under nitrogen. Several ratios of water/AOT were used. The polymerization of monomers was carried out withAIBN at 55 °C [82].

Dynamic light scattering was used to obtain information on the average size and size distribution of polymeric magnetite particles [82].

DLS studies have shown that the microspheres obtained had RH values ranging from 90 to 320 nm, depending on the water/AOT ratio. These particles have a very narrow size distribution when compared with that of a "monodisperse" polystyrene latex suspension that is often used as a reference standard [82].

The saturation magnetization was found to be equal to 2.72 emu/g, representing a magnetic content of 3.3 wt % by using the reference value for the previously synthesized pure magnetite particles of 81 emu/ g. It is superparamagnetic.

The magnetite particles synthesized in solution and in microemulsion showed fairly narrow size distributions [82].

Polymerization in microemulsions offers the most promising versatile technique for the synthesis of a wide variety of polymeric nanoparticles with the ability to control precisely both the size of the core and that of the particles formed. In this respect, microemulsions offer the best reaction media utilizing the small size and uniform distribution of the microdroplets to produce ultrafine particles. The polymeric shell size can be controlled in the range 80-320 nm by varying the size of the microdroplets. The technique of synthesizing a core and a shell in a single microemulsion has improved the particle structure and size distribution. New magnetic hydrogel particles, made of a superparamagnetic magnetite core coated with a polymeric shell of PMA-PHEMA random copolymer, have been synthesized. The smallest radius for the polymeric magnetite particles that had been synthesized was about 160 nm, with a magnetite concentration as high as 3.3 wt % [82].

According to Jiaguo Deng and his coworkers study magnetic and conducting Fe_3O_4–polyaniline (PANI) nanoparticles with core–shell structure have been prepared in the

presence of Fe_3O_4 magnetic fluid in aqueous solution containing dodecylbenzene sulfonic acid sodium salt (NaDS) as a surfactant and dopant. The conductivity of the composites at room temperature depended on Fe_3O_4 content and doping degree. The magnetic properties of the resulting composites showed ferromagnetic behavior, such as high-saturated magnetization (Ms = 4.22–48.4 emu/g) and high coercive force (Hc = 8–55.3 Oe). The saturated magnetization increased with the increasing Fe_3O_4 content. A structural characterization by elemental analysis, Fourier transform infrared, transmission electron micrograph (TEM) and powder X-ray diffraction (XRD), proved that nanometer-sized Fe_3O_4 (20–30 nm) in the composites was attributed to the ferromagnetic behavior of the composites. The average size of Fe_3O_4–polyaniline nanoparticles with core–shell structure was about 80 nm, and polydisperse. The results of TG, IR and UV spectra indicated that Fe_3O_4 nanoparticles could improve the composite thermal stability possibly due to the interaction between Fe_3O_4 particles and polyaniline backbone. In this study they have been presented a novel approach to synthesize core–shell Fe_3O_4–PANI nanoparticles, where Fe_3O_4 is the magnetic core, and PANI is the conducting shell. The Fe_3O_4 nanoparticles primarily prepared by precipitation–oxidation method, and the Fe_3O_4–PANI nanoparticles with core–shell structure is synthesized via an in situ polymerization of aniline monomer in an aqueous solution, which contains well-dispersed Fe_3O_4 nanoparticles and surfactant NaDS. The influence of Fe_3O_4 content with respect to the electrical and ferromagnetic properties of PANI composite has been investigated. The origin of their electrical and ferromagnetic properties is also discussed based on the structural characterizations including elemental analysis, transmission electron micrograph (TEM), Fourier transform infrared (FTIR), ultra-visible spectrum (UV), X-ray diffraction (XRD), thermogravimetric analysis (TG) [94].

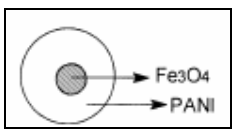

Figure 2.29: The structure of Fe_3O_4-PANI nanoparticle.

Another study by Jianguo Deng and his coworkers have also been carried out. Acorrding to this study, magnetic and conducting Fe_3O_4-cross-linked polyaniline

(CLPANI) nanoparticles with core-shell structure have been prepared in the presence of magnetic fluid in aqueous containing polyethylene glycol as a surfactant. The magnetic properties of the resulting composites showed ferromagnetic behavior, such as high saturated magnetization (M_s=4.22-19.22 emu/g), and coercive force (H_c=2-8 Oe). The saturated magnetization increased with the increasing Fe_3O_4 content. Th conductivity of the composites at room temperature depended on the Fe content and doping degree. A structural characterization by elemental analysis, Fourier transform infrared, transmission electron micrograph (TEM) and X-ray diffraction proved that nanometer-sized (about 10 nm) Fe_3O_4 in the composites was responsible for the ferromagnetic behavior of the composites. The average size of Fe_3O_4-CLPANI nanocomposites with core-shell structure was about 40 nm, and polydisperse. The results og TG, IR and UV spectra indicated that the Fe_3O_4 particles could improve the composite thermal stability due to interaction between the Fe_3O_4 particles and CLPANI polymer backbone [94].

2.7.6. Applications of Magnetic Polymeric Particles

2.7.6.1. Biomedical Applications

Magnetite (Fe_3O_4), due to its strong magnetic properties, was used first in biology and then in medicine for the magnetic separation of biochemical products and cells as well as the magnetic guidance of particle systems for site-specific drug delivery[3]. The use of superparamagnetic iron oxide as a contrast agent for magnetic resonance imaging (MRI) has been the subject of extensive studies over the past decade. Magnetite particles have nearly a 50-fold greater magnetic susceptibility than gadolinium chelates approved for use in MR imaging. However, the size, charge, and surface chemistry of magnetic particles could strongly influence their biodistribution. Another important point is that the magnetic properties depend strongly on the size of the magnetite particles. An advance in the use of magnetic particles for medical applications depends on new synthetic methods with better control of the size distribution and of particle surface properties. The wellknown microemulsion synthesis of polymeric microspheres was used on one occasion to develop magnetic particles, but they were in the micron size range [82].

Magnetic polymer nanoparticles should fulfill some criteria to fit further biomedical application: no sedimentation, uniform size and size distribution, high and uniform

magnetic content, superparamagnetic behavior, no toxicity, no iron leaking, high selectivity in case that these particles are used for hyperthermia purposes, and sufficient heat generation at lower frequencies to enhance selective heating. Therefore, magnetite particles homogeneously encapsulated in a hydrophobic polymer which keep away water-soluble components from contacting the magnetite particles are of high interest [76].

There are several reasons to use polystyrene as hydrophobic encapsulation material in biomedical applications, e.g., it is inexpensive and it is a hydrophobic polymer which allows physical adsorption of antibodies or proteins, it can also be functionalized, e.g., by carboxylic groups which enables covalent binding of antibodies, proteins, or cells [76].

In recent years, magnetic polymeric particles (i.e. polymer composites), due to their relatively rapid and easy magnetic separation, have been used in biomedical and bioengineering such as cell separation, immunoassay and nucleic acids concentration. In addition, magnetic polymeric particles offer a high potential in several areas of application such as detoxification of biological fluid and the magnetic guidance of particle systems for specific drug delivery process [76].

So as to investigate the temperature dependence of the magnetic resonance field and the resonance linewidth of magnetite nonoparticles in a copolymer matrix, the mesoporous Sty-DVB copolymer particles used as the template were prepared by suspension polymerization in the presence of inert diluents, as described elsewhere. The copolymer was sulfonated using concentrated sulfuric acid in the presence of dichloroethane. The composite sample preparation follows a three step procedure. First, the sulfonated resin is dispersed in aqueous solution of ferrous sulfate, with iron (II) concentration running in the range of to mmol/L. Second, the polymer particles were separated by filtration and washed with water until no iron is detected in the eluent. Third, alkaline oxidation of iron (II) is performed using a mixture of potassium hydroxide and sodium nitrate, following the standard recipe used to synthesize magnetite microcrystals. Finally, a black and strongly magnetic composite is obtained after the third step. The synthesized composites were characterized by X-ray diffraction. Magnetic resonance measurements were performed in the range of 100–260 K, using a commercial Bruker ESP200 X-band spectrometer. The

resonance data has indicated that the nanoparticle average diameter (D) increases as iron (II) concentration increases [95].

In special, magnetic nanoparticles with or without polymer encapsulation can be used as magnetic drug targeting, tissue engineering, magnetic resonance imaging, and hyperthermia [76].

Ideally, magnetically active particles applicable in separation processes should be larger units composed of a high concentration of superparamagnetic nanoparticles, with each of the larger entities monodisperse in size and uniform in magnetic particle concentration. Magnetically inactive "duds" reduce separation efficiency. Proper encapsulation of the magnetic nanoparticles protects them from degradation and endows biocompatibility. However, a survey of the scientific literature shows rare achievement of such ideal particles, and achievement only occurs using complicated multistep processes. In much of the published literature, questions remain as to the completeness of encapsulation and homogeneity of size and pigment loading achieved [86].

These medical applications require biocompatibility. Highly magnetic materials such as cobalt and nickel, toxic and susceptible to oxidation, remain of little interest. However, even particulate magnetic iron oxide (magnetite or maghemite) must first be coated for biocompatibility. Hydrophilic organic coatings such as albumin, dextran, or hydroxethylmethacrylate often enhance biocompatibility [86].

Furthermore, medical applications require particles with magnetism that turns "on" upon application of a strong magnetic field and turns "off" upon removal of the field. Superparamagnetic particles fulfill this requirement, but superparamagnetism only occurs with magnetic iron oxide particles smaller than 10 nm in diameter. Endowed with unique magnetic properties, superparamagnetic nanoparticles find great scientific interest in the form of ferrofluids and in mesoscopic magnetic composites. To increase magnetic activity, many of these nanomagnets must first be gathered together into one larger particulate entity [86].

2.7.6.2. Electronic Applications

Well dispersed magnetic particles have also been found of great interest for magnetic tape, disks and toner in laser printing [80]. There are also several applications for

mechanical and electrical devices which take advantage of the magneto-rheological properties of ferrofluids, e.g., in loudspeakers, seals, sensors, dampers, etc.

Encapsulation of inorganic pigments into organic polymers endows pigments with important properties that bare uncoated pigments lack. Polymer coatings on pigments enhance compatibility with organic ingredients, reduce susceptibility to leaching, and protect pigment surfaces from oxidation. Consequently, encapsulation improves dispersibility, improves chemical stability, and reduces toxicity. Therefore it is not surprising that polymercoated pigments find great interest in the preparation of paint, ink, pharmaceutical, and cosmetic formulations. One class of pigments, magnetic particles, generates interest in traditional applications such as magnetic recording, though new applications in the medical field currently demand attention. In vitro applications such as separation, purification, and immunoassay methods rely on coating magnetic particles with proteins or monoclonal antibodies which endow the particles with the ability to bind to the specific cancer cell, DNA fragment, or enzyme of interest and remove that entity from the fluid upon application of a magnetic field. In vivo, small magnetite particles enhance image contrast in magnetic resonance methods (MRI) magnetic fields guide magnetic particles with attached anticancer drugs toward tumors, and high frequency magnetic fields heat up magnetic particles attached to a tumor, destroying the tumor tissue ("intercellular hyperthermia") [86].

One of the useful magnetic materials may be magnetic fiber. Magnetic fibers are used for applications such as magnetic paper, health-care cloth, magnetic filters, electromagnetic wave adsorbents, and various other application because of their high forming abilities. Preparation of magnetic fibers has been reported by coating magnetite particles on the surface of pulp, cellulosic fibers, and spider silk [79].

In 1984, Abe et al. reported that the magnetic Fe_3O_4 film could be anodic-oxided from aqueous solution at relatively low temperature ($T < 80^0C$). This technique removed the high heat resistance restriction of the substrate, and their research encouraged us to synthesize doubly-functionalized magnetic-conducting polymer composite film with both high conductivity and ferromagnetic properties by means of the technique anodic-oxidation. To their knowledge, no similar results have been reported [96].

Since the anodic oxidation was applicable only to conductive substrate, and the key of this method is to choose a conducting polymer which is very stable in water and elavated temperatures during the process of electropolymerization of the conducting polymer materials investigated, heavily doped PPy film (especially when m-sulfobenzoic acid is used as dopand) exhibits good stability and high conductivity (about 10^2 S cm^{-1}) in air, elevated temperatures even in the reductive agent (such as NH_4OH). For this reason, the doped PPy film was chosen as a conductive substrate on which Fe_3O_4 particles were electrodeposited [96].

It was described in Abe's work that the good quality magnetite film could not be electrodeposited directly on the metal electrodes until the surfaces of working electrodes were oxidized or covered with some intermediate layer. However, in this work, magnetite film could be electrodeposited on the PPy film with a mirror-like surface and exhibited strong adhesive, it could not be scratched by a nail or knife. According to the theory provided by Abe, the formation reaction of magnetite films could be illustrated as the following process:

$$x\mathrm{FeOH}^{2+} + y\mathrm{FeOH}^{+} + z\mathrm{FeOH}^{(n-1)+} + \mathrm{OH}^{-} \rightarrow (\mathrm{Fe}^{3+}, \mathrm{Fe}^{2+}, \mathrm{Fe}^{n+})_3\mathrm{O}_4 + 4\mathrm{H}^{+} (x + y + z = 3)$$

And it could be assumed here that it was the polar group of the PPy film surface (such as NH-) enhanced the adsorbing of magnetite particles, thus the magnetite film on the PPy was more easily formed [96].

Two novel methods for imparting magnetic properties to the hollow polyelectrolyte capsules were proposed. The first one includes the impregnation of the capsules with pre-formed Fe_3O_4 magnetite nanoparticles; the second approach is based on selective synthesis of magnetic Fe_3O_4 inside the polyelectrolyte capsules filled with polycations. Synthesized Fe_3O_4 core/polyelectrolyte shell composites were characterized by transmission electron microscopy (TEM) and WAXS techniques. Perspectives of the usage of hollow polyelectrolyte capsules as microreactors for spatially restricted inorganic synthesis were demonstrated [97].

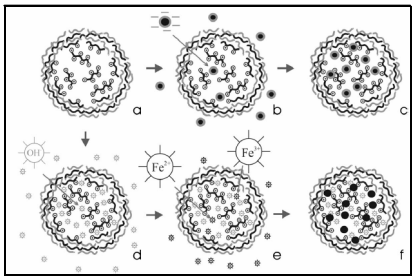

Figure 2.30: Schematic illustration of the preparation of polyelectrolyte capsules loaded with magnetite.

Figure 2.30 depicts two procedures of the imparting magnetic properties to hollow polyelectrolyte capsules. The idea of the first one (Figure 2.29a,b,c) is to impregnate hollow interior of the capsule with preformed Fe_3O_4 nanoparticles from water-based magnetic fluid stabilized by citronic acid. Mixing the poly(allylamine hydrochloride) (PAH) containing capsules with magnetic fluid leads to the impregnation of magnetite nanoparticles into the capsules interior followed by their fixing on the inner side of the PAH/PSS wall caused by electrostatic interaction between PAH polycation and negatively charged surface of the Fe_3O_4 particles. Five hours of exposition with subsequent cleaning from non-captured material result in the filling of capsules interior with nanosized Fe_3O_4. The other method (Figure 2.29a,d,e,f) employs both the difference in pH between capsule interior and surrounding solution and the presence of dissolved PAH inside capsule which allow us to carry out selective precipitation of the magnetite only inside the capsules. As shown in Figure 2.29, at first PAH/PSS capsules were exposed to the 0.01 M NaOH for 4 h. Then they were washed and 3 ml of 0.66M $FeSO_4$ + 0.62 M $Fe_2(SO_4)_3$ solution were added to 200 ml of aqueous solution containing 5% v/v of activated capsules for 6 h. During the reaction combined precipitation of both Fe(II) and Fe(III) ions and the formation of the Fe_3O_4 possessing magnetic properties were observed. After synthesis, the excess of Fe(II) and Fe(III) ions was removed from bulk solution by repeated magnetic decantation [97].

Here it is important to emphasize that Fe_3O_4 formation inside polyelectrolyte capsules is caused not only by pH but also by specific interaction between dissolved PAH molecules and Fe^{2+}, Fe^{3+} ions resulting in the obtention of colloidal Fe_3O_4. Addition of acidic PAH solution (pH = 1) in the absence of polyelectrolyte capsules to the mixture of 0.66 M $FeSO_4$ + 0.62 M $Fe_2(SO_4)_3$ provokes the appearance of the Fe_3O_4 sol possessing similar characteristics (crystallinity, particle size) as those of

Fe_3O_4 formed inside polyelectrolyte shells. Such interaction between polymer amines and metal cations followed by formation of corresponding hydroxides and oxides was previously described [97].

Another application of magnetic polymeric particles is the fabrication of magnetic spider silk fibers. Since silk fibers could have important applications in impact-proof textiles or other structural fabrics where strong and flexible materials are desirable, bundles of ca. 200 individual silk fibers were prepared by cutting 3 cm lengths of dragline spider silk from a continuous spool produced by Nephila edulis. It has been used dragline silk originating from the Major Ampullate glands, and the threads were drawn mechanically from immobilized but fully awake spiders at a speed of 2 cm/s onto either 1 cm diameter glass tubes or photographic slide frames. These bundles were suspended by tweezers and mechanically lowered into either a water or water/methanol sol of 10 to 20 nm diameter superparamagnetic magnetite (Fe_3O_4) particles for 2 min. Alternatively, single fibers, mounted across a twin-pronged variable caliper, were mechanically submerged into the nanocolloidal suspensions. After submersion, the fibers were slowly withdrawn from the colloidal sol and allowed to dry in air at ambient temperatures. The resulting dark brown fibers were coated with a dense coherent film of the magnetite nanocrystallites. High magnification images showed that the magnetite±silk composites displayed some surface roughness, indicating that the thickness of the mineral films was substantial. The mineralized fibers, however, retained their natural flexibility without significant disruption of the magnetite coating [98]. Moreover, the combination of intrinsic mechanical and fabricated magnetic properties enabled dried fibers to be oriented in the presence of an external magnetic field because fibers suspended against gravity tracked the position of a strong magnet. This was observed by fixing the fibers with tweezers in the presence of a 1.5 cm diameter neodymium±iron±boron slug [98].

2.7.6.3. Environmental Applications

It has also been reported by SenGupta and his coworkers that Nanoscale Inorganic Particles (NIPs) and their agglomerates offer excellent opportunities conducive to selective removal of a wide array of target compounds from contaminated water bodies. For example, magnetite (Fe_3O_4) crystals are capable of imparting magnetic activity. Very high surface area to volume ratio of these nanoscale particles offers

favorable sorption and/or reaction kinetics. Harnessing these inorganic nanoparticles and their aggregates appropriately within polymeric beads offers new opportunities that are amenable to rapid implementation in the area of environmental separation and control. While the NIPs retain their intrinsic sorption / desorption, redox, acid–base or magnetic properties, the robust polymeric support offers excellent mechanical strength, durability and favorable hydraulic properties in the flow-through systems. The polymer supported nanoparticles are reusable and can be easily reprocessed over many cycles of operation [99].

Imparting magnetic activity into already available polymeric sorbent materials with specific sorption affinities towards various environmental contaminants, namely, heavy metals, metalloids, inorganic and organic ligands, chlorophenols and pesticides. Once magnetized, these polymeric particles can be immensely effective in scavenging target contaminants from the background of complex environmental matrices such as slurries or sediments with high-suspended solids content, viscous or radioactive liquid or a medium with high concentration of biomass. Also, for environmental monitoring or forensic purpose, Magnetically Active Polymer Particles (MAPPs) can be judiciously used to track down the origin of a particular contaminant present in natural water bodies [99].

3. EXPERIMENTAL PART

3.1. Chemicals

All the chemicals used were analytical grade commercial products.

Table 3.1: List of chemicals used in this study.

Name- Molecular Formulas	Brand	Properties
Poly (vinyl alcohol) $[CH_2CH_2]_n$ OH	DuPont/Elvanol	grade 70-05 99 % hydrolyzed Mw = 26.000 Da Viscosity 5.5 cP 4 % aqueous solution, Molar volume 34.7 cm^3 mol^{-1}
Iron (II) sulfate $FeSO_4$. $7H_2O$	E. Merck	M_w=278,02 g mol^{-1}
Ammonia NH_4OH	E.Merck	25 % aqueous solution M_w=17,03 g mol^{-1} d=0,90 g cm^{-3}
Hydrogen peroxide H_2O_2	Fluka	35 % aqueous solution M_w=34,01 g mol^{-1} d=1,13 g cm^{-3}
Toluene C_7H_8	E.Merck	

They were used without any further purification.

3.2. Instruments

Table 3.2: List of instruments used in this study.

Instrument	Brand
Magnetic stirrer	RH basic KT/C IKAMAG®
Hot plate	HP 30 IKATHERM®
Shaker	IKA-HS 501 digital
Ultra-Turrax	IKA-TURRAX, 220 W
Scanning Electron Microscope	JEOL 6310 SEM
Vibrating Sample Magnetometer	Homemade design
UV-Visible	Perkin-Elmer

3.3. Characterization

3.3.1. Determination of Hydroperoxy Content of Commercial PVA

Hydroperoxide content of the commercial PVA was determined by Fe (II) in the presence of sulfosalicylic acid. In this procedure Fe (II) is oxidized to Fe (III), by reacting with hydroperoxide of PVA. Sulfosalicylic acid complex of Fe (III) has absorption maxima around 500 nm. This method allows the determination of Fe (III) in presence of Fe (II). Thus, 0.5 g of sulfosalicylic acid was dissolved in 10 mL acetic acid and diluted to 100 mL.

50 mL of 2 M PVA solution was transferred into two-necked flask and nitrogen was flushed through the solution for 15 minutes. Then, 1 g $FeCl_3.6\ H_2O$ was dissolved in

PVA solution under nitrogen stream. The flask was closed and the mixture was stirred with a magnetic bar for 24 h at room temperature. 1 mL of this solution was mixed with 10 mL of sulfosalicylic acid solution and stirred for 5 min in a closed bottle. The absorbance of the colored complex was measured at 500 nm against the blank. Concentration of hydroperoxide was estimated based on calibration curve produced by a series of Fe (III) standards in 10^{-4}-10^{-3} M concentration range and found to be 6.1 10^{-4} M. This corresponds to 0.36 mmol hydroperoxide per mol of PVA repeat unit. In another words 10^5 repeat units have 36 hydroperoxide units.

3.3.2. Swelling Measurements

Swelling measurements were performed in water using sintered crucibles. For this purpose 0.1 grams of dry samples were placed in the crucibles and immersed in water. The system was left to stand for 24 hours at room temperature. Final mass of the gel samples were removed and their final masses were measured by weighing.

Swelling ratios were defined as;

$$\text{Swelling ratio} = w/w_0 \qquad (3.1)$$

Where, w and w_0 denote the final and initial weights of the samples respectively.

3.3.3. Scanning Electron Microscopy (SEM)

Scanning electron microscopy (SEM) analysis studies were carried out using a JEOL 6310 SEM operating at 20 kV. The images were obtained directly or by gold coated samples as usual. The pictures were taken by 4000-8000 times of magnification. No differences were detected in both measurements.

3.3.4. Magnetic Measurements

Magnetic measurements were carried out at room temperature using Vibrating Sample Magnetometer (homemade design) prior to the measurements, the magnetometer was calibrated with Nickel standard having the same shape with the samples. The samples were prepared in cylindric form (1.5 cm diameter, 0.5 cm of height) by pressing (4.2 Tones cm^{-2}). The saturation magnetizations were obtained by scanning the field from -15 kOe to + 15 kOe. Coeservities were estimated simply by measuring from half width of the hysterisis curves. The results are tabulated in Table 4.1.

3.4. Crosslinking of PVA by Fenton reagent

A representative example is as follows:

$FeSO_4.7H_2O$ (2.78 g, 10 mmol) is dissolved in 20 mL distilled water. 0.6 mL of concentrated H_2SO_4 (96 %) is added to this solution. The acidified solution is then added to 50 mL of PVA solution (4.4 g, 100 mmol repeat unit) while stirring. 1.03 mL of 30 % H_2O_2 (10 mmol) is diluted to 20 mL and added dropwise to above solution under vigorous stirring. A sudden gelation took place. The gel precipitate was filtered by suction and dried under vacuum for 24 h at 50 ^oC.

This procedure was repeated for various Fe (II) / PVA ratios.

3.5. Preparation of Submicron Magnetite Particles

A typical procedure is as follows:

To a 40 mL PVA solution (containing 3.52 g dry PVA) there were added 1.67 g (6 mmol) ($FeSO_4.7H_2O$) in 10 mL of water and 0.22 mL (4 mmol) concentrated H_2SO_4 (d: 1.84) under nitrogen atmosphere. The solution was added to 300 mL of toluene in a flat-bottomed flask under vigorous stirring with an Ultraturrax high speed homogenizer. A nitrogen stream was introduced with a delivery tube dipped into the solution. Meanwhile, 0.34 mL 35 % H_2O_2 (4 mmol, d: 1.13) was diluted to 25 mL and this solution was added dropwise to the flask while aggitating. Then the mixture was stirred for another 20 minutes. At this time, 2.5 mL of (36 mmol) 26 % ammonia solution was added all at once. The mixture turned to be deep green. The homogenizer and nitrogen inlet were removed. The flask was tightly closed and placed on a continuous shaker to be shaken for 36 hours. Then the color turned to dark black. The reaction content was poured onto Büchner funnel to be filtered under gravitational force. It took 3 days and the residue on the filter paper was dryed until a constant weight (for about 24 hours) under vocuum at 50 ^0C.

The same procedure was followed for the samples with different PVA/H_2O_2 ratios.

4. RESULTS AND DISCUSSION

In this work it was observed that, Fenton Reagent causes to a rapid crosslinking of PVA in aqueous solution. The crosslinking is so rapid that, a sudden gelation takes place as soon as the hydrogen peroxide droplets contact with acidified aqueous solution containing PVA and Fe(II) ions. For this reason drop wise addition of diluted hydrogen peroxide (3%) is essential to obtain more homogenous crosslinking. This process gives light green precipitates, in which ferric sulfate is entrapped into crosslinked PVA. By using 1.5 mole of Fe (II) per mole of hydrogen peroxide the gel particles containing a mixture of iron salts with 2 / 1 molar ratio of Fe (III)/ Fe (II). The crosslinking is believed to occur by hydrogen abstraction preferably from the methylol carbons of PVA and combination of the radicals as depicted in Figure 4.1. Reaction of low molecular weight alcohols with Fenton Reagent proceeds in similar fashion.

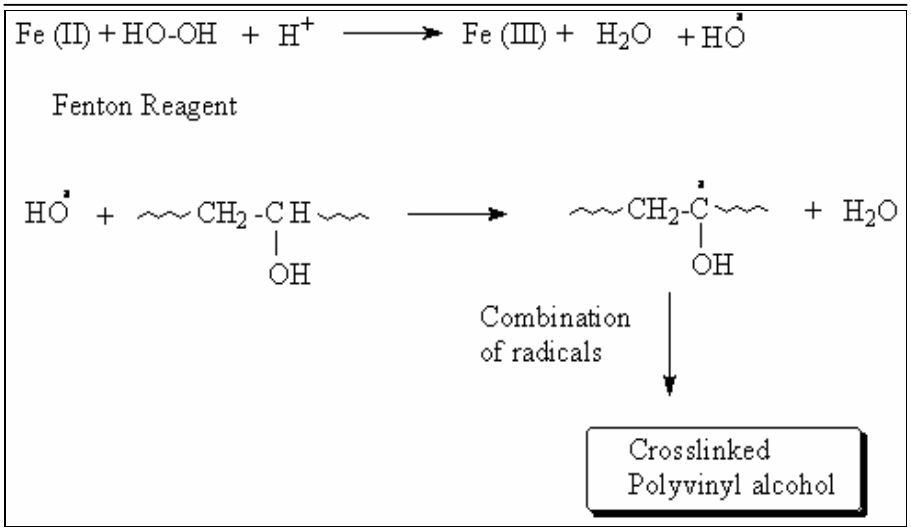

Figure 4.1: Crosslinking of Poly (vinyl alcohol) with Fenton Reagent.

The crosslinking density and iron contents can be adjusted by proper combination of PVA, H_2O_2 and Fe (II) ratios.

This ratio is crucial to prepare a good quality of magnetite by subsequent treatment with ammonia. However, commercial PVA may contain trace amounts of hydroperoxides depending on its preparative and storage conditions.

Fenton Reagent is a well-known oxidizing agent of which reactivity is based on decomposition of hydrogen peroxide to give hydroxyl radicals.

Since stoichiometry of Fe (II) and Fe (III) is crucial to attain good magnetite forming combination, amount of hydroperoxide present in PVA structure must be known exactly. In this work the hydroperoxide content of the PVA was estimated by an additional experiment. In this experiment an aqua solution of PVA was reacted with Fe (II) solution. The hydroperoxide content was assigned by determination of Fe (III) colorimetrically. This measurement showed that hydroperoxide content of the commercial product is of order of 0.036 mole hydroperoxide per 100 mole of PVA repeat unit. This amount in fact is neglicible.

4.1. Evaluation of the Crosslinked Material

Post crosslinking of PVA in aqueous solution resulted in rapid precipitation. The precipitate was no longer soluble. Attempts to remove iron salts retaining in the crosslinked matrix by extraction with acetic acid, HCl solution and EDTA solutions were failed. No chlorination was observed in HCl solution while contacting with the PVA-precipitates for more than one week. This reveals dense crosslinking of PVA.

The crosslinked polymer samples (containing iron sulfates) showed modest swelling ratios in water (Figure 4.2).

For instance swelling ratio was only 471 % for the sample obtained using 5 % (mol/mol) Fe(II) (as crosslinker) per mole of PVA repeat unit.

The swelling ratios were found to be inversely proportional to iron contents as expected.

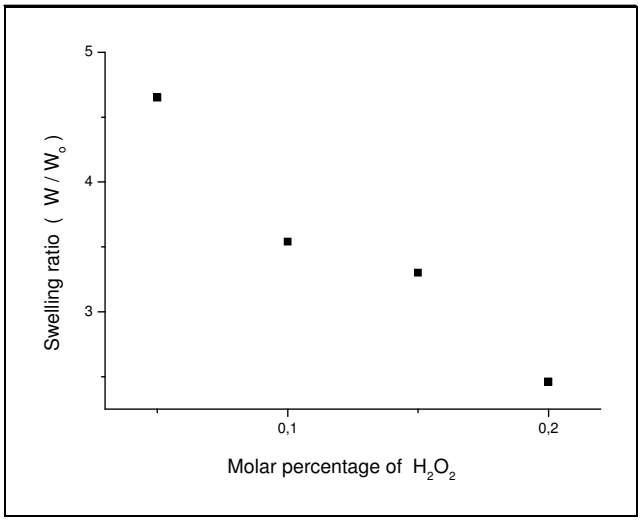

Figure 4.2: Swelling ratios of crosslinked PVA samples versus molar percantages of H_2O_2 used in the crosslinking.

By using the swelling ratios, we have attempted to estimate the crosslinking densities based on Flory-Reigner approach:

$$\ln(1-v_2)+v_2+\chi v_2^2+\frac{\rho v_1}{\bar{M}_C}\left(v_2^{1/3}.v_2^{0^{2/3}}-v_2/2\right)-fv_2=0 \qquad (4.1)$$

v_2: Volume ratio of dry polymer in swollen state

ρ : Density of polymer in dry state

v_1: Molar volume of solvent (for water: 18 mL/mol)

$\bar{M}_c$: Molecular weight of the polymer segments between two crosslinking points

v_2^0 : Molar ratio of the dry polymer at the beginning

f: Degree of ionization, if present ionic groups in the polymer.

Calculations using χ=0.48 (PVA-water interaction parameter) and v_2^0=1 (to phase separation during the crosslinking)

In those calculations, iron free portions of the PVA were taken into consideration. The iron sulfates were assumed to be in non-hydrated forms.

Those calculations showed that the crosslinking densities are not inconsistent with the theoritical values.

Of course the iron sulfates are expected to be in hydrated form. Perhaps the best results can be obtained by taking hydrated water contents of iron sulfates in swollen

state. However we are unable to detect the number of water molecules surrounding the iron sulfates.

Calculations by assuming 6 mole of water per mol of iron sulfate were also not in agreement with those predicted by the feed compositions.

This might be largely due to the complexing tendency of the ferric and ferrous ions with PVA.

This can be avoided by formation of magnetite in crosslinked polymer nanoparticles. For biological applications, polyvinyl alcohol has been considered as host matrix. Post-crosslinking of polyvinyl alcohol by acid catalyzed cyclic acetale formation with glutar dialdehyde has been demonstrated to be useful method of preparing. On the other hand; coating of magnetite particles with a bio-compatible polymer is sought. For long term stabilities

In fact, these procedures are applicable not only for magnetite but also nanoparticles of metals or metal oxides.

4.2. Magnetite Formation

In magnetite formation 1.5 mole of $FeSO_4$ were used per mole of H_2O_2, together with 1 mole H_2SO_4. The excess of $FeSO_4$ (0,5 mole) was chosen deliberately to have a mixture with 1 mole Fe(III) and 0,5 mole Fe(II) which is exact stoichiometry to form magnetite. This was performed water in oil emulsion (inverse emulsion) without using emulsifier. While stirring with an ultrahigh speed homogenizer (IKA-TURRAX, 220 W) at 4000-5000 rpm, ammonia was added dropwise under nitrogen stream. Color of the mixture was turn to be green to pitch dark.

The dispersions resulted were highly stable, so that no coagulation or precipitation was observed upon standing at room temperature for longer than 20 days.

4.3. The Magnetite Contents

Percentage magnetite contents of the products can be calculated based on the initial compositions.

Since crosslinking is quantitative, for 1 mole of PVA repeat unit (44), there must be one mole of Fe_3O_4 per three moles of initially used $FeSO_4$.

For instance; in case of 0.3 crosslinking, 0.3 mole of Fe (III) is produced beside the PVA (44 g). Since each Fe (III) is accompanying with 0.5 mole of Fe (II) this accounts for 0.45 mole of total iron, which corresponds to 0.15 mole of Fe_3O_4.

Then total weight of theresulting formulations would be 0.15x232+44=78.8 g.

This reads,

$$\frac{0.15 * 232}{78.8} = 44.16 \text{ \% of } Fe_3O_4$$

Compositions of other formulations were calculated similarly (See Table 4.1)

Table 4.1: Preparation and physical characteristics of PVA coated magnetite particles.

Run	$Fe(II)/H_2O_2$ (mol/mol)	H_2O_2/PVA[(a)] (mol/mol)	Practical Yield (%)	Swelling (w/w_0)%	Saturation[(b)] magnetization (emu/g)	Coecervity (Hc) (Oe)	Fe_3O_4 Content (w/w_0 %)
1	1.5	5/100	83	471	13	2,6	11,65
2	1.5	10/100	96	352	23	11,8	20,86
3	1.5	15/100	90.3	331	28,5	38,8	28,34
4	1.5	20/100	87	218	34,5	-----	34,52
5	1.5	30/100	88.9	ND	46,9	51,3	44,16

(a): in 1/5 water/toluen ratios

(b): saturation magnetizations were measured from -15 kOe to + 15 kOe

4.4. Magnetic Properties

The resulting dark colored products show strong magnetization. Saturation magnetizations measured are proportional to Fe_3O_4 contents of te samples, as expected.

The highest magnetization is attained for the samples with 52.91 % Fe_3O_4 (w/w_0 %). This indicates a $\frac{42.9}{0.4416} = 97.15$ emu g^{-1} of saturation magnetization, which is slightly higher than those of natural magnetite minerals (94-95 emu g^{-1}).

Moreover, the hydroxy groups on outer surface of the particles, provide various modification possibilities based on esterification, urethane formation etc.

Apparently those transformations allow preparing many composite materials possesing strong magnetic properties.

The magnetite dispersions obtained by this procedure are all stable. No precipitation or phase separation was observed upon standing at room temperature for longer than 20 days.

5. CONCLUSIONS AND RECOMMENDATION

Fenton Reagent with 50 % excess Fe (II) gives iron sulfate mixture entrapped in the crosslinked PVA matrix. Following reaction with NH_3 solution (pH= 10-11) results in magnetite coated particles in submicron size.

The Fenton Reagent serves not only as crosslinking agent, but also take part as magnetite forming component.

Overall process can be carried out in one pot.

Being coated by crosslinked PVA, the resulting material is promising as candidate to use in biomedical applications, and in preparing ferromagnetic composites.

The process performed without additional stabilizer yields submicron magnetic particles with strong saturation magnetizations.

REFERENCES

[1] **Turkevitch, J.,** 1985. Colloidal Gold, *Gold Bulletin*, **18**, 86-91.

[2] **Watzky, M.A., Finke, R.G.,** 1997. Transition metal nanocluster formation kinetic and mechanistic studies. A new mechanism when hydrogen is the reductant: slow, continuous nucleation and fast autocatalytic surface growth, *Journal of the American Chemical Society,* **119**, 10382-10400.

[3] **Blum, J., Amer, I., Peter, K., Vollhardt, C., Schwarz, H., Hoehne, G.** 1987. Hydrogenation of arenes by the RhCl3-Aliquat 336 catalyst. 4. Hydrogen-deuterium exchange and other mechanistic features**,** *J. Org. Chem.;* **52**(13); 2804-2813.

[4] **Lin, Y., Finke, R.G.,** 1994. A More General Approach to Distinguishing "Homogeneous" from "Heterogeneous" Catalysis: Discovery of Polyoxoanion- and Bu4N+-Stabilized, Isolable and Redissolvable, High-Reactivity Ir.apprx.190-450 Nanocluster Catalysts *Inorg. Chem.;* **33**(22); 4891-4910.

[5] **Finke, R. G.**, 2002. In *Metal Nanoparticles: Synthesis, Characterization and Applications*; Feldheim, D. L., Foss, C. A., Jr., Eds.; Marcel Dekker: New York, 2002; Chapter 2, pp 17-54.

[6] **Evans, M.**, 1999. *In The Colloidal Domain*, 2nd ed., Wiley-VCH, Newyork.

[7] **Roucoux, A., Schulz, J., Patin, H.,** 2002. Reduced Transition Metal Colloids: A Novel Family of Reusable Catalyst, *Chem. Rev.,* 102, 3757-3778.

[8] **Tadros, Th. F.,** 1987. Solid/Liquid Dispersions, pp 17-61, Academic Press Inc., Florida.

[9] **Lin, Y., Finke, R.G.,** 1994. Novel Polyoxoanion- and Bu_4N^+-Stabilized, Isolable, and Redissolvable, 20-30-.ANG. Ir300-900 Nanoclusters: The Kinetically Controlled Synthesis, Characterization, and Mechanism of Formation of Organic Solvent-Soluble, Reproducible Size, and Reproducible Catalytic Activity Metal Nanoclusters, *J. Am. Chem. Soc.* **116**(18); 8335-8353.

[10] **Amiens, C., Caro, D., Chaudret, B., Bradley, J.S., Mazel, R., Roucau, C.,** 1993. Selective synthesis, characterization, and spectroscopic studies on a novel class of reduced platinum and palladium particles stabilized by carbonyl and phosphine ligands, *J. Am. Chem. Soc.;* **115**(24); 11638-11639.

[11] **Chen, S., Kimura, K.,** 2001. Synthesis of Thiolate-Stabilized Platinum Nanoparticles in Protolytic Solvents as Isolable Colloids *J. Phys. Chem. B.*; **105**(23); 5397-5403.

[12] **Schmid, G., Emde, S., Maihack, V., Meyer-Zaika, W. and St. Peschel,** 1996. Synthesis and catalytic properties of large ligand stabilized palladiumclusters , *95-104.*

[13] **Rodriguez, A., Amiens, C., Chaudret, B.; Casanove, M.-J., Lecante, P.,** 1996. Synthesis and Isolation of Cuboctahedral and Icosahedral Platinum Nanoparticles. Ligand-Dependent Structures**,** J. S. *Chem. Mater.,* **8**(8); 1978-1986.

[14] **Franke, R., Rothe, J., Pollmann, J., Hormes, J., Bonnemann, H., Brijoux, W.,** 1996. A Study of the Electronic and Geometric Structure of Colloidal Ti^{0}·0.5 THF *J. Am. Chem. Soc.,* **118**(48), 12090-12097.

[15] **Churaev, N. V. and Derjaguin, B. V.,** 1985. Inclusion of structural forces in the theory of stability of colloids and films*, J. Coll. Interface Sci.* **103**, *542-553*

[16] **Verwey, E.J.W. and Overbeek, J.Th.G.,** 1948. Theory of Stability of Lyophobic Colloids., Elsevier, Amsterdam

[17] **Lyklema, J., and Van Leeuwen, H.P.,** 1982. Dynamic properties of the AgI-solution interface: Implications for colloid stability *Adv. Coll. INTERFACE Sci,* **16,** 127

[18] **Polder, R.B.**, 1984. Electrodynamics of the AgI/solution interface, The Netherlands, *PhD Thesis*, Agricultural University, Wageningen.

[19] **Mahanty, J. and Ninham, B.W.,** 1976. Dispersion Forces, Academic Press, London

[20] **Hogg R. and Yang K.C.,** 1976. Secondary coagulation , *J. Coll. Interface Sci.*, **56**, 573

[21] **Napper, D.H.,** 1983. Polymeric Stabilization of Colloidal Dispersions, Academic Press, London

[22] **Vincent, B. and Whittington, S.,** 1982. *Surface and Colloid Science*, **12**, Wiley, Newyork.

[23] **Fleer, G.J. and Scheutjens, J.M.H.M., and Vincent, B.,** 1984. Polymer Adsorbtion and Dispersion Stability (ed. E.D. Goddard and B. Vincent). *Am. Chem. Soc. Symposium, 1984,* Vol. 240, 245-253.

[24] **Vincent, B.,** 1973. The van der Waals attraction between colloid particles having adsorbed layers. II. Calculation of interaction curves, *J. Coll. Interface Sci.* **42**, 270-285.

[25] **Vincent, B.,** 1974. The effect of adsorbed polymers on dispersion stability, *Adv. Colloid and Interface Sci.* **4**, 193-277

[26] **Barret, K.E.J.,** 1974. Dispersion Polymerisation in Organic Media, Wiley, Newyork.

[27] **Ugelstad, J., Hansen, F.K., Lange,S.,** 1974. Emulsion polymerization of styrene with sodium hexadecyl sulphate/hexadecanol mixtures as emulsifiers. Initiation in monomer droplets, *Die Makromolekulare Chemie,* **175**, 507-521.

[28] **Durbin, D.P., El-Aasser, M.S., Poehlein, G.W., Vanderhoff, J.W.,** 1979. Influence of monomer preemulsification on formation of particles from monomer drops in emulsion polymerization, *Journal of Applied Polymer Science,* **24**, 703-707.

[29] **Landfester, K.,** 2001. Polyreactions in Miniemulsions, *Macromol. Rapid Commun.,* **22**, 896-936.

[30] **Landfester, K.,** 2001. The Generation of Nanoparticles in Miniemulsions, *Advanced Materials* **13**, 10-22.

[31] **Landfester, K., Tiarks, F., Hentze, H.P., Antonietti, M.,** 2000 Polyaddition in miniemulsions: A new route to polymer dispersions, *Macromolecular Chemistry and Physic* **201,** 1-5.

[32] **Tadros, T.P., Izquierdo, J., Esquena, C.,** 2004. *Advances in Colloid and Interface Science*, **108-109**, 303-318.

[33] **K., Shinoda and Saito, H.,** 1968. The effect of temperature on the phase equilibria and the types of dispersions of the ternary system composed of water, cyclohexane, and nonionic surfactant, *J. Colloid Interface Sci.,* **26,** 70-74.

[34] **Brooks, B.W., Richmond, H.N., Zerfa, M.,** 1998. Modern Aspects of Emulsion Science, Royal Society of Chemistry Publication, Cambridge.

[35] **El- Aasser, M.,** 1997. Polymeric Dispersions, Kluwer Academic Publications, The Netherlands

[36] **Shinoda, K., Kunieda, H.,** 1983. in P. Becher (Ed), Encyclopedia of Emulsion Technology, Marcel Dekker, Newyork

[37] **Walstra, P., Smoulders, P.E.A.,** 1983. Encyclopedia of Emulsion Technology, Marcel Dekker, Newyork

[38] **Welin-Berger, K., and Bergenståhl, B.,** 2000. Inhibition of Ostwald ripening in local anesthetic emulsions by using hydrophobic excipients in the disperse phase, *Int. J. Pharm.,* **200,** 249-260

[39] **Davis, S.S., Round, H.P., and Purewal, T.S.,** 1981. Ostwald ripening and the stability of emulsion systems: an explanation for the effect of an added third component, *J. Coll. Interface Sci.,* **80,** *508-511*

[40] **Danov, K.D., Denkov, N.D., Petsev, D.N., Ivanov, I.B., and Borwankar, R.**, 1993. Coalescence dynamics of deformable Brownian emulsion droplets, *Langmuir,* **9,** 1731-1740

[41] **Azad, A.R.M, Ugelstad, J., Fitch, R.M., Hansen, F.K.,** 1976. Emulsion polymerization, *Am. Chem. Soc. Publications, Washington, DC*

[42] **Chou, Y. J. El-Aasser, M. S., Vanderhoff, J. W.,** Mechanism of emulsification of styrene using hexadecyltrimethylammonium bromide-cetyl alcohol mixtures, *Journal of Dispersion Science and Technology*, **1,** 129-150.

[43] **Landfester, K., Bechthold, N., Tiarks, F., Antonietti, M.,** 1999. Miniemulsion Polymerization with Cationic and Nonionic Surfactants: A Very Efficient Use of Surfactants for Heterophase Polymerization, *Macromolecules*, **32** (8), 2679-2683.

[44] **Antonietti, M.; Hentze, H.-P.,** Microemulsion polymerization: New surfactant systems by counterion variation, *Advanced Materials*, **8**(10), 840-844

[45] **Zu Putlitz, B., Hentze, H.P., Landfester, K., Antonietti, M.,** 2000. New cationic surfactants with sulfonium headgroups, *Langmuir*, **16**(7), 3214-3220

[46] **Zu Putlitz, B., Landfester, K., Fischer, H., Antonietti, M.,** 2001. The generation of "armored latexes" and hollow inorganic shells made of clay sheets by templating cationic miniemulsions and latexes, *Advanced Materials*, **13** (7), 500-503

[47] **Chern, C.S., Liou, Y.C.,** 1999. Kinetics of styrene miniemulsion polymerization stabilized by nonionic surfactant/alkyl methacrylate, *Polymer*, **vol.40**, no 13, p 3763-3772

[48] **Lim, M.S., Chen, H.,** 2000., Miniemulsion polymerization of styrene with a block copolymer surfactant, *Journal of Polymer Science, Part A: Polymer Chemistry*, vol.38, no 10, p 1818-1827

[49] **Wang, S., Schork, F.J.,** 1994. Miniemulsion polymerization of vinyl acetate with nonionic surfactant, *Journal of Applied Polymer Science*, **vol.54,** no 13, p 2157-2164

[50] **Baskar, G., Landfester, K., Antonietti, M.,** 2000. Comblike polymers with octadecyl side chain and carboxyl functional sites: scope for efficient use in miniemulsion polymerization, *Macromolecules*, **33**, 9228-9232

[51] **Abismail, B., Canselier, J.P., Wilhelm, A.M., Delmas, H., Gourdon, C.,** 1999, Emulsification by ultrasound: Drop size distribution and stability *Journal of Histochemistry and Cytochemistry*, **47,** 75-83

[52] **Walstra, P.** 1993. Principles of emulsion formation, *J. Chemical Engineering Science*, **48**, 333-386

[53] **Landfester, K., Bechthold, N., Tiarks, F., Antonietti, M.,** 1999. Formulation and stability mechanisms of polymerizable miniemulsions *Macromolecules*, **32,** 5222-5228

[54] **Attwood, D., Florence, A.T.,** 1980. *Surfactant Systems-Their chemistry, pharmacy and biology*, Chapman and Hall, London

[55] **Landfester, K., Willert, M., Antonietti, M.,** 2000. Preparation of polymer particles in nonaqueous direct and inverse miniemulsions *Macromolecules*, **33**, 2370-2376.

[56] **Ugelstad, J., Mork, P.C., Kaggerud, K.H., Ellingsen, T., Berge, A.,** 1980. Swelling of oligomer-polymer particles. New methods of preparation of emulsions and polymer dispersions, *Advances in Colloid and Interface Sci.*, **13,** 101-140.

[57] **Reimers, J.L., Schork, F.J.,** 1996. Predominant droplet nucleation in emulsion polymerization, *Journal of Applied Polymer Science*, **60,** 251-262.

[58] **Candau, F.,** 1992. Polimerization in Organized Media pp. 215-282, E.C. Paleos, Ed., Gordon and Breach Science Publisher, Philadelphia.

[59] **Hunkeler, D., Candau, F., Pichot, C., Hemielec, A.E., Xie, T.Y., Barton, J., Vaskova, V., Guillot, J., Dimonie, M.V., Reichert, K.H.,** 1994. Heterophase polymerization. A physical and kinetic comparison and categorization, *Advances in Polymer Science*, **112**, 115-133.

[60] **Walstra, P.** 1983. P. Becher (Ed), Encyclopedia of Emulsion Technology, Marcel Dekker, Newyork.

[61] **Pusey, P.N.,** 1973. Green, J.H.S. Dietz, R. (Eds.), Industrial Polymers: Characterisation by Molecular Weights, Transcripta Books, London.

[62] **Kitamoto, Y., Nakayama, Y., Abe, M.,** 2000. Spin-dependent intergranular transport in magnetite films deposited by ferrite plating, *Journal of Applied Physics*, **87,** 7130-7136.

[63] **Ziolo, Ronald F., Giannelis, E.P., Weinstein, B.A., O'Horo, M.P., Ganguly, B.N., Mehrotra, V., Russell, M.W., Huffman, D.R.,** 1992. Matrix-mediated synthesis of nanocrystalline γ-Fe_2O_3. A new optically transparent magnetic material, *Science*, **257,** 219-223.

[64] **Hai Lin, H., Watanabe, Y., Kimura, M., Hanabusa, K., Shirai1, H.,** 2003. *Journal of Applied Polymer Science,* **87,** 1239–1247.

[65] **Ding, X.B., Sun, Z.H., Zhang, W.C.; Peng, Y.X., Wan, G.,X., Jiang, Y.,Y.,** 2000._Adsorption/desorption of protein on magnetic particles covered by thermosensitive polymers, *J Appl Polym Sci*, **77**(13), 2915-2920.

[66] **Yang, J., Ding, Y., Cheng, Z., Sun, K., Wang, H., Wang, Y., Zhang, W., Zheng, Z.,** 2000. Experimental study of radiative ablation to low and medium-Z material *Colloid polym. Sci. Qiangjiguang Yu Lizishu/High Power Laser and Particle Beams(chinese)*, **12,** 459-462.

[67] **Haas, W., Zrinyl, M., Kilian, H.G., Heise, B.,** 1993. Structural analysis of anisometric colloidal iron (III)-hydroxide particles and particle-aggregates incorporated in poly(vinyl-acetate) networks *Colloid Polym. Sci.*, **271***,* 1024 – 1034.

[68] **Sauzedde F., Elaïssari A., Pichot C.,** 1999. Hydrophilic magnetic polymer latexes. 1. Adsorption of magnetic iron oxide nanoparticles onto various cationic latexes, Colloid Polym. Sci.**, 277,** 846 – 855.

[69] **Moore L.R., Zborowski M., Nakamura M., McCloskey K., Gura S., Zuberi M., Margel S., and Chalmers J.J.,** 2000. The use of magnetite-doped polymeric microspheres in calibrating cell tracking velocimetry, *J. Biochem. Biophys. Methods.***, 44,** 115-130.

[70] **Furusawa, K., Nagashima, K., Anzai, C.,** Synthetic process to control the total size and component distribution of multilayer magnetic composite particles, *Colloid Polym Sci*, **272,** n 9, p. 1104-1110.

[71] **Sauzedde, F., Elaïssari A., Pichot C.,** 1999. Hydrophilic magnetic polymer latexes. 2. Encapsulation of adsorbed iron oxide nanoparticles Colloid Polm. Sci. **277**, 1041-1050.

[72] **Ugelstad, J., Berge, A., Ellingsen, T., Schmid, R., Nilsen, T.-N., Mork, P. C., Stenstad, P., Hornes, E., and Olsvik, O.,** 1992, Preparation and application of new monosized polymer particles, *Prog. Polym. Sci.* **17,** 87-95.

[73] **Zaitsev, V. S., Filimonov, D. S., Presnyakov, I. A., Gambino, R. J., and Chu, B.,** 1999. Physical and Chemical Properties of Magnetite and Magnetite-Polymer Nanoparticles and Their Colloidal Dispersions *J. Colloid Interface Sci.* **212,** 49-55.

[74] **Shimoiizaka, J., Nakatsuka, K., Fujita, T., Kounosu, A.,** 1980 ‘‘Fineparticles’’, in: Processing – Proceedings of the international symposium on fine particles processing, **2,** P. Somasundaran, Ed., New York.

[75] **V. Veiga, D. H. Ryan, E. Sourty, F. Llanes, R. H. Marchessault,** 2000. Formation and characterization of superparamagnetic cross-linked high amylose starch Carbohydr. Polymer, **42,** 353-365.

[76] **Landfester, K.** 2003. Magnetic Polystyrene Nanoparticles with a High Magnetite Content Obtained by Miniemulsion Processes *Macromol. Chem. Phys.*, **204** (1), 22-31.

[77] **Shimoiizaka, J., Nakatsuka, K., Fujita, T., Kounosu, A.,** 1980. *Fine particles*, in: Processing – Proceedings of the international symposium on fine particles processing, **2,** P. Somasundaran, Ed., New York.

[78] **Deng, Y., Wang, L., Yang, W., Fu, S.,** 2003. Elaissari A., *Journal of Magnetism and Magnetic Materials,* **257**, 69–78.

[79] **Lin, H., Watanabe, Y. Kimura, M., Hanabusa, K., Hirofusa, S.,** 2003. *Journal of Applied Polymer Science,* **87,** 1239–1247.

[80] **Zaitsev, V. S., Filimonov, D. S., Presnyakov, I. A., Gambino, R. J., Chu, B.,** 1999. Physical and Chemical Properties of Magnetite and Magnetite-Polymer Nanoparticles and Their Colloidal Dispersions *Colloid Interface Sci.* **212**, 49-99.

[81] **V. S. Zaitsev, D. S. Filimonov, I. A. Presnyakov, R. J. Gambino, B. Chu, J.** Physical and Chemical Properties of Magnetite and Magnetite-Polymer Nanoparticles and Their Colloidal Dispersions Colloid Interface Sci. 1999, **212**, 49-99.

[82] **Zaitsev, Vladimir S.; Gambino, Richard J.; Chu, Benjamin.** 1999, Preparation and properties of magnetite and polymer magnetite nanoparticles, *Langmuir*, **15**, 1945-1951.

[83] **Yanase, N., Noguchi, H.; Asakura, H., Suzuta, T.,** 1993. Preparation of magnetic latex particles by emulsion polymerization of styrene in the presence of a ferrofluid Source, *Journal of Applied Polymer Science*, **50** (5), 765-776

[84] **Cooper, E. C., and Vincent, B.,** 1989. Encapsulation of filler particles in polymethylmethacrylate beads by a double-dispersion method *J. Colloid Interface Sci.* **132,** 592-594.

[85] **Gupta, P. K., Hung, C. T., Lam, F. C., and Perrier, D. G.,** 1988. Albumin microspheres. III. Synthesis and characterization of microspheres containing adriamycin and magnetite, *Int. J. Pharmaceutics* , **43,** 167-177.

[86] **Wormuth, K.**, 2001. Superparamagnetic Latex via Inverse Emulsion Polymerization, *Journal of Colloid and Interface Science* **241,** 366–377.

[87] **Mülller-Schulte, D., and Brunner, D.,** 1995. Novel magnetic microspheres on the basis of poly(vinyl alcohol) as affinity medium for quantitative detection of glycated haemoglobin *J. Chromatogr. A* **711,** 53-60.

[88] **Candau, F., Leong, Y. S., Pouyet, G., and Candau, S.** 1984. Inverse microemulsion polymerization of acrylamide: Characterization of the

water-in-oil microemulsions and the final microlatexes , *J. Colloid Interface Sci.* **101**, 167-183.

[89] **Lopez-Qunitela, M. A., and Rivas, J.,** 1993. Chemical Reactions in Microemulsions: A Powerful Method to Obtain Ultrafine Particles *J. Colloid Interface Sci.* **158**, 446-451.

[90] **C., Graillat, C., Pichot, A., Guyot, M. S., El Aasser,** 1986. Inverse emulsion polymerization of acrylamide. I. Contribution to the study of some mechanistic aspects, *Journal of Polymer Science Part A*, **24**(3) 427-449.

[91] **Hernandez-Barajas, J., and Hunkeler, D.,** 1997. Heterophase water-in-oil polymerization of acrylamide by a hybrid inverse-emulsion/inverse-microemulsion process, *Polymer,* **38**, 5623.

[92] **Kriwet, B.,Walter, E., and Kissel, T.,** 1998. Synthesis of bioadhesive poly(acrylic acid) nano- and microparticles using an inverse emulsion polymerization method for the entrapment of hydrophilic drug candidates *J. Controlled Release* **56**, 149.

[93] **Landfester, K., Willert, M, Antonietti, M.,** 2000. Preparation of polymer particles in nonaqueous direct and inverse miniemulsions, *Macromolecules*, **33**(7), 2370-2376.

[94] **Deng, J., He, C., Peng, Y., Wang, J., Long, X., Li, P., Chan, A**., 2003. Magnetic and conductive Fe_3O_4-polyaniline nanoparticles with core-shell structure, Synthetic Metals, **139**, 295-301

[95] **Morais, P.C., Lima, E.C.D., Rabelo, D., Reis, A.C., Pelegrini, F.,** 2000. Magnetic resonance of magnetite nanoparticles dispersed in mesoporous copolymermatrix, *IEEE Transactions on Magnetics*, **36** (5I), 3038-3040.

[96] **Yan, F., Xue, G., Chen, J., Lu, Y.,** 2001. Preparation of a conducting polymer/ferromagnet composite film by anodic-oxidation method, *Synthetic Metals,* **123**, 17-20.

[97] **Shchukin, D.G., Radtchenko, I.L., Sukhurov, G.B.,** 2003. Micron-scale hollow polyelectrolyte capsules with nanosized magnetic Fe_3O_4 inside. *Mat. Lett.,* **57**, 1743-1747.

[98] **Mayes, E., Vollrath, F., Mann, S.,** 1998. Fabrication of Magnetic spider silk and other silk-fiber composites using inorganic nanoparticles, *Adv. Mater.,* **10**, 801-805

[99] **Cumbal, L., Greenleaf, J., Leun, D., SenGupta, A.K.,** 2003. Polymer Supported Inorganic Nanoparticles: Characterization and Environmental Applications, *Reactive and Functional Polymers*, **54**, 167-180.

BIOGRAPHY

Meral Akdüzen was born in 1979 in Istanbul. In 1997, he graduated from Bornova Anatolian High School and attemped to the Chemistry Department of Istanbul University within the same year.

In 2003, he was accepted as a master student to Istanbul Technical University, Polymer Science and Technology Department of the Institute of Science and Technology.